Preparation of Heparin Surface for Quantification of Fibroblast Growth Factor-2 (FGF-2) Binding Using Surface Plasmon Resonance (SPR).

David Rand Kirtland

Thesis submitted to the Faculty of the
Virginia Polytechnic Institute and State University
In partial fulfillment of the requirement for the degree of

Masters of Science
In
Biomedical Engineering

Kimberly Forsten-Williams, Chair
Raymond E. Dessy
Richey M. Davis

May 04, 2005
Blacksburg, Virginia

Keywords: Fibroblast Growth Factor-2 (FGF-2) basic Fibroblast Growth Factor (bFGF), Mixed Self Assembling Monolayer (mSAM), Surface Plasmon Resonance (SPR), Biosensor, Heparin, Growth Factor, Mixed Self-Assembled Monolayer

Copyright 2005, David Rand Kirtland

Preparation of Heparin Surface for Quantification of Fibroblast Growth Factor-2 (FGF-2) Binding Using Surface Plasmon Resonance (SPR).

David Rand Kirtland

(Abstract)

A mixed self assembling monolayer (mSAM) chip with attached heparin was developed to analyze heparin-protein interactions using a Reichert Inc, SR7000, surface plasmon resonance (SPR) instrument. The heparin was attached via streptavidin-biotin linkage where the streptavidin was covalently coupled to the mSAM and biotinylated heparin bound to it. These chips were then used to quantify the interactions of fibroblast growth factor-2 (FGF-2) with the surface bound heparin. Kinetic rate constants of association and disassociation were calculated. The association data of FGF-2 with heparin was fit to a single compartment, well-mixed model as the data did not exhibit mass transfer limitations. The results suggested that rebinding was prevalent and observed disassociation rates differed significantly in the presence of competing soluble heparin during disassociation. Our results indicate that the Reichert instrument and mSAM chips can be used to analyze heparin-protein interactions but that a careful protocol, outlined in this thesis, should be followed to obtain optimal data.

Author's Acknowledgements

I would like to thank all of those who have helped me in the completion of the thesis.

Dr Kimberly Williams for the opportunity to work in her lab and for all of her help and patience she provided in completing this project.

Dr. Thomas Ryan, Reichert Inc, for all of trouble shooting, explanations, and suggestions; for providing the mSAM chips, and for taking time to help figuring out that the SPR instrument was not functioning properly.

My Parents, Dr. and Mrs. Howard Kirtland, for their support, patience, and encouragement.

Dr. and Mrs. Cenedella for persistent encouragement to further my education..

Mr. John Autry for his generous assistance.

Table of Contents

List of Figures

List of Tables

Chapter 1 : Introduction

The ability to accurately model complex cellular pathways is predicated on knowing the rates of association and disassociation for the chemical species. Basic fibroblast growth factor, now more commonly referred to as fibroblast growth factor-2 (FGF-2), is a cytokine that influences cell behavior and development with direct applications to tissue growth and repair. FGF-2 is a member of the broad class of heparin-binding proteins and, as a result its interactions with heparin are of biological relevance. In this thesis, ours aims are to:

(1)- couple heparin to mixed self-assembled monolayer (mSAM) chips for use in the Reichert surface plasmon resonance (SPR) instrument,

(2)-quantify the interactions of FGF-2 with heparin using the Reichert SPR instrument.

Completion of these aims will allow us to demonstrate the applicability of the Reichert system for studying heparin-binding proteins and provide quantitative numbers useful for the modeling of heparin regulation of FGF-2.

Fibroblast Growth Factor Family

FGF-2 is a member of the fibroblast growth factor family that contains at least 23 other members (Ornitz & Itoh, 2001). The FGF family has a common 120-residue homologous region that forms a structure known as a beta-trefoil (Ibrahimi) where a beta-trefoil is three simple 4-strand anti-parallel beta sheets (Ornitz & Itoh, 2001). This group has a common core amino acid sequence that binds to heparin and heparan sulfate making them arguably the best studied of the heparin binding growth factors (Nugent & Iozzo, 2000; Berry et al., 2004). FGF proteins have been shown to induce effect in

mesodermal and neuroectdermal cells and play a role in angiogenesis, cell growth, tissue patterns, embryo development, metabolic regulation, cell migration, tissue repair, and maintenance (Nugent & Iozzo, 2000; Rifkin & Moscatelli, 1989).

FGF-2

Basic fibroblast growth factor, now referred to as FGF-2, is an 18 kD signal protein that varies little between organisms, typically exhibiting sequence homology in excess of 90% (Nugent & Iozzo, 2000). The sequence is comprised of a large number of basic resides that give the molecule an iso-electric point of 9.5 pH (Nugent & Iozzo, 2000).

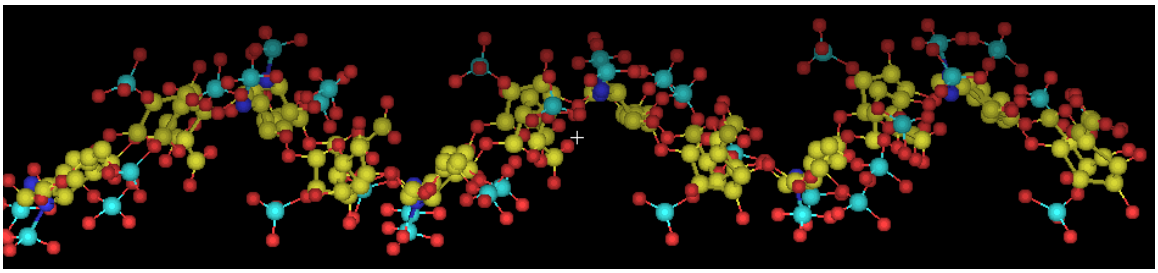

Figure 1.1, Homology model of heparin fragment generated using Molw PDB Viewer, version 4.0, and the NMR studies of heparin by Mulloy et al. (1993). Yellow represents carbon atoms; red represents oxygen atoms; light blue represents sulfur atoms; dark blue represents nitrogen atoms.

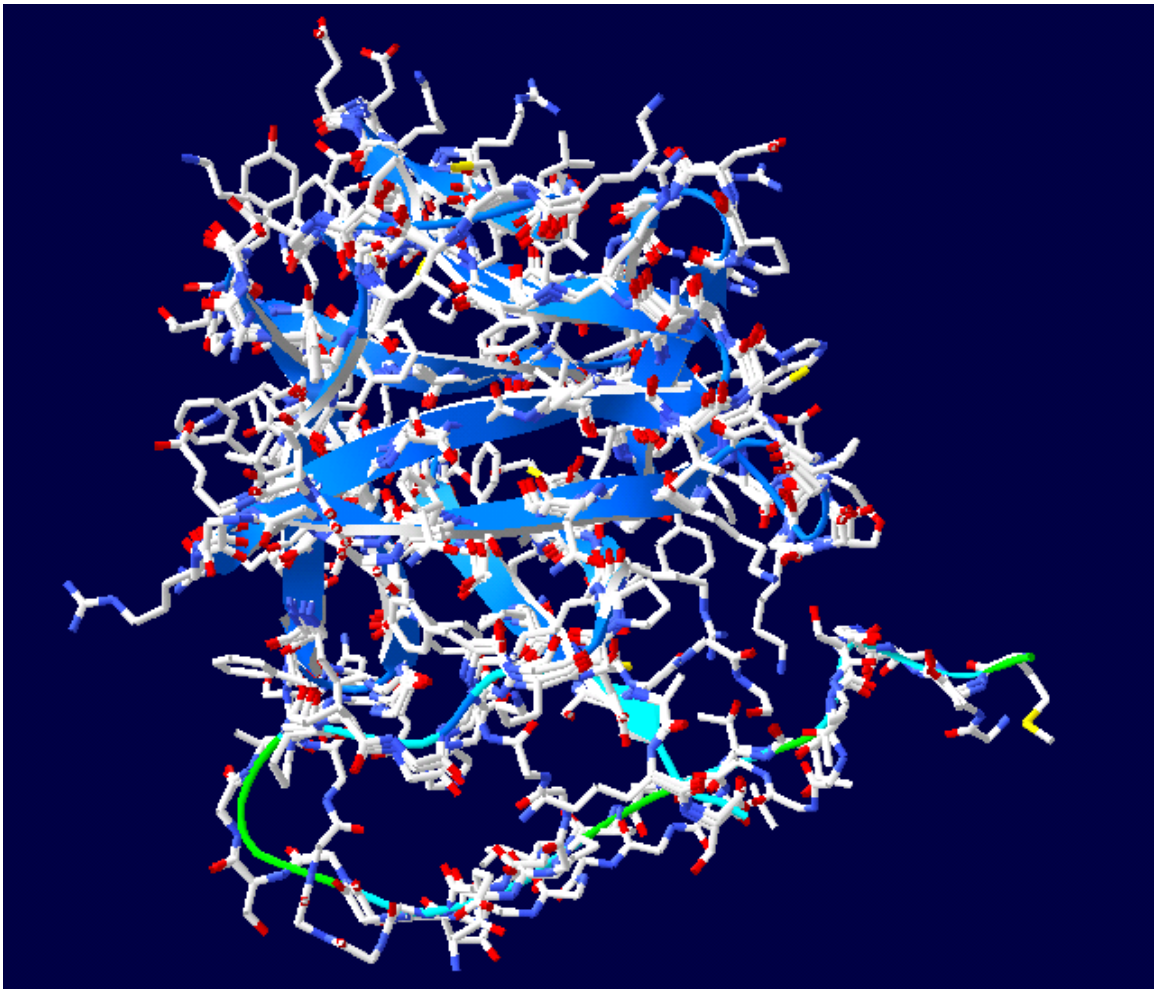

Figure 1.2, Homology model of FGF-2 generated using Deep View PDB Viewer, version 3.7, and the PDB generated by Swiss Model from the sequence of human FGF-2. White represents carbon atoms; red represents oxygen atoms; yellow represents sulfur atoms; dark blue represents nitrogen atoms. The blue ribbon represents beta sheets.

FGF-2 has been shown to mediate a mitogenic response in mesoderm and neuroectoderm cells such as fibroblasts, osteoblasts, endothelial cells, and smooth muscle cells primarily through transmembrane receptors (Ornitz & Itoh, 2001). It is probably best known for its role in the growth and function of vascular cells (Nugent & Iozzo, 2000). The interaction between FGF-2 and heparin is part of the beginning of a complex cellular pathway. This is controlled through interactions between heparin-like

proteoglycans and receptors to selectively effect discrete cellular pathways (Berry et al., 2004).

Heparin

Heparin is not a protein; rather it is a complex sugar. It is composed of repeating disaccharide units of D-glucosamine and L-idurinic acid with periodic substitutions of D-glucuronic acid, N-acetylated D glucosamine, and D-glucosamine. These repeated units form a negatively charged polymer ribbon with sulfate and carboxyl groups along its edge (Faham et al., 1998). Heparin is highly heterogeneous. It is a sulfated polysaccharide, much like heparan sulfate, but contains on average more sulfate groups (Osmond et al., 2002).

It should be noted that heparin is very similar to the glycosaminoglycan heparan sulfate. Heparan sulfate is a component of the outer surfaces of nearly all mammalian cells, while heparin is limited to connective tissue mast cells (Walker et al., 1993). Both are members of the glycosaminoglycan family and both bind members of the FGF family (Faham et al., 1998; Walker et al., 1993). Heparan sulfate is made up primarily of D-glucuronic acid and N-acetyl D-glucosamine components, and heparin is constituted primarily of alpha-D-glucosamine and L-iduronic acid (Guerrini et al., 2005). Heparin and heparan sulfate have similar overall structure and differ primarily in the greater amount of sulfate found in heparin (Faham et al., 1998).

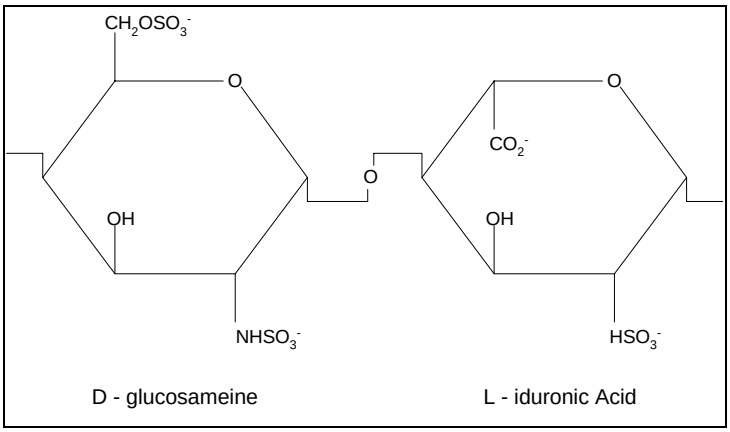

Figure 1.3, Basic repeating disaccharide of Heparin.

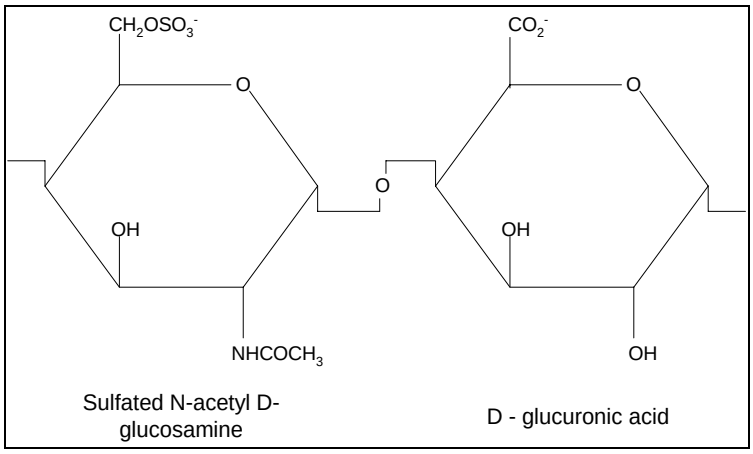

Figure 1.4, Basic repeating disaccharide of heparan sulfate featuring a sulfated N-acetyl D-glucosamine.

Heparin has many functions and physiological implications. Free heparin is used in medial applications as an anti-coagulant and anti-thrombosis drug (Guerrini et al., 2005), but this is just a specialized use of the molecule. Normally it is found in the extracellular matrix of connective tissue mast cells. It interacts with many different proteins to aid in the formation of certain protein-protein interactions, prevent other interactions, and affect molecular concentrations (Rahul et al., 2005). Heparin not only binds with all members of the FGF family, but also binds to many other growth factors like vascular endothelial growth factor (VEGF), placental growth factor (PlGF), platelet-

derived growth factor (PDGF), and hepatocyte growth factor (HGF) (Liekens et al., 2001). Heparin does not interact with all growth factors. For example, it does not bind insulin like growth factor I (IGF-I), transforming growth factor beta (TGF-β), or epidermal growth factor (EGF) (Liekens et al., 2001).

The extracellular matrix is filled with proteoglycans, including those with heparan sulfate glycosaminoglycan side-chains, and these molecules can have a strong impact on cell signaling pathways. Their roles can include prevention of degradation of FGF-2, prolonged retention at cellular membrane surface of the growth factor, and even acting directly as a member of the pathway activation sequence (Faham et al., 1998). For example, heparin has been shown to protect FGF-2 from degradation and denaturing from heat, enzymes, or acid (Sommer & Rifkin, 1989; Faham et al., 1998). Heparan sulfate molecules in solution that do not interact with the cell surface have also been shown to inhibit cell activity (Forsten et al., 2000; Fannon et al., 2000). Binding to heparan sulfate proteoglycans by FGF-2 has been shown to prolong retention of FGF-2 near the cellular surface of bovine endothelial cells resulting in prolonged stimulation of DNA synthesis (Moscatelli, 1992; Cochran, 2003). Cells that lack extra-cellular heparin / heparan sulfate via chemical modifications exhibited a reduced receptor binding and response to FGF-2 (Fannon & Nugent, 1996). Understanding heparin binding to FGF should lend insight into how heparin, and by extension heparin sulfate, impact FGF-2 signaling.

Interaction of FGF-2 and Heparin

FGF-2, as well as other heparin-binding proteins, binds to specific locations on heparin, and due to the heterogeneity of the molecule may interact in complex ways. For

example, Walker and coworkers (1994) found that longer heparan sulfate oligosaccharides were more active then shorter segments. These studies examined the extent that FGF-2 activated DNA synthesis in heparan sulfate deficient Swiss mouse fibroblast cells grown in the presence of different heparan sulfate fragments. These fragments consisted of heparan sulfate that had been digested with heparinases and acid followed by separation into groups with lengths of 3,4,5,6,7, and 8 disaccharides. The results showed that the extent of DNA synthesis activation depended on fragment size with extremely limited activation occurring with fragment lengths of 5 disaccharides or less in length. The author suggests this is due to the necessity of FGF-2 dimers forming on the heparan sulfate for activation to occur.

While FGF-2 can bind heparin in multiple separate locations, FGF-2 has been shown to contain heparin-binding domains that lie in close proximity on the surface of the protein making binding of a single protein to multiple heparin molecules unlikely (Nugent & Iozzo, 2000). Further, binding of FGF-2 to heparin does not change the protein conformation, but it does induce a conformational change in heparin (Berry et al., 2004). The change in heparin and the lack of change in FGF-2 have been shown using x-ray crystallography by Faham et al. (1996) of FGF-2 bound to heparin fragments and by analysis of homology models derived from crystalline structures of FGF-2 and heparan sulfate by Raman et al. (2003).

The role of heparin/heparan sulfate proteoglycans in the binding of FGF-2 to the FGF receptor (FGF-R) is not completely understood. There are different theories about the role of these glycosaminoglycans. The theories that heparin/heparan sulfate merely serves as a reservoir for the FGF-2 until it can form a binary complex with FGF-R or that

FGF-2 simply binds to FGF-R independent of proteoglycans are extremely unlikely. Several studies have strongly suggested that surface heparin / heparan sulfate binding is required for enhanced pathway activation (Forsten et al., 2000).

The prevalent theory places heparin as an essential component for pathway activation under physiological conditions. The stoichiometry of the interaction between FGF-2, FGF-R, and heparin/heparan sulfate is highly debated (Ibrahimi et al., 2004; Schlessinger et al., 2000; Pellegrini, 2001; Faham et al., 1996; Raman et al., 2003), but the predominate view that a ternary complex of heparin/heparan sulfate, FGF-2, and FGF-R is what activates the cellular pathway (Nuggent & Iozzo, 2000).

What has been shown is that there are many ways that FGF-2 pathway activation can occur. In addition to the heparin dependent activation mentioned above, activation of receptors can occur without heparin/heparan sulfate (Padera et al., 1999; Fannon & Nugent, 1996). In more recent work, heparan sulfate proteoglycans, particularly syndecans, have been shown to transducer an FGF-2 mediated signal independent of FGF-R (Chua et al., 2004; Tkacenko et al., 2004).

Figure 1.4 illustrates the suspected pathways that lead to formation of an activation complex. In the heparin dependent model the proteoglycans serves a means to maintain a concentration gradient of FGF-2 near the cell surface. The dimerization and binding to the receptor occurs independent of the heparin. While in the heparin dependent pathways the heparin serves as a necessary component for pathway activation.

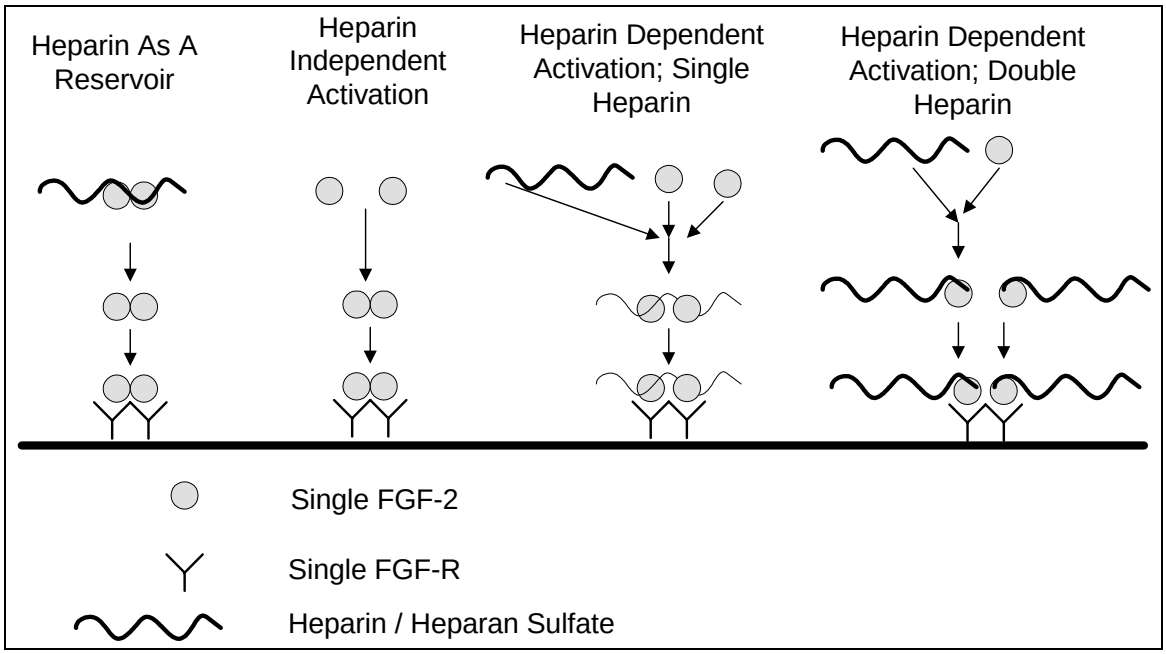

Figure 1.5, Summary of proposed pathway activation involving FGF-2 to form activating complex.
a-In the path that shows heparin as a reservoir the heparin merely serves to keep FGF-2 near the cell surface and increase its concentration the cell.
b-In the heparin independent pathway, heparin plays no role in the activation. This could represent cells that have been modified to not possess heparin.
c-In the heparin dependent, single strand, pathway, the heparin serves as site for FGF-2 to dimerize. The whole FGF-2, heparin, FGF-R complex is needed for activation.
d-In the heparin dependent, double strand heparin, pathway, a single FGF-2 and heparin bind initially. This complex then binds with a single FGF-R to form a trimer. Finally to complete activation two trimers bind.

Safran et al. (2000) and Padera et al. (1999) proposed that heparin serves as a site to promote the dimerization of FGF-2 as illustrated in the heparin dependent, single heparin model shown in Figure 1.5. This dimerization, as shown in the heparin independent pathway in Figure 1.5, can occur without the aid of heparin, but at a much lower rate. They also propose that the heparin/heparan sulfate, while not absolutely

essential, provides a structure that promotes the formation of dimers and stabilizes the FGF-2 dimer FGF-R interaction. This leads to increased and prolonged pathway activation.

Ibrahimi et al. (2004) propose that the heparin, FGF-2, and a receptor protein such as FGF-R form a complex that activate cellular pathways, as illustrated in the heparin dependent pathway with two separate heparin molecules (Figure 1.5). In this model there is a 2:2:2 ratio of heparin: FGF-2: FGF-R. The stable configuration of 2:2:2 of heparin, FGF-2, and FGFR has been shown to exist with x-ray crystallography studies (Schlessinger et al., 2000).

While the stoichiometry of the entire system is important, we have chosen to focus simply on the FGF-2-heparin binding at this point rather than including a receptor protein or trying to use purified heparan sulfate. This is much simpler but forms a strong foundation for future studies.

Surface Plasmon Resonance

Surface plasmon resonance (SPR) is a technique that enables one to obtain real time measurement of surface binding of unlabeled compounds to protein-coated surfaces (Schuck, 1997). With SPR, p-polarized light is generally used to excite a thin gold layer on a glass wafer attached to a prism. The setup, also known as a Kretschmann prism (Figure 1.6) arrangement, consists of a prism with a thin glass slide in optical contact. The slide has a thin metal coating and is the site where the surface binding will be measured (Earp & Dessy, 1998; Schuck, 1997).

The SPR process uses total internal reflection to excite non-radiative surface plasmon, waves of oscillating surface charge density, in the gold film. This excitatory

process can only occur when the polarizing light is at certain angles to the prism. Altering the substances bound to the gold film alters the angle at which the surface plasmons form (Schuck, 1997; Cooper, 2003). From the change in angle that resonance occurs at, one can determine the extent of surface binding.

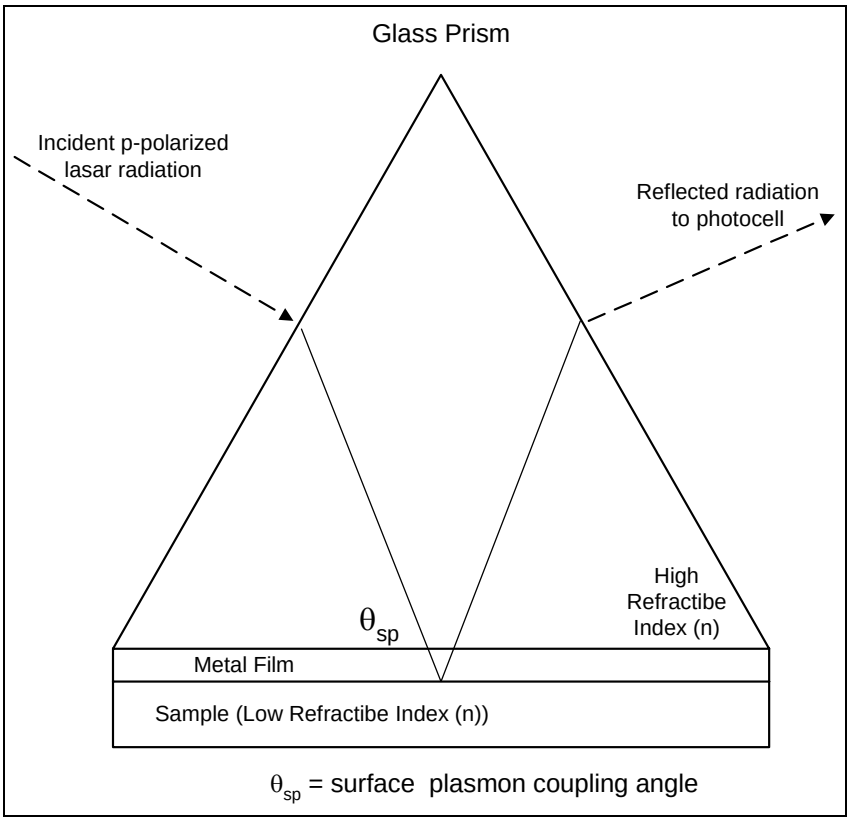

Figure 1.6, Schematic of an idealized Kretschmann Prism. P-polarized light is projected on a prism with a metal film and sample surface bound to one side. At a particular coupling angle complete internal refraction occurs, which is a marked by a significant reduction in the measured intensity of the reflected light. The angle at which internal reflection occurs can be related to the amount of material in the sample (Based on Earp & Dessy, 1998).

The SPR process measures changes in the refractive index on and near the chip surface with measurements typically limited to 200 to 300 nm from the surface (Earp & Dessy, 1998). This means that the protein in solution can affect the refractive index, but

the effect is likely only 1.8 x10-5 RIU per 100ug/ml of protein (Earp & Dessy, 1998). This is likely to be insignificant in comparison to the effects of surface binding on the refractive index. This study will analyze protein concentrations of less then 1.0 ug/ml.

There is a proportional relationship between the resonance angle and the concentration of macromolecules near the film surface. According to Reichert Analytical Instruments, 1 ng/mm^2 of surface binding will cause a refractive index change of 1.36x10^{-3} refractive index units (RIU) (Reichert, 2004). Stenberg et al. (1991) measured a response of 1.1x10^{-3} RIU per ng/mm^2 using radiolabeled antibodies on a Biacore SPR instrument (Stenberg et al., 1991). The response varies little, when examined on a mass basis between various biomolecules, as their individual refractive indices are nearly identical (Earp & Dessy, 1998; Lahiri et al., 1999). This was determined by measuring the response from binding radiolabeled proteins and antibodies of a range of masses with a Biacore AB SPR unit and then measuring the actual amount of binding (Biacore Methods Manual, 1991). Therefore one would anticipate that refractive index change can be used to quantify the amount bound of a certain molecule without first developing a standard curve.

Reichert SR 7000 Market Position

The Reichert SR 7000 and the Biacore 3000 both can be used for SPR analysis. The Reichert unit has a single flow cell and each solution change must be initiated by the user. It has a single 1 μl flow cell and a typical system volume, the total volume of the flow cell and tubing, in excess of 30 μl (Reichert, 2004). The BIAacore 3000, is a completely automated unit designed to integrate with other laboratory equipment. It has 4 flow cells and can analyze samples a small as 20-80 μl (Biacore, 2004). The BIAcore

3000 is a very capable and widely used SPR unit, but it is an expensive unit and the automation does somewhat limit the flexibility for the user. Cost conscious researchers can utilize a Reichert SR 7000 to perform most of the same studies at a lower cost while obtaining excellent quality data.

Chip Surface/Composition

SPR is not limited to using mixed self-assembled monolayer (mSAM) chips. Several different types have been used in the past, each with their positive and negative implications. The most commonly used type is the carboxyl-modified dextran surface (CMD). This surface is composed of a matrix or carboxymethylated dextran covalently bound to a gold layer (Biacore Product information), is negatively charged, and proteins for study can be bound to it by amine coupling. Unfortunately, the surface is prone to non-specific binding especially when analyzing complex proteins (Pei et al., 2000; Lahiri et al., 1999). This reasons makes this surface chemistry unsuitable for FGF-2 studies. Further, coupling generally occurs throughout the layer making transport limitations prevalent and preventing the binding of large molecules (Lahiri et al., 1999).

The mSAM layer we used was composed of alkanethiol-polyethene glycol and alkanethiol-polyethylene glycol carboxyl produced by Reichert, Inc. These chips have a well-characterized composition that places the carboxyl groups only at the interface of the chip and the solution. The advantages of this chip type include resistance to non-specific binding and a planar surface increasing uniformity when proteins are coupled to the chip. This uniform surface binding limits the extent of mass transfer limitations that may occur (Lahiri et al., 1999). Similar to the CMD chips, proteins can be coupled to the chip with amine chemistry.

Activation Chemistry

The chemical process to attach proteins to the surface via amine chemistry is illustrated in Figure 1.7. The chemistry of activation has one intermediate form in its progression to form a surface that can bind proteins. First, the carboxylic acid, of alkanethiol-polyethylene glycol carboxyl in our case, reactions with the EDC to form EDC esters. The attached EDC group is then replaced by NHS to form reactive NHS esters. At this point the surface is ready to bind the protein of interest. The protein is flowed over the surface and the amine groups of the protein take the place of the NHS to become covalently coupled to the surface. At the end of the process, ethanolamine removes any reactive NHS esters on the surface to prevent the binding of other proteins to the system surface during later associations/disassociation phases (Lahiri et al., 1999).

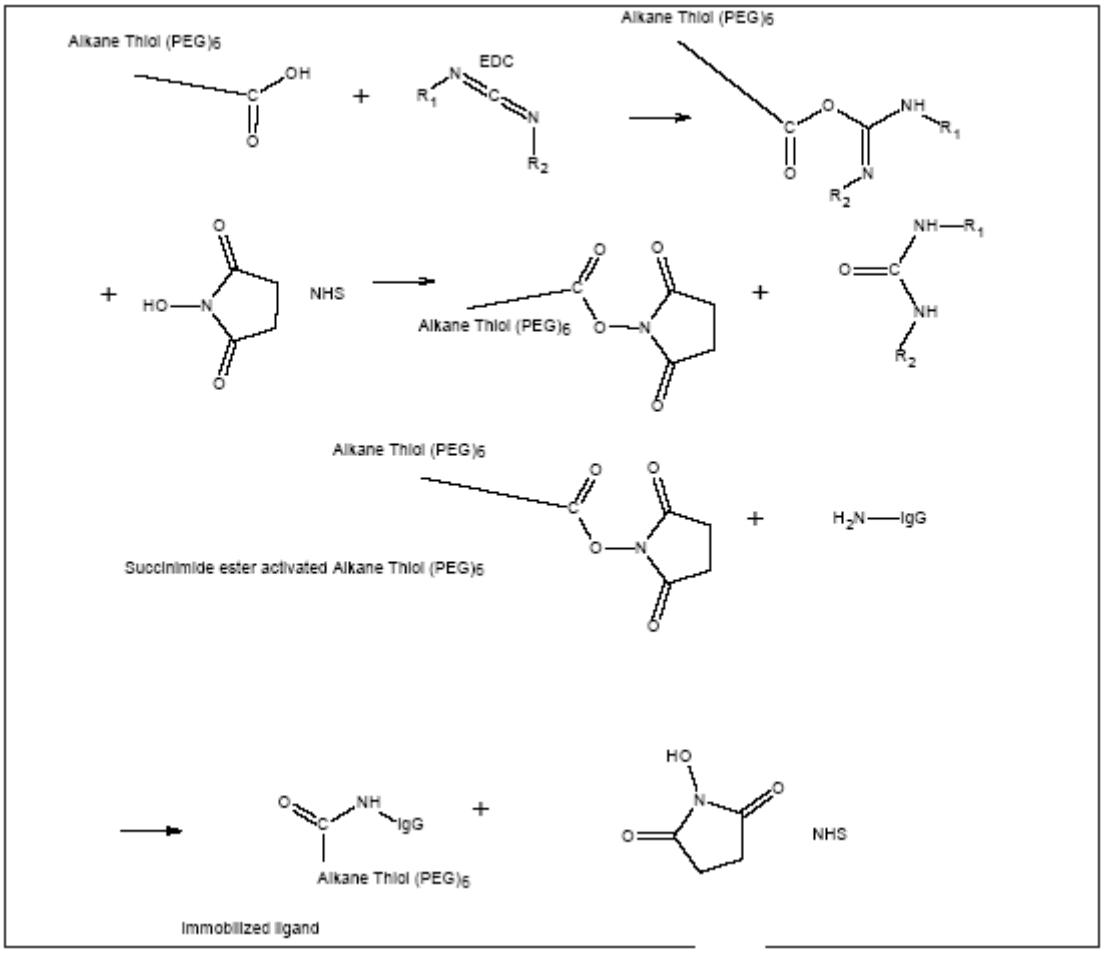

Figure 1.7, Amine coupling of an antibody to mSAM surface. This figure illustrates the amine coupling of an antibody, IgG, to alkanethiol-polyethylene glycol carboxyl. First, the carboxyl group on the surface reacts with the EDC to form EDC esters. This EDC ester is then replaced by NHS to form reactive NHS esters. Next the protein to be bound, in this case IgG, is passed over the chip and it takes the places of the NHS ester to covalently bind to the surface. Finally the remaining reactive NHS esters are removed with ethanolamine solution (Figure used with permission from Reichert Inc. (2004)).

Data Analysis

To fully quantify the binding of specific proteins to proteins immobilized on SPR chips, one must collect quality data and analyze the data using a model that reflects the

physical reality. There are several different units of measure used to describe the binding detected with SPR analysis. The change in pixels reported by the Reichert SPR unit is proportion to the amount of material bound to the surface. One refractive unit (RU), the unit commonly used with BIAcore SPR instruments, has been determined to be equal to 1 pg per mm of bound protein (Stenberg et al., 1991).

A pixel, the unit of measure outputted by the Reichert system, is a measure of the surface thickness or concentration. It is effected by the thickness and effective refractive indexes for it constituent components (Silin et al., 1996). All of the various measurement units can be inter-converted and for the Reichert system with 1 pixel being equivalent to 90 μRIU which is equivalent to 66 RU and 0.0066 degrees (Reichert, 2004; Silin & Plant, 1997; Dr T.E. Ryan, Reichert, Inc., personal communication).

The simplest and most common model to utilize for data analysis is the rapid mixing bi-molecular model shown in Equation 1. This model is based on a well-mixed uniform, constant concentration solution interacting with a homogeneous binding surface. No mass-transfer limitations or variations in the individual binding properties of the surface binding sites are assumed present (BIAtechnology Handbook, 1994; Morton et al., 1995).

$$A + B \underset{k_d}{\overset{k_a}{\leftrightarrow}} AB$$

Equation 1

Rapid-Mixing Model, First Order Model Where A represents the protein free in solution, B represents the free binding sites on the chip surface, and AB is the complex formed from binding A to B.

Equation 1 can be written as a rate equation for the association phase in terms of the time rate of change of bound surface complexes (Equation 2). *d[AB]/dt* is the rate of change for the amount of protein bound to the surface with k_a being the kinetic rate constant for the association of protein to the surface binding sites and k_d being the rate constant for the release of protein from the binding sites. [AB] is quantified by the change in pixels reported by the SPR unit during the association and disassociation phases.

$$\frac{d[AB]}{dt} = k_a[A][B] - k_D[AB]$$

Equation 2

Rate equation for association phase of Rapid-Mixing Model

$$\frac{d[AB]}{dt} = -k_D[AB]$$

Equation 3

Rate equation for disassociation phase of Rapid-Mixing Model

Equation 2 is simplified for the disassociation phase when the concentration of free protein in the solution is considered to be negligible (Equation 3). In order to relate the amount of free and bound binding sites, Equation 5 is used. $[B_{max}]$ is the total number of free binding sites at the beginning of an association. It is assumed that all binding sites are the same and that $[B_{max}]$ does not change during the time frame of interest.

$$[B] = [B_{\max}] - [AB]$$

Equation 4

Relationship between bound and free binding sites

$$\frac{d[AB]}{dt} = k_a[A]([B_{Max}] - [AB]) - k_D[AB]$$

Equation 5

$$\frac{d[AB]}{dt} = k_a[A][B_{Max}] - ([A]k_a - k_d)[AB]$$

Equation 6

Equations 5 and 6 show the progression and development of equation 2 to produce a solvable form where equation 6 is simply a rearrangement of Equation 6. Since the collected data is in the form of RU or pixels, $[B_{max}]$, [AB], and [A] are substituted to with R_{max}, R, and C in Equation 7 to reflect the form of the data collected. From there Equation 7 is integrated to Equation 8 using the initial conditions of $R_0 = 0$ at t = 0.

$$\frac{dR}{dt} = k_a CR_{Max} - (Ck_a - k_d)R$$

Equation7

$$R = \frac{k_a CR_{Max}}{Ck_a - k_d}\left(1 - e^{-(Ck_a - k_d)t}\right)$$

Equation 8

Biotin-Streptavidin Interaction

Biotin and streptavidin have a very specific, high affinity interaction that is utilized in many laboratory procedures. This non-covalent interaction is significantly stronger than even antibody-antigen interactions (Diamandis & Christopoulos, 1991). The disassociation constant between streptavidin and biotin ranges from 10^{-13} to 10^{-16} M depending on the assay conditions (Queshi & Wong, 2002). Once the streptavidin- biotin complex is formed, it is difficult to dissociate and generally believed to break only under extreme pH changes or in the presence of chaotropes (Diamandis & Christopoulos, 1991) like sodium dodecyl sulfate. This strong binding can produce a specific, stable interaction that has been utilized to couple biotinylated proteins to bound streptavidin (Cochran et al., 2003; Smith et al., 2003).

In this study streptavidin was bound to the mSAM chip using amine coupling and biotinylated heparin will be bound to the streptavidin. This produces an ideal environment to measure the interactions between FGF-2 and heparin. The use of the streptavidin biotin association has been used successfully in SPR systems in the past. Biotinylation of compounds is a relatively simple procedure for which many chemical companies offer kits to perform.

Past Studies Utilizing Surface Bound Heparin

Many SPR studies have been previously performed to investigate protein interactions with heparin bound to the chip surface as presented in Table 1.1, however none have been done with the Reichert System. A variety of techniques were utilized with the most common being biotinylated heparin bound to streptavidin coupled by amine chemistry to the surface. A second common technique was to attach a protein-

heparin to the surface directly by amine chemistry. Both accomplish the same goal, but there are many variations that can impact the end result.

The majority of the studies outlined in Table 1.1 use streptavidin bound by amine chemistry to a carboxymethyl dextran chip followed by the introduction of biotinylated heparin. Chips can be purchased with just carboxymethyl dextran surface, like the CM5 produced by BIAcore, or with the streptavidin already coupled to a carboxymethyl dextran surface, like the SA produced by BIAcore. The streptavidin has been used to successfully attach 20 to 824 RU of biotinylated heparin in studies (Futamura et al., 2003; Utt et al., 2000). Based on the multitude of studies presented in Table 1.1, the extent of addition of biotinylated heparin has been controlled primarily by adjusting the length of association, concentration of association solution, and surface density of streptavidin. Once streptavidin has been attached to the surface, adding biotinylated heparin done by introduction through the flow cell to produce a chip for studying interactions with surface bound heparin.

Another common means to attach heparin to a surface for analysis by SPR, as presented in Table 1.1, is to couple a heparin molecule that has been modified to include peptide fragments. These peptide fragments, like bovine serum albumen (BSA) or albumen, can be attached to the carboxymethyl dextran surface by amine coupling. This method has been used to successfully attach 250 to 300 RU of heparin in studies (Akhouri et al., 2004; Zhang et al., 2002). This method has the advantage of being a single step coupling and is not dependent on the strength of the biotin-streptavidin link. Unfortunately, commercial sources of BSA coupled heparin were no longer available at the time of this thesis.

We have thus chosen to bind heparin to the surface by attaching biotinylated heparin to streptavidin that has been amine coupled to the surface. As mentioned above, commercial sources of protein-heparin conjugate were no longer available and, due to its size, streptavidin might be expected to project the heparin further away from the surface then albumen heparin. This would be expected to diminish mass transfer limitations (Myszak, 1997) and improve binding (Osmond et al., 2002).

The previous studies differ from our work though in that all were performed using a Biacore SPR units and a different chip type. Our studies were performed using a Reichert SR 7000 with biotin labeled heparin bound to streptavidin that had been attached using amine coupling to a mSAM chip.

Investigator(s)	Year	Protein in Solution That Was Studied	Chip Type	Heparin Attachment Technique	Heparin Bound (RU)	SPR Unit
Futamura et al.	2005	apoE	SA	Biotinylated Heparin to Streptavidin	20-300 RU	Biacore 2000, Biacore X
Presta et al.	2005	FGF-2	SA	Biotinylated Heparin to Streptavidin	Not Listed	Not Listed
Alexakis et al.	2004	FGF-2	CM5	Amine Couple Streptavidin to Chip; Biotinylated Heparin to Streptavidin	100 RU	Biacore
Ibrahimi et al.	2004	FGF-2	C1	Amine Couple Albumen-Heparin to Chip	300 RU	Biacore 3000
Jang et al.	2004	TNI-3,4,5	CM5	Amine Couple Streptavidin to Chip; Biotinylated Heparin to Streptavidin	Not Listed	Biacore X
Zhang et al.	2004	Slit proteins	C1	Amine Couple Albumen-Heparin to Chip	300 RU	Biacore 3000
Neuenschwander	2004	IxA-B	SA	Biotinylated Heparin to Streptavidin	7.2; 265; 824 RU	Biacore 3000
Akhouri et al.	2004	ECD protein	SA	Biotinylated BSA Heparin to Streptavidin	250 RU	Biacore 2000
Ricard-Blum et al.	2004	Endostatin	F1	Amine Couple Streptavidin to Chip; Biotinylated Heparin to Streptavidin	70-200 RU	Biacore 3000
Cochran et al.	2003	VEGF	CM5	Amine Couple Streptavidin to Chip; Biotinylated Albumen Heparin to Streptavidin	60-200 RU	Biacore 3000

Smith et al.	2003	Viral Protein Fragments	CM5	Amine Couple Streptavidin to Chip; Biotinylated Albumen Heparin to Streptavidin	2762 RU	Biacore X
Garcia-Olivas et al.	2003	PDGF	F1	Amine Couple Streptavidin to Chip; Biotinylated LMW Heparin to Streptavidin	Not Listed	Biacore 2000
Barth et al.	2003	Hepitis C Viral Envelope	C1	Amine Couple BSA-Heparin to Chip	250 RU	Biacore 3000
Yakovlev et al.	2003	Fibrinogen	SA	Biotinylated Heparin to Streptavidin	300 RU	Biacore 3000
Eckert et al.	2003	Heparin Cofactor 2	SA	Biotinylated Heparin to Streptavidin	Not Listed	Biacore 3000
Kett et al.	2003	Avaidin	CM5	Amine Couple Streptavidin to Chip; Biotinylated Heparin to Streptavidin	Not Listed	Biacore 2000
Guerrini et al.	2002	FGF-1	CM5	Amine Couple Streptavidin to Chip; Biotinylated LMW Heparin to Streptavidin	170 RU	Biacore 1000
Vives et al.	2002	rANTES 9	F1	Amine Couple Streptavidin to Chip; Biotinylated Heparin to Streptavidin	Not Listed	Biacore 1000
Osmond et al.	2002	Thrombin	B1	Amine Couple Streptavidin to Chip; Biotinylated Heparin to Streptavidin	52-66 RU	Biacore 2000
Laffont et al.	2002	LDL	SA	Biotinylated Heparin to Streptavidin	Not Listed	Biacore X
Miyamoto et al.	2002	Fibronectin	SA	Biotinylated Heparin to Streptavidin	91 RU	Biacore 2000
Zhang et al.	2002	FGF-1	C1	Amine Couple Albumen-Heparin to Chip	300 RU	Biacore 3000
Guerrini et al.	2002	FGF-1	CM5	Amine Couple Streptavidin to Chip; Biotinylated LMW Heparin to Streptavidin	170 RU	Biacore 1000
Stenlund et al.	2002	FusCC	CM5	Amine Couple Avidin to Chip; Biotinylated Albumen Heparin to Avidin	650 RU	Biacore 2000
Birkmann et al.	2001	Herpes Virus 8	SA	Biotinylated Heparin to Streptavidin	160 RU	Biacore
Badellino et al.	2001	FXIa	SA	Biotinylated Heparin to Streptavidin	100-150 RU	Biacore
Martin et al.	2001	RANTES	F1	Amine Couple Streptavidin to Chip; Biotinylated Heparin to Streptavidin	100-200 RU	Biacore 2000
Capila et al.	2001	Annexin V	SA	Biotinylated Heparin to Streptavidin	Not Listed	Biacore
Friedrich et al.	2001	Anti-thrombin	SA	Biotinylated Heparin to Streptavidin	Not Listed	Biacore 2000
Hoffman et al.	2001	Peptide Sequences	SA	Biotinylated Heparin to Streptavidin	300 RU	Not Listed
Utt et al.	2001	Cytotoxin	SA	Biotinylated Heparin to Streptavidin	400-600 RU	Biacore 1000

Dong et al.	2001	Apolopoproetin E4	SA	Biotinylated Heparin to Streptavidin	Not Listed	Not Listed
Nielsen & Yamanda	2001	Synthetic Peptides	SA	Biotinylated Heparin to Streptavidin	300 RU	Biacore 1000
Sadir et al.	2001	SDF-1Alpha	F1	Amine Couple Streptavidin to Chip; Biotinylated Heparin to Streptavidin	50 RU	Biacore
Bengtsson	2000	PRELP	CM5	Amine Couple Streptavidin to Chip; Biotinylated Heparin to Streptavidin	Not Listed	Biacore 2000
Lin et al.	2000	HMW Kiniogen	CM5	Amine Couple Streptavidin to Chip; Biotinylated Heparin to Streptavidin	50-150 RU	Biacore 2000
Nielsen et al.	2000	LG4	SA	Biotinylated Heparin to Streptavidin	300 RU	Biacore 1000
Pethe et al.	2000	HBHA	CM5	Amine Couple Streptavidin to Chip; Biotinylated LMW Heparin to Streptavidin	250 RU	Biacore 2000
Kappler et al.	2000	netrin-1	SA	Biotinylated Heparin to Streptavidin	200 RU	Biacore 1000
Arteel et al.	2000	Selenoprotein P	C1	Amine Couple Biocytin to Chip; Biotinylated Heparin to Biocytin	100 RU	Biacore 1000
Lookene et al.	2000	Lipoproteins	CM5	Amine Couple Streptavidin to Chip; Biotinylated Heparin to Streptavidin	Not Listed	Biacore 1000
Moulard et al.	2000	HIV-1 proteins	B1	Biotinylated Heparin to Streptavidin	65,35,20 RU	Not Listed
Lookene et al.	2000	Dismutase	CM5	Amine Couple Streptavidin to Chip; Biotinylated Heparin to Streptavidin	Not Listed	Biacore 2000
Shuvaev et al.	1999	Apolipoprotein	SA	Biotinylated Heparin to Streptavidin	Not Listed	Biacore X
Amara et al.	1999	Cell Derived Factor 1 Alpha	F1	Amine Couple Streptavidin to Chip; Biotinylated Heparin to Streptavidin	50 RU	Biacore
Gaus & Hall.	1999	LDL	SAM	Amine Couple N-Acetyl Heparin Couple to Chip	Not Listed	Not Listed
Lustig et al.	1999	PDGF	CM5	Amine Couple Streptavidin to Chip; Biotinylated LMW Heparin to Streptavidin	Not Listed	Biacore
Capila et al.	1999	Annexin V	SA	Biotinylated Heparin to Streptavidin	100 RU	Biacore 2000
Joyce et al.	1999	BPV particles	CM5	Amine Couple Carbohydrazide; Oxidized Heparin to Carbohydrazide	Not Listed	Biacore
Caldwell et al.	1999	Esterase inhibitor	SA	Biotinylated Heparin to Streptavidin	100 RU	Biacore 2000
Lookene et al.	1997	Lipoproteins	CM5	Amine Couple Streptavidin to Chip; Biotinylated Heparin to Streptavidin	Not Listed	Biacore

Lustig et al.	1996	PDGF-AA	CM5	Amine Couple Streptavidin to Chip; Biotinylated LMW Heparin to Streptavidin	Not Listed	Biacore
Mach et al.	1993	FGF-1	CM5	Amine Couple Streptavidin to Chip; Biotinylated Heparin to Streptavidin	50,200 RU	Biacore

Chip Type Definitions			
Biacore #	Pioneer #	Other	
CM5	C1		Carboxymethyl dextran chip
CM4	B1		a CM5/C1 chip with reduced carboxylation to reduce non specific binding
CM3	F1		a CM5/C1 chip with a reduced length dextran to reduce surface height
SA			CM5 chip with streptavidin covalently attached to the surface
		mSAM	Mixed Self Assembled Monolayer

Table 1.1, Techniques used to bind Heparin to chip surface for SPR studies. Biacore and Pioneer, both produce carboxymethyl dextran chips for use with Biacore SPR instruments

FGF-2 Heparin Studies Utilizing SPR

Probably the most complete study of FGF-2 interactions was done by Ibrahimi, et al. (2004). They used a Biacore 3000 SPR to quantify the interactions between a soluble form of FGF-R, heparin, and FGF-2. In their study, they performed experiments where they flowed heparin over coupled FGF-2 and where they flowed FGF-2 over coupled heparin. 1000 RU of FGF-2 was coupled by amine chemistry to the surface of a carboxymethyl dextran chip, and 300 RU of albumen heparin was coupled by amine chemistry to another carboxymethyl dextran chip. The heparin was associated with a solution of 200 μg per ml albumen heparin in sodium acetate buffer and 2M guanidium hydrochloride at pH 4.0. The FGF was associated with a solution of 25 μg per ml FGF-2 HBS-EP buffer at pH 7.4. For all associations a flow rate of 50 μl per minute was

employed. The chip was regenerated with 2M NaCl, 100 mM sodium acetate at pH 4.0 between all FGF heparin associations.

They examined the binding of 25 nM to 800 nM heparin solutions to the FGF-2 chip and the binding of 500 nM FGF-2 to the heparin chip. The 400 nM heparin solution binding to surface bound FGF-2 showed a higher maximal extent of association than a 500 nM FGF-2 solution with surface bound heparin. Exact difference could not be quantified because of the size and format of the presented graphs and differences in tested concentrations, but differences such as the total amount bound during association were obvious From their results they calculated an association rate, k_a, of $1.1x10^7 \pm 4.71x10^5$ $M^{-1}s^{-1}$and a disassociation rate, k_d, of $.43 \pm 1.92 \times 10^{-2}$ s^{-1}. The authors noted that non-specific binding did not surpass 20% of the maximum RU for any run. It should be noted that the calculations are based on the interactions of heparin in solution with surface bound FGF-2. Furthermore the one association of FGF-2 with surface bound heparin was done at 500 nM; a very concentrated solution.

Presta and coworkers (2005) also examined the interactions of heparin and FGF-2 with a SPR instrument. The study did not mention an instrument make or model, but they did utilize a Biacore streptavidin coated chip (SA). Un-fractionated biotinylated heparin (90 RU) was coupled the chip. They examined the association of FGF-2 to the surface bound heparin using concentrations of 10 nM and 160 nM FGF-2, while varying the concentrations of low molecular weight (LMW) heparin in the association solution from 0 to 900 nM. For situations in the absence of LMW heparin in the association solution they calculated an association rate, k_a, of $9x10^3$ M^{-1} $s^{-1}$and a disassociation rate,

k_d, of 3.8 x10^{-4} s^{-1}. When un-fractionated heparin was added to the association phase a dose dependent reduction in FGF-2: heparin binding was observed.

Wu and coworkers (2003) used an IAsys SPR system to quantify the interactions between FGF-2 and surface bound heparin. Glycol chitosan was amine coupled to a carboxymethyl dextran chip. This was followed by the binding of glycaminated heparin to the surface bound glycol chitosan. Associations of 20 to 350 nM FGF-2 were performed, and an association rate, k_a, of 5.4± 0.7 x10^4 M^{-1} $s^{-1}$and a disassociation rate, k_d, of 3.85± 0.9 x10^{-3} s^{-1} were calculated.

Alexakis and coworkers (2004) explored the binding of FGF-2 with surface bound heparin with a Biacore SPR instrument. Streptavidin was amine coupled to a carboxymethyl dextran chip that was then bound with biotinylated heparin (100 RU). No mention of specific FGF-2 concentrations that were studied were presented, but an equilibrium dissociation constant, K_d, of 10.6± 1.4 x10^9 M was offered.

Authors	SPR System	Method To bind Heparin to System	Rate Constants
Alexakis et al.	Biacore	Amine Couple Streptavidin To Surface; Bind Biotinylated Heparin To Streptavidin	K_d =10.6+/1.4.4 nM where $K_d = k_d/k_a$
Ibrahimi et al.	Biacore 3000	Amine Couple Albumen Heparin To Surface; Amine Couple FGF-2 To Surface	k_a=1.1 x 10^7 +/- 4.71 x 10^5 ($M^{-1}s^{-1}$) k_d=.43+/-1.92x10^{-2} (s^{-1})
Presta et al.	Not listed	Couple Biotinylated Heparin To Streptavidin Coated Surface	k_a=9 x 10^3 +/- 4.71 x 10^5 ($M^{-1}s^{-1}$) k_d=3.8x10^{-4}+/-1.92x10^{-2} (s^{-1})
Wu et al.	IAsys	Amine Couple Glycol Chitosan To Surface; Glycaminated Heparin To Glycol Chitosan	k_a=5.4 +/- 0.7 x 10^4 ($M^{-1}s^{-1}$) k_d=3.85+/-0.9 x 10^{-3} (s^{-1})

Table 1.2, A compilation of results from studies that quantified the binding of FGF-2 and heparin using SPR.

Clearly there is a large variation in the results from these four studies despite looking essentially at the same interaction. Our study differs in that we will be using an

mSAM chip, which should provide a better chip surface than that of the carboxymethyl dextran and permit better data to be collected, as well as the Reichert instrument.

Heparin Binding Orientation

A product of the long ribbon like structure of heparin is that when bound to a surface; the point of attachment for the heparin can affect the capacity and affinity for proteins. Superior results have been obtained by using heparin that is attached at the reducing terminus (Osmond et al., 2002). In this configuration, Osmond and coworkers suggest that the heparin that is farther from the surface is more available for interactions. For there studies they utilized a Biacore 2000 and carboxymethyl dextran chips. When performing experiments utilizing heparin bound to a surface, one must be conscious of the effects of its orientation. For our studies we are using a biotinylated heparin from CalBiochem that is biotinylated at carboxyl groups of the uronic acid residues with a 12-atom spacer between the heparin and biotin groups (Stearns et al., 1997). This spacer moves the heparin away from the surface and should be more available for interactions. This spacer makes the biotinylated heparin we utilized different than any of the types Osmond et al. tested. The Osmond et al. study does illustrate the important of separating the bound molecule of interest away from the surface, and we believe that the distance from the surface because of the streptavidin and the spacer will allow for optimal FGF-2: heparin binding.

Summary

This purpose of this study was to couple heparin to mSAM chips for analysis using a Reichert SR 7000 SPR instrument. This type of interaction has not previously been studied using this instrument and, as outlined above, differences in chip availability

as well as flow cell meant that optimization was necessary. Following heparin coupling, we used these chips and instrument to quantify the interactions of FGF-2 with heparin. We present the methods used to obtain our results, the problems that we overcame, and processes employed to optimize our results. We also note that limited testing with a second heparin-binding protein, insulin-like growth factor binding protein-3 (IGFBP-3), was also performed.

The overall aims of the work and the general background necessary to place this work in context were included in Chapter 1. In Chapter 2, the reader will find a comprehensive presentation of the methods employed. Chapter 3 is an analysis of the process of developing a method to bind heparin to the mSAM surface, while Chapter 4 contains our analysis of the interactions of heparin and FGF-2. In Chapter 5, we will discuss our results and suggest future research possibilities. An appendix describing additional work using the Reichert instrument but studying a different protein system is included.

Chapter 2 : Materials and Methods

Binding heparin to a mSAM chip so that quantification of the interaction between heparin with FGF-2 could be evaluated required the development of a specific protocol. This chapter describes all of the substances, instruments, and techniques that were used to attach heparin to the chip, purify biotin heparin, and quantify the binding of FGF-2 to heparin using SPR.

Hardware Setup

The data included in this thesis was collected using the layout depicted in Figure 2.1. A Reichert SR 7000 SPR refractometer (Figure 2.2) was attached to a Dell Optiplex SX260 desktop computer running National Instruments Labview Run-time version 6.02 software. A Cole-Parmer Masterflex L/S model 7519-20 peristaltic pump was used to move solutions through Upchurch Scientific 0.02 I.D. Teflon polymer tubing. All connections were made with plastic compression fittings. A manual six input valve was utilized on the suction side to allow trouble-free changes of solution without inducing air into the system. A one ml injection loop (Figure 2.3) was situated on the pressure side between the pump and the flow cell for coupling of streptavidin to the SPR chip. The exact layout is shown in Figure 2.1.

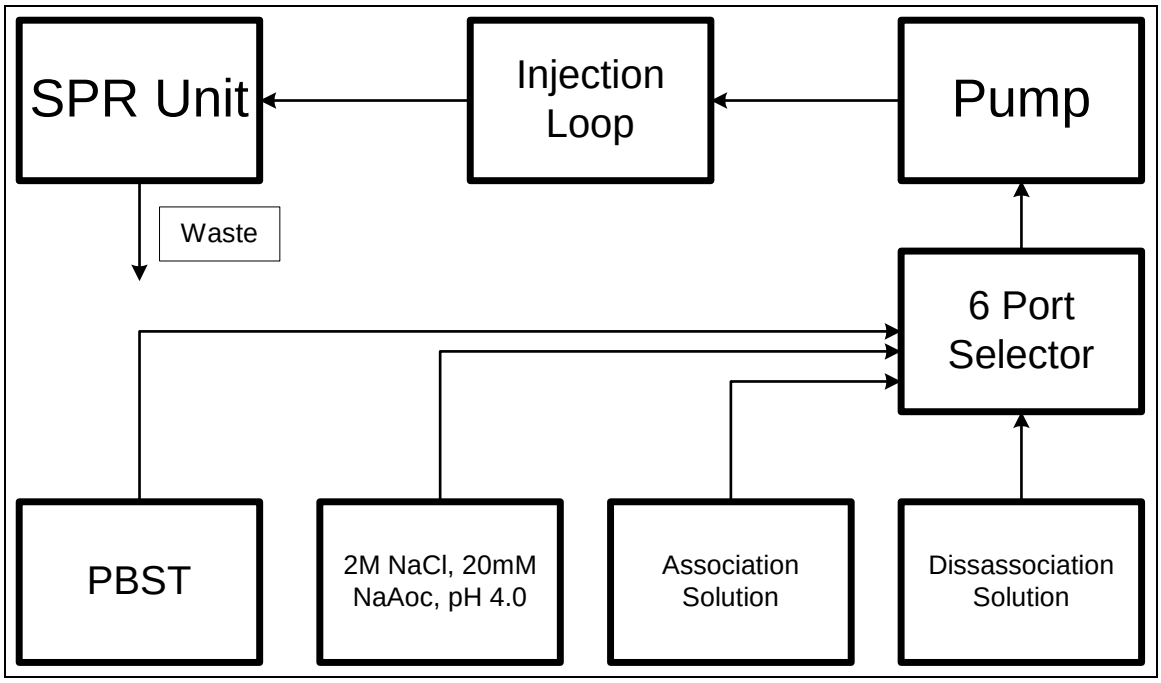

Figure 2.1, Hardware Layout

Figure 2.2, Picture of actual hardware setup depicted in Figure 2.1

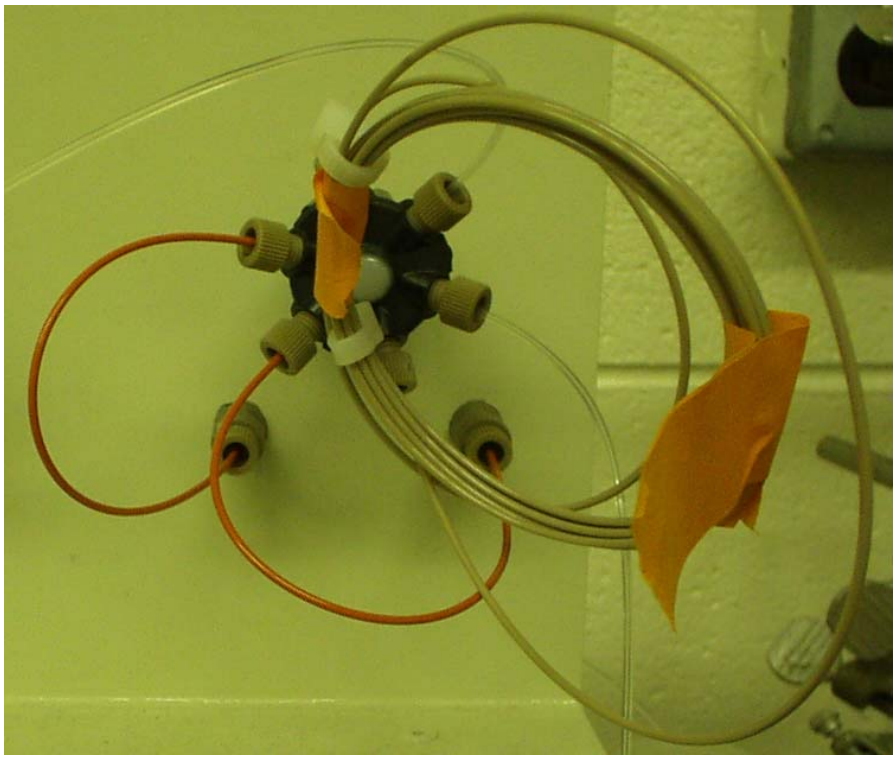

Figure 2.3, Picture of actual 1.0 ml injection loop.

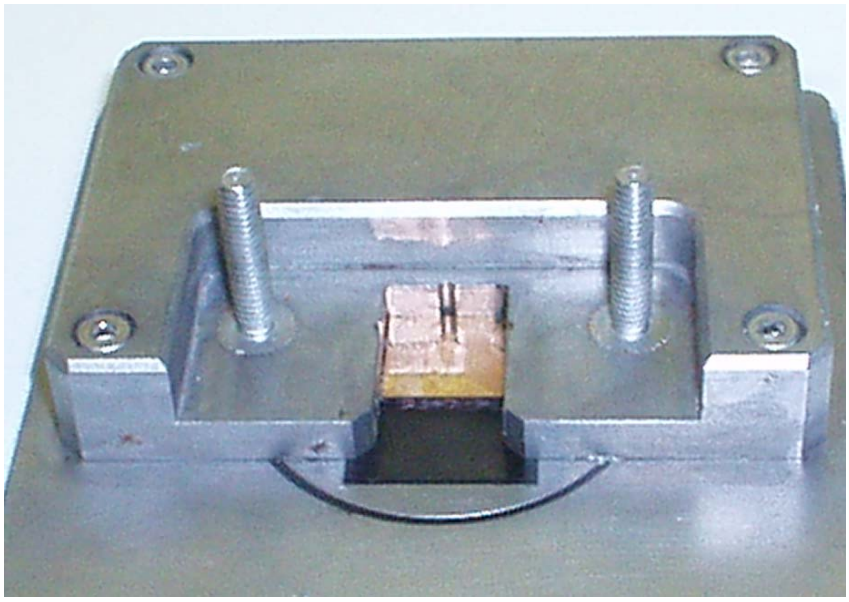

Figure 2.4, Picture of chip mounted on SPR stage.

Chip Mounting

A mixed self-assembled monomer (mSAM) chip (Toronto Research Chemicals Inc., North York, ON, Canada) was mounted to the Reichert Surface Plasma Resonance unit as shown in Figure 2.4. The chips consist of a 12.5 mm x 12.5 mm x 0.9 mm thick glass slide with one side that has been coated with 50 nm of gold. Attached to this gold layer is a mixed monolayer of 10% 23-(9-mercaptononyl)-3,6,9,12,15,18,21-heptaoxatricosanoic acid and 90% 1-(9-mercaptononyl)-3,6,9-trioxaundecan-11-ol (Figure 2.5). These chips were produced as described in Lahiri et al (1999).

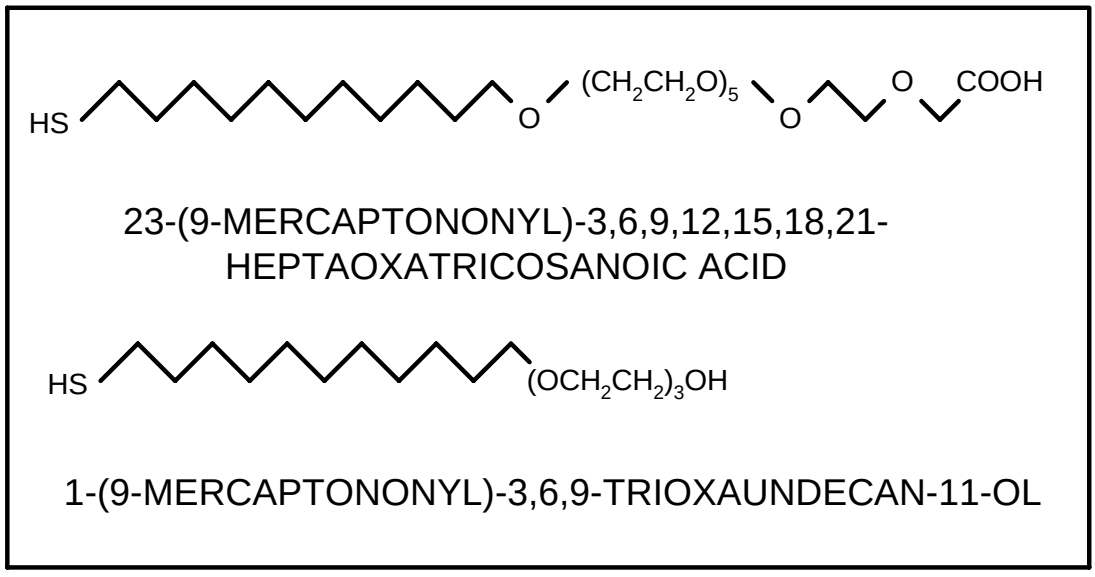

Figure 2.5, Illustrations of the components in the mSAM chip surface.

Prior to mounting the chip, the glass stage and surrounding area were cleaned twice with a cotton swap dipped in HPLC grade 99.9+% acetone (Burdick & Jackson, Muskegon, MI). Next, the glass stage and the plastic cover were wiped down with a kimwipe dipped in HPLC grade 99.9+ % acetone. After allowing any remaining acetone to evaporate, 2µl of immersion oil (Cargill Laboratories (Cedar Grove NJ), type A

refractive index 1.515) was placed on the center of the glass stage where the chip will be positioned. Then the chip was placed, glass side down, on the stage. Finally, the plastic cover with rubber o-ring in place was lowered into position and the retaining nuts tightened down by hand.

Initialization

The SPR unit was turned on and allowed it to warm up for 30 minutes with ultra pure water flowing through it. The instrument was then initialized and calibrated as instructed in the Reichert manual. At this point the unit is ready to collect data. A shadow line was collected to ensure the chip and coupling of the slide to the prism are of sufficient quality to allow high-quality data readings.

The shadowline is a graph of light intensity versus angle. When the machine is operating properly and the chip has been properly coupled to the prism, two narrow minimums will be observed. These minimums are angles at which the internal resonance occurs and allow measurement of surface binding. Runs where the machine was not functioning properly were marked by two shallow minimums. Runs that showed proper sensitivity and low system noise had two distinct minimums with a difference in excess of 8,000 units from the maximum to the minimum.

Streptavidin Binding

The binding of streptavidin (Calbiochem, La Jolla, CA, Cat# 189730, Lot# D24453) to the mSAM chip surface was completed through several steps each utilizing the 1.0 ml injection loop. A flow rate of 0.086 ml/min was utilized for each of these steps. First, the chip surface was activated using a solution of 0.2 M 1-Ethyl-3-(3-dimethylaminopropyl) carbodiimide HCl (EDC)(Pierce, Rockford, IL) and 0.05 M N-

hydroxysuccinimide (NHS)(Aldrich Chemical, St. Louis, MO) passed over the chip for 10 minutes. The EDC/NHS solution was made immediately before its use to ensure complete activation of the chip surface. The activation allows the binding of proteins to the chip surface using the amine chemistry presented in Chapter 1. Then the streptavidin was bound to the chip surface by passing a solution of 30 μg/ml streptavidin, 20 mM sodium acetate, pH 5.2, over the chip for 13 minutes. The chip was then deactivated by passing 1.0 M ethanolamine (Sigma, St. Louis, MO), pH 8.5, over the chip for 10 minutes. Ultra pure water was flowed over the chip between steps to allow the chip to reach a steady state baseline after each step and to act as a wash prior to inject of the next solution. An example activation and coupling of the streptavidin is shown in Figure 2.6. PBST was run at the start and end of the streptavidin association to provide a reference and allow quantification of the amount of streptavidin bound to the surface. The PBST solution is supposed to replicate the extracellular conditions found in the body where FGF-2-heparin interactions normally occur. Figure 2.5 shows a gain in baseline of 7.88 pixels from before (725.97 pixels) the association to after (733.85 pixels). This corresponds with the binding of 4.8 μg of streptavidin to the chips surface giving a surface density of 547 pg/mm^2.

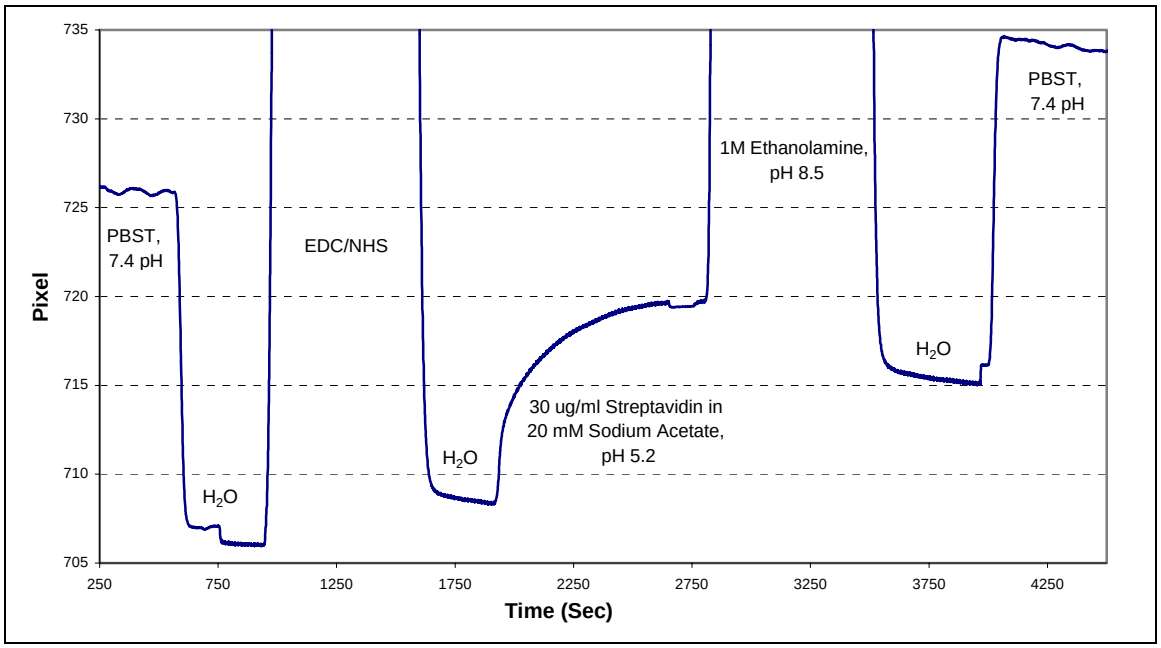

Figure 2.6, Sample Streptavidin Association

Biotinylated Heparin – Cleaning & Coupling

Early attempts to bind biotin labeled heparin to the surface showed insufficient binding as discussed in Chapter 3. Briefly, during the heparin association phase, essentially no increase in pixels was evident indicating a negligible level of heparin binding. This lack of bound heparin became apparent by the low amount of detected FGF-2 binding during protein associations. The lack of bound heparin was determined to be caused by free biotin in the biotin labeled heparin solution. Removal of the free biotin with a desalting column (Pharmacia Biotech, Uppsala Sweden), allowed more biotin labeled heparin to bind the surface and helped produce a sufficient level of FGF-2 binding for data analysis.

Briefly, a PD-10 Sephadex G-25 M desalting column (Pharmacia Biotech, Uppsala, Sweden) was utilized to remove free biotin from the concentrated biotinylated heparin (Calbiochem, La Jolla, CA, Cat# 375754, Lot# B48469). The column was equilibrated with 25 ml of phosphate buffered saline with Tween 20 (PBST) (Sigma, St.

Louis, MO, P-3563), at pH 7.4. The PBST was prepared by combining ultra pure water and dry powered concentrate to make a solution that was then filtered, degassed, and titrated to pH 7.4. Then 2.5 ml of PBST containing 410 ug of biotinylated heparin was added to the top of the column and the resulting 2.5 ml flow-thru discarded. Finally 3.5 ml of PBST was added to the column and the flow thru collected.

DMB Assay

To accurately determine the recovery of the biotinylated heparin from the desalting procedure a proteoglycan assay utilizing 1,9, dimethylmethylene blue (Aldrich Chemical, St. Louis, MO) was used as described by Forsten, Courant, and Nugent (1997). A 500 ml solution was generated with nearly 500 ml ultra pure H_2O (400 ml initially and filled to 500 ml after the other chemicals were added), 0.47 ml 36-38% concentrate HCL (EM Science, Gibbstown, NJ), 1.185g NaCl (Fischer Scientific, Pittsburgh, PA), 1.520g glycine (Bio-Rad Laboratories, Hercules, CA), and 0.008 dimethyl methylene blue (Aldrich Chemical, St. Louis, MO), and was prepared and stored in an opaque bottle. Samples of heparin in PBST (50 μl total volume) were mixed with 1 ml of the DMB solution. The absorbance of the solution at 525 nm was measured after zeroing the spectrometer (Spectronic Genesys 5) to 1 ml DMB solution and 50 μl PBST. Plastic disposable cuvettes (Fisher Scientific, Pittsburgh, PA) were used for all samples. A standard curve was developed for 0.1 μg to 5 μg of heparin (Celsus Laboratories, Cincinnati, OH, porcine intestinal mucosa, Cat # 03003, Lot # 39899) to compare with biotinylated heparin. Desalted and unprocessed biotinylated heparin solutions were compared using the standard curve and there was an average recovery of 92% +/- 0.7 %

was determined based on 3 separate desalting with triplicate testing of the pre and post purification solution.

The collected flow-thru from the desalting column (3.5ml) was at a concentration of 120ug /ml, assuming 92% recovery, and was used as is for the biotin heparin association. To minimize the loss of purified biotinylated heparin volume for association with the surface, we tested the recovery of heparin from the desalting procedure by testing and desalting samples not destined to be used for heparin association. The three purifications showed little variance in their performance, so testing every purified sample was not implemented.

Following free biotin removal from the biotinylated heparin, PBST was pumped over the streptavidin bound chip until a stable baseline was reached, generally in less than 2 minutes. Desalted biotin labeled heparin (120μg/ml) was then circulated over the surface at a flow rate of 0.128 ml/minute. A higher flow rate then the streptavidin association was utilized for this step because the heparin solution was recycled thus eliminating the problem of limited material. After 1 minute of heparin association, the exit line was recycled into the heparin stock container so sufficient quantity was available without having to use large quantities of material. The assumption was that the chip coupling did not significantly deplete the heparin stock such that significant amounts of heparin were still available for coupling. The initial association was performed for 100 minutes. In many of the described studies subsequent biotin labeled heparin associations were done before every heparin binding protein association run and were performed for 20 minutes using the same solution from the initial coupling.

Protein Association

FGF-2 (BD Bioscience, San Jose, CA, Cat #35-4060), insulin-line growth factor(IGF-I) (Peprotech, Rocky Hill, NJ, Cat #100-11) and insulin like growth factor binding protein 3 (IGFBP-3) (Protigen, Inc., Sunnyvale, CA) were used in the studies described in this thesis. The association assays were all run at a flow rate of 0.64 ml/min with the exit line recycled 1.4 minutes after the initiation of the association. This flow rate was chosen because it was high enough to avoid mass transfer issue while low enough to avoid serious pump noise problems. The 1.4-minute lag corresponded with the amount of time required for the solution to travel from the start of the association tube to the end of the exit line. Recycling of the protein solution allows the use of a high flow rate and extended association phases without preparing large amounts of protein solution. There may be some dilution of the solution from the formation of surface complexes or non-specific binding, but it is assumed that this will be negligible. The high flow rate is needed to avoid mass transfer limitations affecting the observed rates of binding (Mysaka 1997; Schuck 1997) and the prolonged association phases allow the collection of more data to produce more accurate calculations.

Protein Disassociation

After a 35-minute association period, PBST or PBST and heparin was passed over the chips surface at the same flow rate as the association phase. The use of the selector valve allowed a smooth transition of solutions without introducing air into the system. Heparin at between 0 and 15 μM in PBST, pH 7.4, was utilized for many of the disassociation phase runs. This concentration of heparin was used because it had a strong impact on the disassociation process as discussed in Chapter 4 without causing a

refractive index shift of its own. Concentrations of 1 uM and 5 uM heparin were examined to see the effects varying heparin concentrations on the rate of disassociation.

Surface Regeneration

To regenerate the surface of the chip by disassociating the protein-heparin complexes, a 5-minute wash cycle was used. A solution of 2M NaCl (Fischer Scientific, Pittsburgh, PA), 20 mM sodium acetate (Fischer Scientific, Pittsburgh, PA), pH 4.0, was used for this step. This solution was shown to be most effective at disassociation of FGF-2 from cellular heparan sulfate by Fannon and Nugent (1996) and used with success by Ibrahimi and coworkers (2004) in SPR studies of FGF-2 and heparin.

Chapter 3: Binding heparin to the mSAM chip using the SPR Reichert System.

The Reichert SPR system has not been previously used to analyze the interactions of proteins with heparin bound to the surface of an mSAM chip. A protocol had to be developed and optimized to bind sufficient heparin to the surface for studies. Many problems were encountered and overcome to produce a system that successfully allows for the analysis of protein-heparin binding interactions. The details of binding heparin to the surface will be presented in this chapter.

Instrument Noise & Minimization

The Reichert SPR unit produces a continuous output of data that for these studies was recorded every two seconds. Like all instruments there is some degree of variance and noise in this output. As long as the amplitude of the noise is significantly less than the change in signal produced by protein association or disassociation, proper data analysis of the results can be performed and relevant facts determined. With a properly operating Reichert SR 7000 there is a small amount inherent system noise, but the greatest contributor to system noise is variations solution flow. For optimal data collection, one should attempt to minimize the amount of noise present.

A proper functioning SPR unit is necessary to collect good data. Early in the optimization process, the SPR unit produced an unacceptably low signal to noise ratio. Figure 3.1 illustrates the extent of the system noise of one of the better pre-repair studies with noise that averaged in amplitude 0.17 pixels peak to peak. Figure 3.2 highlights the problem one faces when dealing with a system with a high noise and low signal.

While the data appeared noisy, as evident by the many spikes and oscillations in the data; some specific FGF-2 binding was evident causing us to focus on the low coupling of heparin to the surface as the primary problem. Many months were thus spent attempting to optimize the procedure until the unit was examined by Dr. Thomas Ryan of Reichert and determined to be defective. Reichert repaired the SPR unit in October 2004.

Following these repairs, the baseline noise was significantly reduced (0.028 pixels amplitude with 0.25 Hz) and the signal generated was superior (Figure 3.2). The improvements in binding in Figure 3.2 are the results of the additional steps of purifying the biotinylated heparin and changing the washing procedure between FGF-2 associations, but the critical reduction in system noise is from the repairs made by Reichert.

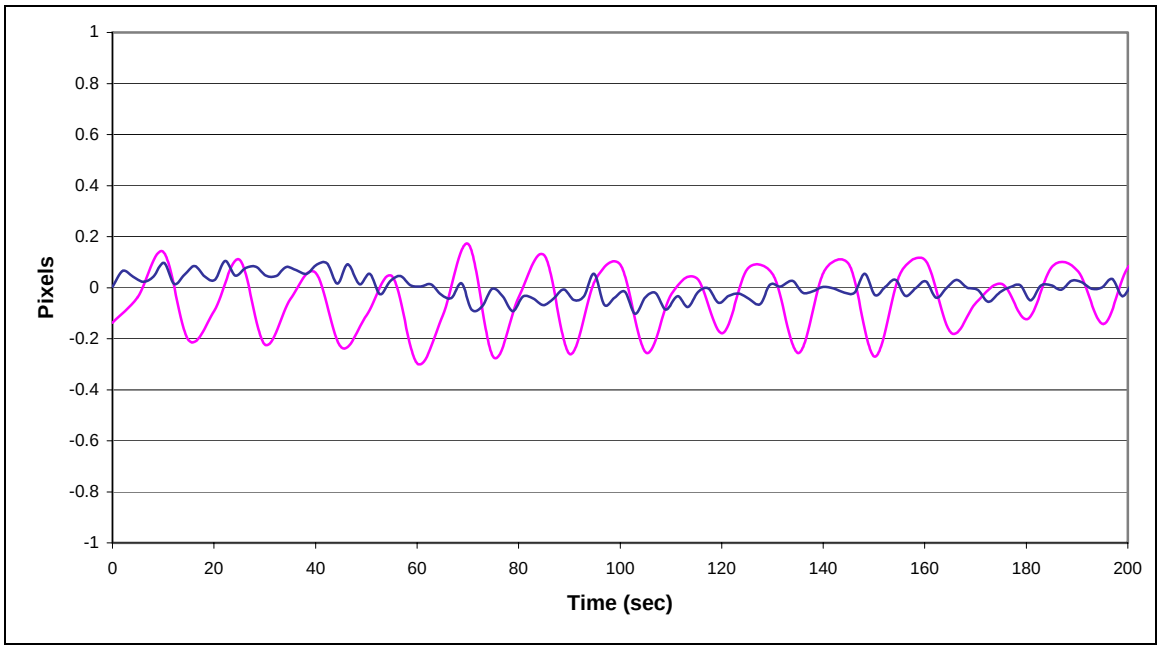

Figure 3.1, Comparison of baseline noise pre and post SPR unit repair. Shown is the signal in pixels from PBST, pH 7.4 pumped through the system at 0.64 ml/min before (pink, October 12, 2004) and after (blue, May 16,2005) system repair.

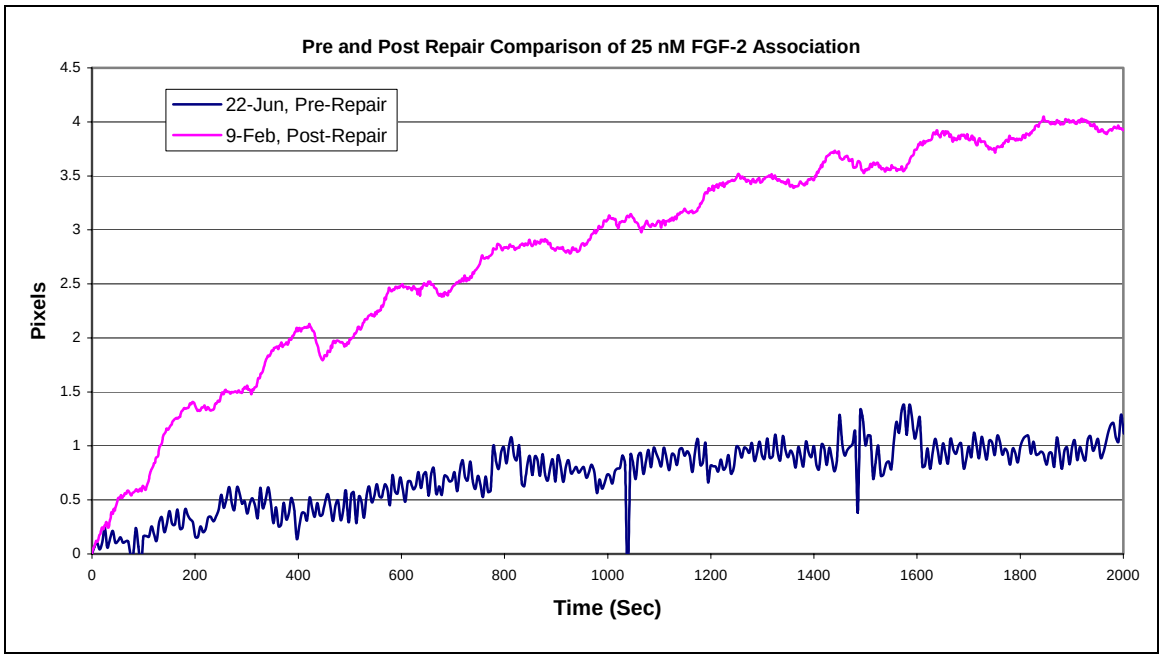

Figure 3.2, Comparison of the association of 25 nM FGF-2 pre and post SPR unit repair. Shown is the signal in pixels from 25 nM FGF-2 in PBST, pH 7.4 pumped through the system at 0.64 ml/min before (pink, June 22, 2004) and after (blue, Feb 9, 2005) system repair. The improvements are the results of optimizations made to the procedure as well as unit repair.

Reichert Inc. reported a defective CCD detector (measures the amount light transmitted by prism), which was replaced; this manifested itself as a low intensity measurement at the receptor was noted. As a result of this issue the unit would increase the intensity of the light source to maximum output in an attempt to compensate for the low readings. This phenomenon was evident in the shadowline (Figure 3.3). An ideal shadowline will have 2 clearly defined narrow minimums with a large absolute difference between the maximum and minimum. While there is no required difference, a larger absolute difference should produce better results due to the absolute difference is a component of how the instrument calculates the angle of resonance (Dr. R. Dessy, personal communication). Our results support the conclusion of a larger absolute

difference being a benefit to the collection of good data. After Reichert repaired the unit, the unit functioned flawlessly. A procedure to collect and analyze the shadowline at the beginning of every run was implemented to ensure a properly functioning machine for all runs.

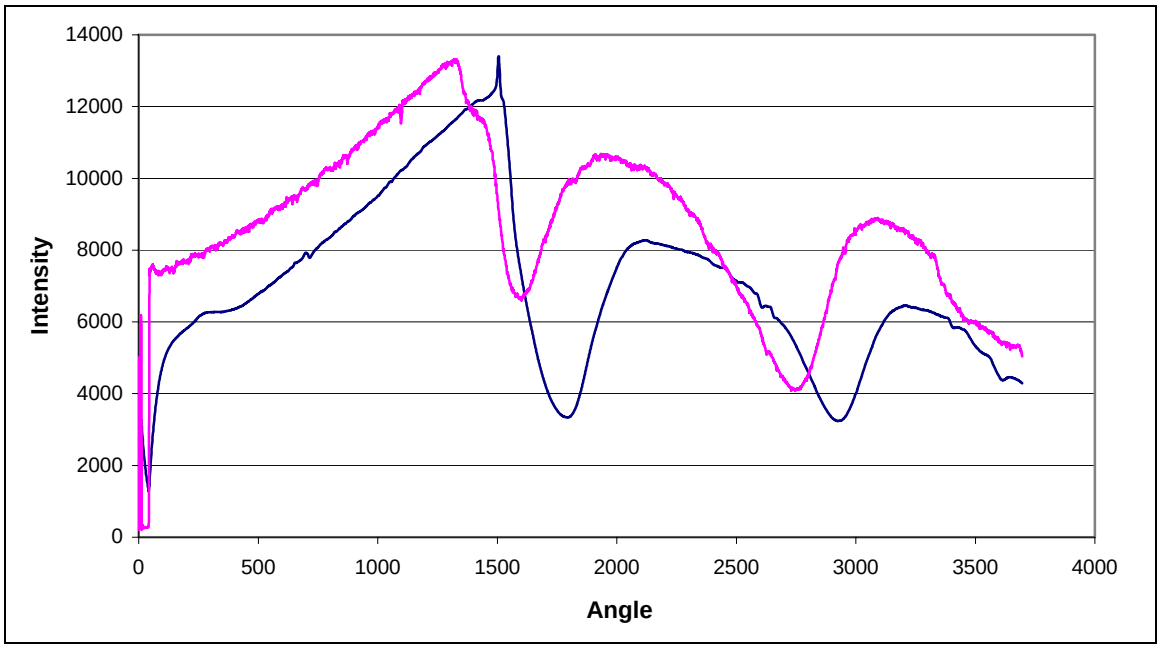

Figure 3.3, Shadowline comparisons between the SPR systems before (pink line, October 12, 2004) and after (blue line, March 16, 2005) the unit was repaired. Note the significant difference between the maximum and minimum for the first dip. The repairs improved the maximal difference from nearly 6500 to almost 9800.

System Configuration

The configuration of the pump and tubing is of significant importance in obtaining quality data. In order to avoid mass transport limitations, a high flow rate of 0.64 ml/min was selected. The use of 0.01" I.D. tubing at such a high flow rate results in the formation of a very low pressure to form on the suction side of the pump. The pressure on the suction was low enough to pull air thru the compression fittings even

when properly assembled. The bubbles of air that formed in the solution had a significantly different refractive index and their presence in the flow chamber extreme amounts of noise to be reported by the system. Installing 0.02" I.D. tubing, to allow the needed flow rate without the pressure drop and introduction of air into the system, was done and the system performance improved.

One of the largest contributors to system noise is the peristaltic pump. It produces a semi-periodic oscillation that is readily apparent in the collected data. This pulsatile variation is caused by the slight changes in flow that occur as the pump functions by compressing the flexible tubing to push the fluid forward. Other pump types were considered, such as a syringe pump, but given the needed flow rate, need to recycle the waste flow, and desire to maintain a clean system; a peristaltic pump best fit our needs.

To produce the lowest amount of pump noise, the pump was set to flow at the desired rate and the tension in the pump head was then adjusted to give the lowest amount of noise. This was repeated until the desired flow rate and a low noise were achieved. We noted that very small adjustments to the tension produced significant changes in the amount of noise present.

Coupling of Streptavidin to mSAM

Amine chemistry was used to couple streptavidin to the surface of an mSAM chip. Several steps were involved in the process, including a baseline measurement of PBST, pH 7.4, shown in Figure 3.4. This served as a reference mark for comparisons to PBST, pH 7.4, post streptavidin coupling to allow determination of how much streptavidin was bound to the surface. A wash with ultra-pure water followed because it

does not contain anything that could interact with the surface and could remove any residual material from the PBST.

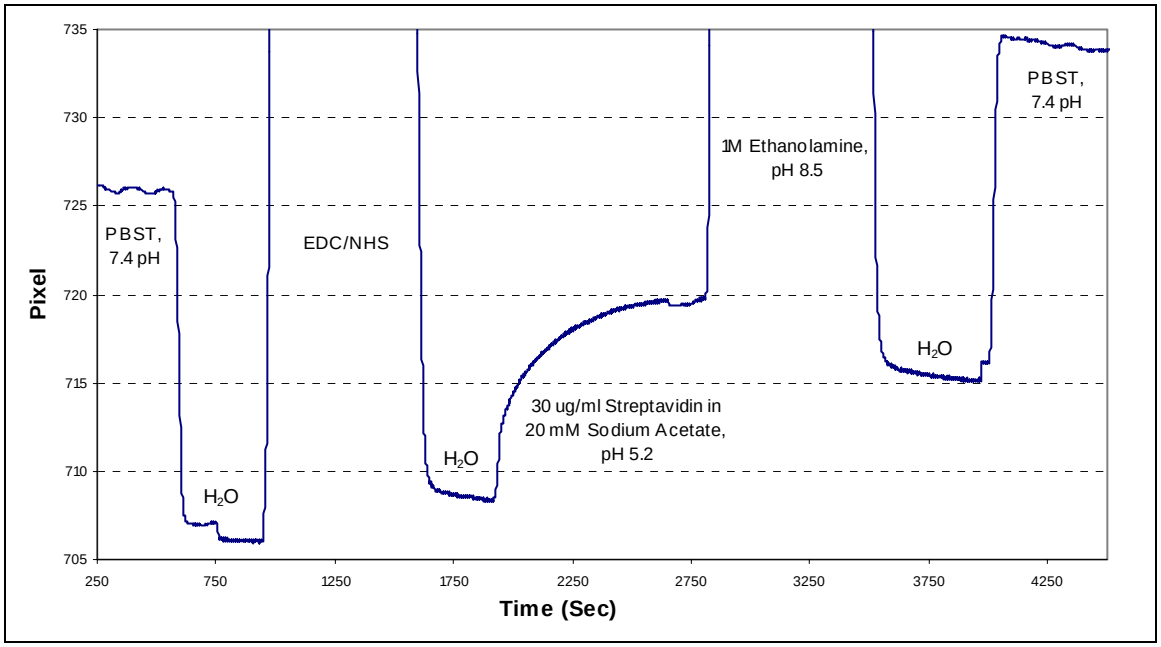

Figure 3.4, Binding of streptavidin to the surface of an mSAM chip using amine chemistry.

To properly activate the chip a solution of EDC and NHS was passed over the chip. This solution must be made fresh for complete activation. This essential fact is not mentioned in many procedures that utilize amine coupling. The use of solutions that are a few hours old may not work as intended. Figure 3.5 shows a streptavidin association that failed because the surface did not activate. Note the drop in baseline after the EDC/NHS step instead of the expected two-pixel rise.

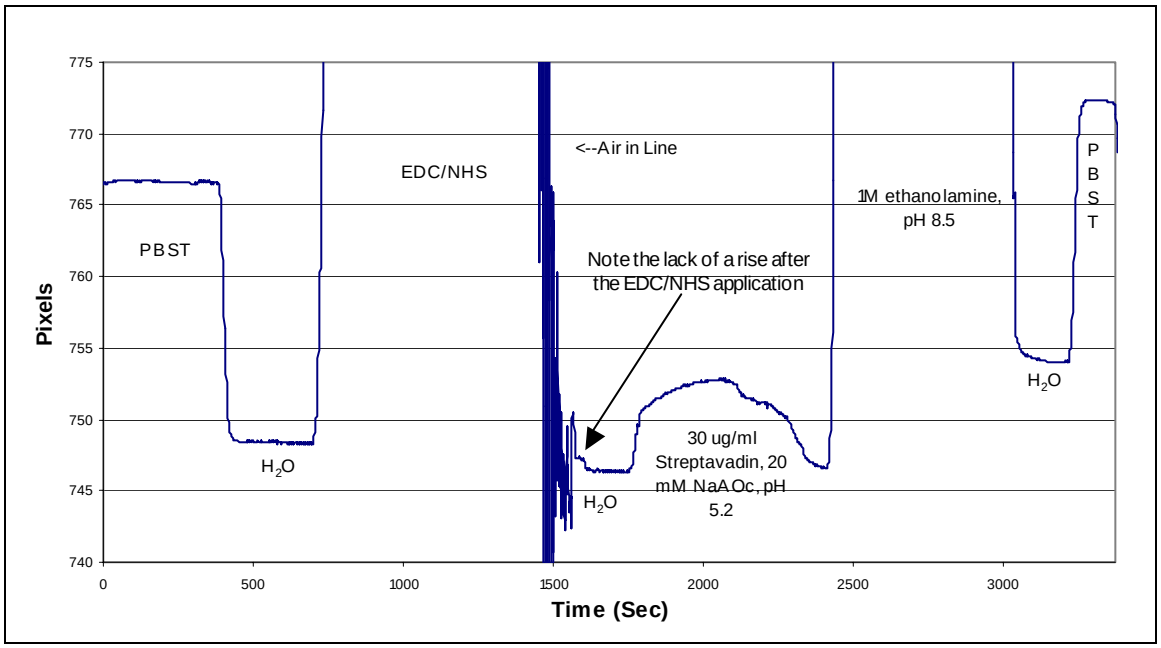

Figure 3.5, Failed Binding of streptavidin to mSAM chip. Note the lack of a pixel rise after the EDC/NHS association. This indicates that reactive NHS esters were not formed on the surface.

For the remainder of the studies the EDC/NHS solution was made up immediately before its use to ensure proper activation. The significant index shift that occurs at 650 seconds is due to the differences in refractive index of ultra-pure water and PBST. The slight shift at 760 seconds is from the decrease in flow rate to 0.068 ml/min from 0.64 ml/min. EDC/NHS was then passed over the surface and results in a large change in pixels due to the large refractive index change of the solution. What should be noted is the difference in index after the EDC/NHS. This two-pixel rise is the result of the formation of reactive NHS esters on the surface that will allow the binding of streptavidin to the surface. Buffered streptavidin at pH 5.2 was then passed over the surface and bound to the surface as evident by the rise from 1900 seconds to 2800 seconds. This replaces the reactive NHS esters with amine compounds. After streptavidin was bound to the surface,

ethanolamine, pH 8.5 was passed over the surface to remove any remaining reactive NHS esters to prevent the surface binding of proteins during future associations runs. Ethanolamine is a small amine containing molecule. Its passage at high concentrations results in the removal of reactive NHS esters and the coupling of the small molecule. No significant pixel changes are noted because of the small size of ethanolamine. At this point the surface was ready for the association of biotinylated heparin.

Biotinylated Heparin Binding

There are limited amounts of streptavidin that can be bound to the mSAM chip surface. This is due primarily to the surface chemistry design of the chip where only a small fraction, 10%, is capable of being activated for coupling. This is desirable in order to maintain a low surface density to try to minimize the effects of mass transport limitations and ligand rebinding.

Desalted Biotinylated heparin

Minimal heparin binding was associated with our initial runs despite heparin association run times of 100 minutes. Figure 3.6 shows the binding of 1.2 pixels of biotinylated heparin to the surface and the wash cycle that reduced it to 0.86 pixels. This corresponds with a surface density of 56.8 pg/mm^2. This technique of associating desalted biotinylated heparin to amine couple streptavidin on mSAM chip created six chips that were used to quantify the interactions of proteins with bound heparin.

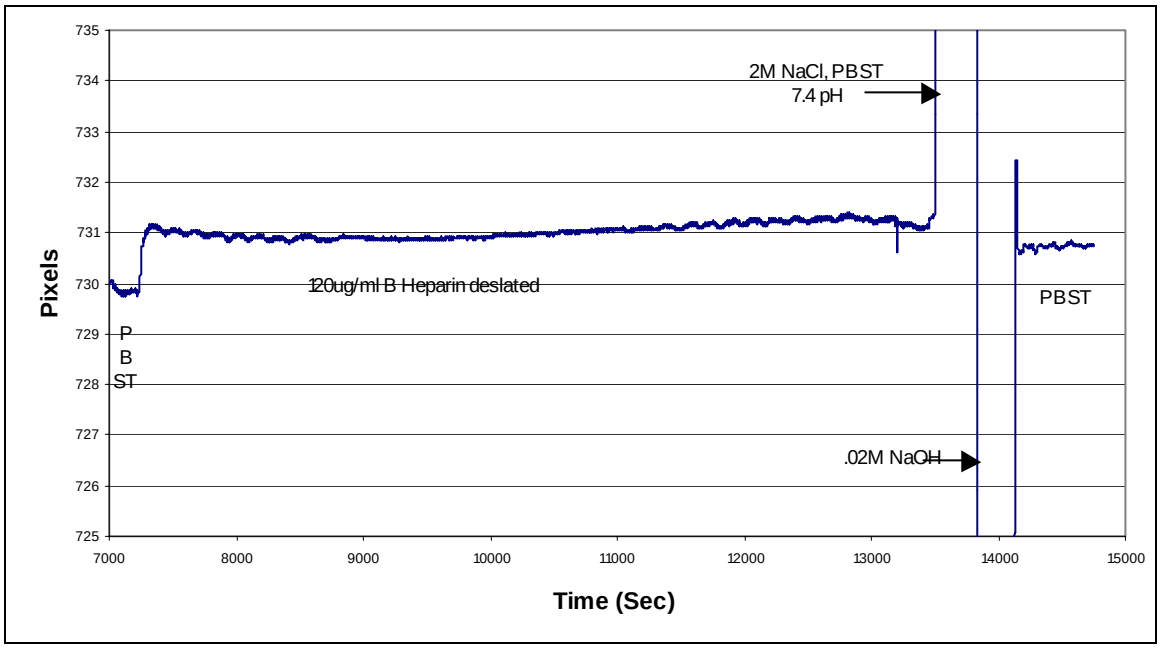

Figure 3.6, Association of desalted biotinylated heparin with amine-coupled streptavidin on a mSAM chip. A 100 minute association produced a 1.2 pixel gain that was reduced to a 0.86 pixel gain by a wash cycle.

Figure 3.2 highlights the effects of machine repairs, but the demonstrated improvements are not simply the result of an instrument repair. Biotinylated heparin (EMD Bioscience) contains free biotin molecules in addition to the biotin-labeled glycosaminoglycan of interest. If not removed, these small molecules will bind to the streptavidin on the chip surface limiting the amount available for binding by biotinylated heparin. Figure 3.7 illustrates this problem with a limited association of only 0.25 pixels when used un-purified biotinylated heparin. The removal of free biotin allows more biotinylated heparin to be bound to the surface and this improvement is seen in the increased binding of FGF-2 to the surface as shown in figure 3.2.

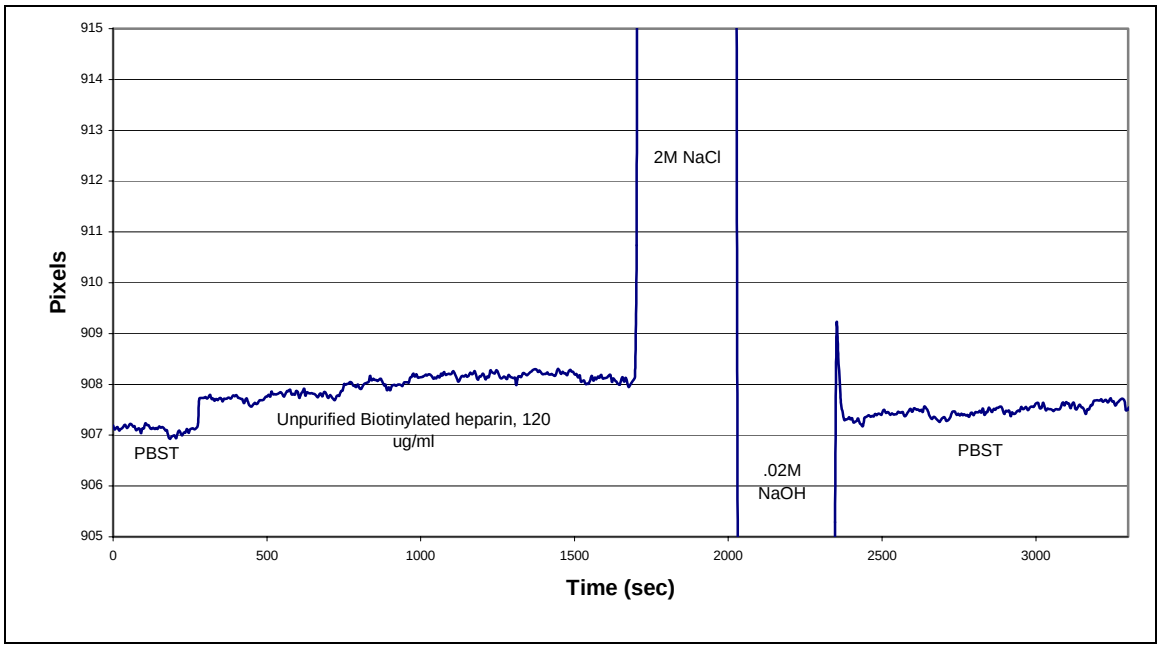

Figure 3.7, Association of unpurified biotinylated heparin with amine-coupled streptavidin on a mSAM chip. A 25 minute second association produced a 1.0 pixel gain that was reduced to a 0.30 pixel gain by a wash cycle.

A desalting column was utilized to remove the free biotin. DMB assays were performed to accurately measure the recovery of purified biotin heparin. Figure 3.8 shows the standard curve that was developed to determine recovery and initial concentration. The addition of this procedure showed a marked increase in the amount of heparin binding to the surface.

In addition to determining the recovery from the desalting procedure, the DMB assay was used to check the presence and concentration of biotin heparin purchased from EMD Bioscience. One of the three 10 mg containers, each from different lots, purchased form EMD bioscience did not contain any glycosaminoglycan (GAG) as the DMB signal was equivalent to PBST alone. This problem initially became apparent during a run when no FGF-2 bound a chip surface after what was believed to be a biotinylated heparin

association. The lack of GAG was then confirmed using a DMB assay. Subsequent vials were tested to confirm the presence and concentration of biotin heparin.

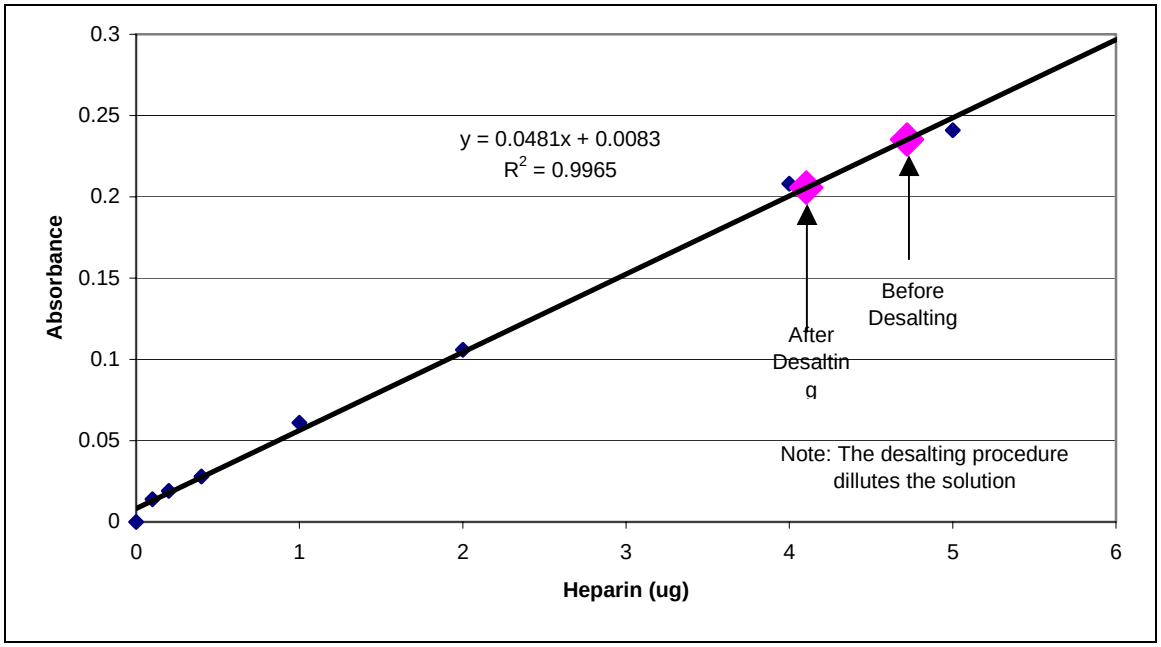

Figure 3.8, Heparin absorbance standard curve

Chapter 3 Conclusions

Chapter 3 presented the steps and optimization need to produce a mSAM chip with surface bound heparin to quantify the interactions of proteins requires. A properly operating Reichert SPR instrument with optimized hardware configuration allows for the accurate detection of molecular interactions with low system noise. The removal of free biotin from the biotinylated heparin is an important part of producing a surface with sufficient density for analysis. The production of this surface relies on proper execution of several steps to bind heparin to the surface.

Chapter 4: Interactions of FGF-2 & Heparin

The interactions of heparin coupled to SPR chips via streptavidin-biotin binding with FGF-2 in solution are measured and quantified in this chapter. The purpose was to determine:

(1) whether the Reichert system could be used to analyze FGF-2-heparin binding,

(2) whether a simple model would fit the data,

(3) values for the binding constants that describe the interactions, and

(4) whether rebinding, an issue found with many growth factor SPR studies, is an issue with this system and if soluble inhibitors can be used

No previous studies that examined FGF-2 and heparin have utilized the Reichert SPR system or the mSAM chip.

Non-Specific Surface Interactions

One of the often-mentioned advantages of the mSAM chip and streptavidin is their resistance to non-specific binding which should facilitate the collection of specific data at lower concentrations. A lack of non-specific binding was verified by passed 37.5 nM FGF-2 in PBST, 7.4 pH, over an mSAM chip that had been successfully coupled with streptavidin by amine chemistry (Figure 4.1). No change in refractive index or binding was noted. The lack of binding was not the result of a bad chip or solutions.

After FGF-2 showed no interaction with a streptavidin covered mSAM chip, Low molecular weight (LMW) biotinylated heparin (Celsus, Cincinnati OH)was passed over the surface. A solution of 37.5 nM FGF-2 in PBST, 7.4 pH, was then successfully associated with the now heparin covered surface (Figure 4.2). LMW biotinylated heparin was utilized because the biotinylated heparin (Calbiochem) that was normally used was

tested with a DMB assay and found to contain no heparin. The use of LMW heparin does not change validity of the observed lack of non-specific binding. This lack of interaction simplified the data analysis because it allow us to assume all observed index shifts were the results of protein interacting with the bound heparin.

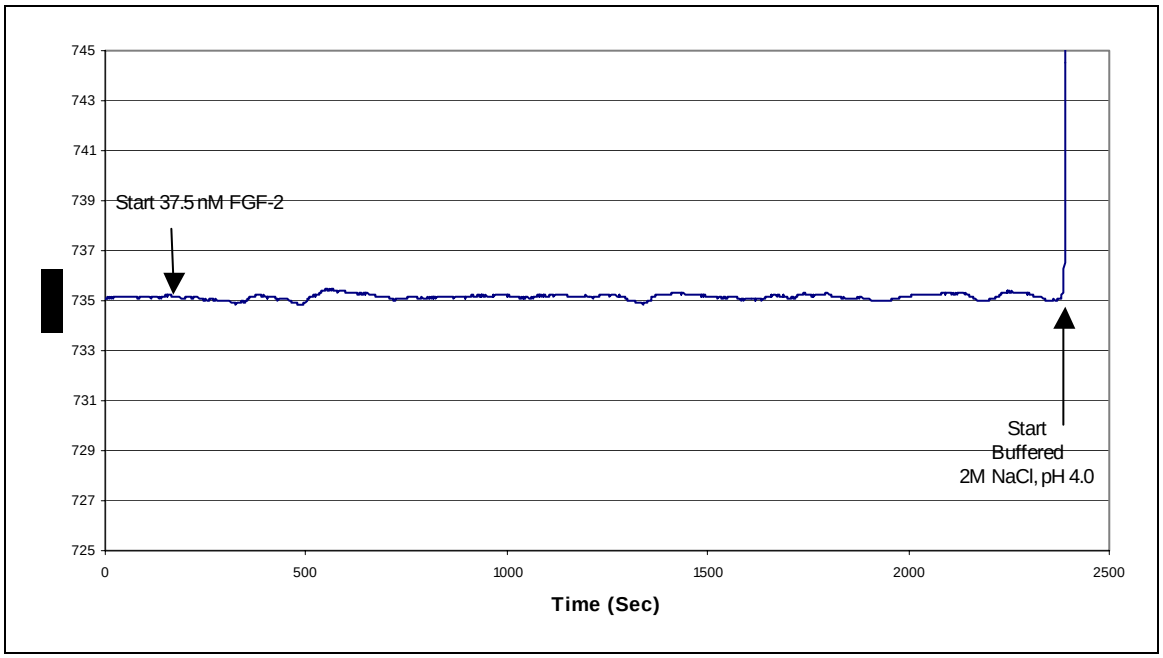

Figure 4.1, Association of FGF-2 with a mSAM chip with only streptavidin coupled to the surface. Note the lack of binding. This is representative of 5 runs on 3 chips.

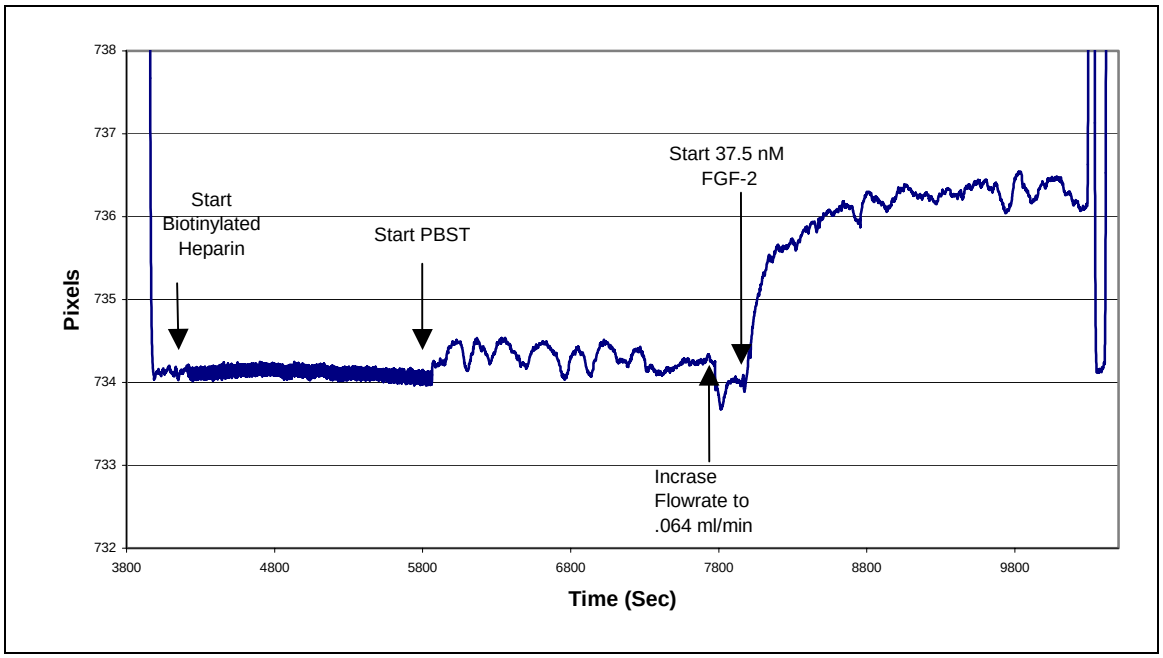

Figure 4.2, 35 minute association of LMW biotinylated heparin with a streptavidin covered mSAM chip. Followed by PBST to wash, then FGF-2 (37.5 nM)

Specific Binding of FGF-2 with Heparin

Obtaining good data for the association of FGF-2 and heparin requires a properly operating and instrument with a chip with sufficient heparin bound to it. Unfortunately, several of our early runs were performed on an improperly operating SPR unit using unpurified heparin. Figure 4.3 shows the 0.25 pixel association that was obtained when using a procedure that utilized unpurified biotinylated heparin and a SPR unit that was not properly functioning. This data was worthless for analysis, but it show that binding was possible.

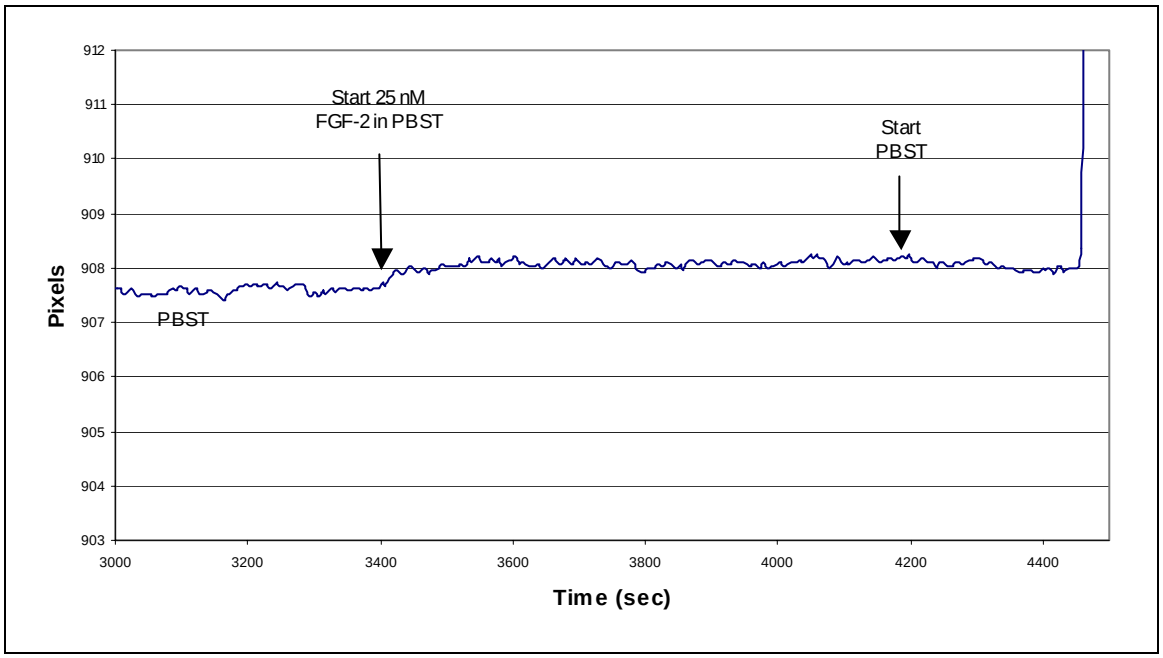

Figure 4,3, Shows a 25 nM FGF-2 association after an unpurified biotinylated heparin association using a unit that was not properly functioning. Note the rise of only a 0.25 pixel during the association. This figure is representative of 16 FGF-2 (25 nM) associations on 6 chips.

After the SPR unit was repaired and desalted biotinylated heparin was used, the quality of the data improved drastically. With the proper procedure, like in Figure 4.4, even a 20 nM solution can display 5.2 pixels of association

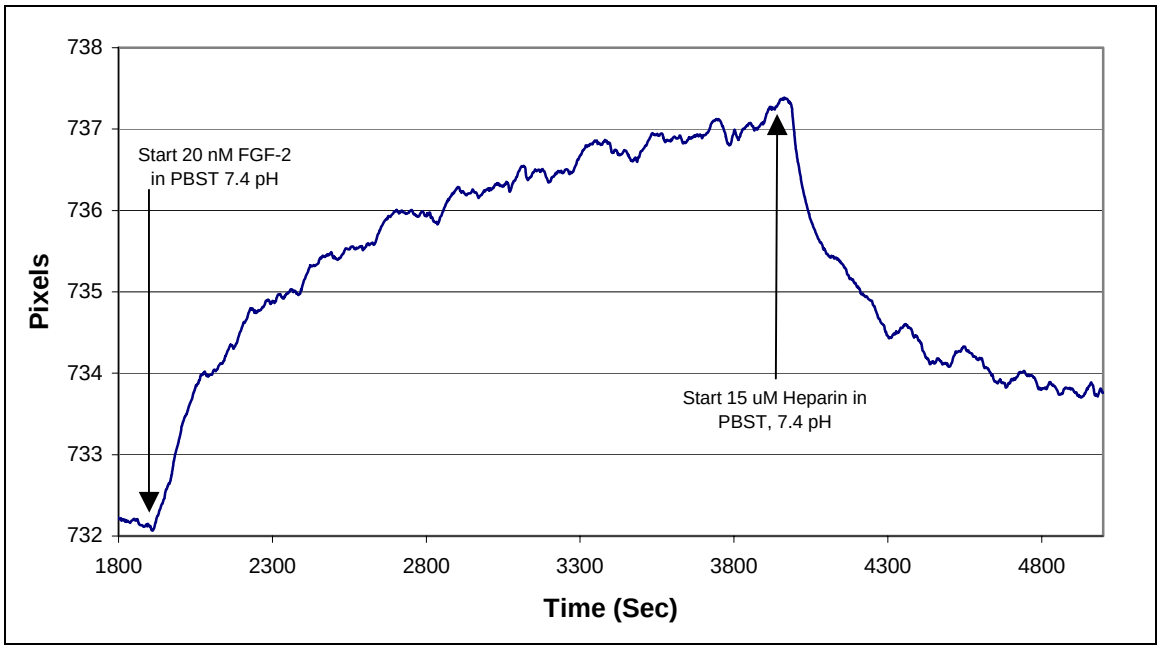

Figure 4.4, 20 nM FGF-2 association after a desalted biotinylated heparin association using a properly functioning SPR unit. Note the 5.2 pixel rise from only a 20nM FGF-2 solution. This figure is representative of 25 FGF-2 associations (2 specifically at 20nM) on 4 chips.

To validate that this interaction was specific, we passed IGF-I, a non-heparin binding protein, over the chip. No binding of IGF-I was noted (Figure 4.5). This suggests the only binding that occurs is to the surface bound heparin

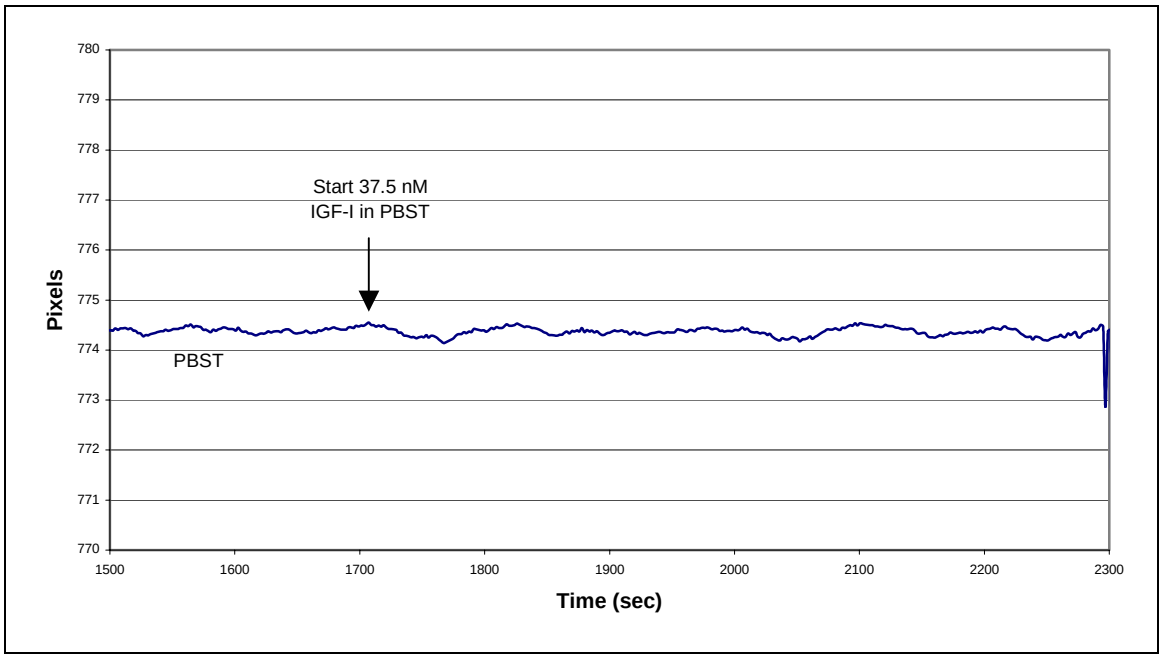

Figure 4.5, 37.5 nM IGF-I2 association after a purified biotinylated heparin association using a properly functioning SPR unit. Note the complete lack of a pixel change. This figure is representative of 5 runs on 3 chips

While the detection of specific binding of FGF-2 with heparin was positive, we noted that the binding was not consistent with multiple runs Figure 4.6 and Figure 4.7 illustrates the differences in binding seen with consecutive runs despite using identical procedures. In Figure 4.6, the first 37.5 nM FGF-2 association shows 6.05 pixels of binding and the second identical associations shows 10.21 pixels when the same procedure is utilized with heparin refreshing between associations. While Figure 4.7 shows how the extent of binding can vary when the heparin is not refreshed between runs. Of interest is the first association, 25 nM FGF-2, that exhibited 0.965 pixels of binding and the third association, also 25 nM FGF-2, that exhibited 0.682 pixels of binding.

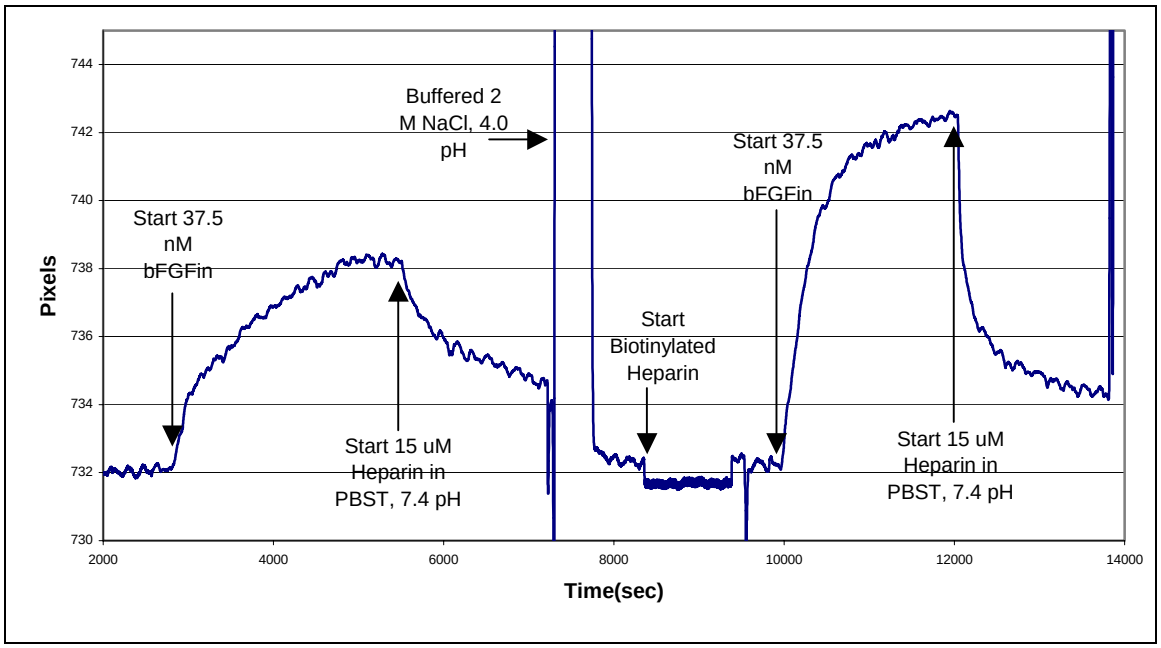

Figure 4.6, Two consecutive 37.5 nM FGF-2 associations to a heparin covered mSAM chip using identical procedures. While not shown, a 20 minute biotinylated heparin association occurred immediately before the first shown association. This figure is representative of over 20 associations (10 specifically of 37.5 nM) on 4 chips. Note, the first shown association shows 6.05 pixels of binding and the second shows 10.21 pixels.

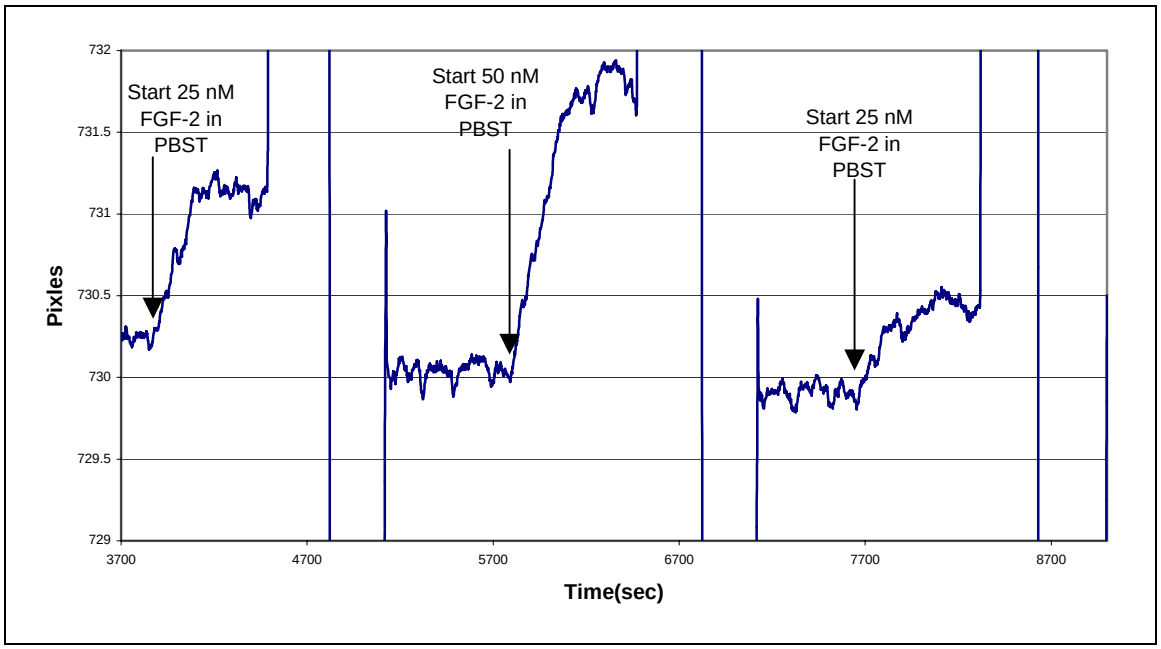

Figure 4.7, Consecutive FGF-2 associations without a biotinylated heparin re-association between runs. Note the reduction of binding that occurs between runs one and three despite the same procedure. Association 1 has 0.965 pixels of binding, association 2 has1.81 pixel of binding, and association 3 has 0.682 pixels of binding. This figure is representative of 3 associations on 2 chips.

Surface Changes

Ideally when one regenerates a mSAM chip's surfaces between protein bindings it will return to its original conditions exactly. Unfortunately some of the proteins used for analysis may remain bound to the surface despite washing and some heparin bound to streptavidin may wash off. Another possible effect of the wash cycle is a denaturing of the surface compounds. This can be permanent or temporary, but it may change the binding characteristics of the surface.

In the early runs, only one initial 100-minute biotin heparin association was performed. The FGF-2 associations showed a limited amount of binding that worsened

with subsequent runs (Figure 4.7). For example in Figure 4.7, the initial 25 nM FGF-2 association for 400 seconds led to a 0.965 pixel rise while a subsequent challenge with 25 nM FGF-2 led only to a 0.682 pixel rise. This indicated a loss of available biotin heparin on the surface. To combat this, 20 minutes refreshing of the surface with desalted biotinylated heparin followed by a wash cycle was implemented. To further reduce the amount of biotin heparin that was washed off or denatured, the wash cycle after the biotinylated heparin refreshing was eliminated. This significantly improved the extent of observed binding.

Figure 4.8 illustrates that importance of removing this wash cycle. Run1 occurs after the 100-minute biotin heparin association. Run-2 shows the marked improvement that an unwashed biotin heparin refreshing produces. Run-3 illustrates the effects of a 2.0 M sodium chloride, 20 mM sodium acetate wash cycle at pH 4.0. This wash cycles greatly stunts the amount of binding. However, run-4 shows that the improvements provided by the biotin heparin refreshing continue for multiple associations.

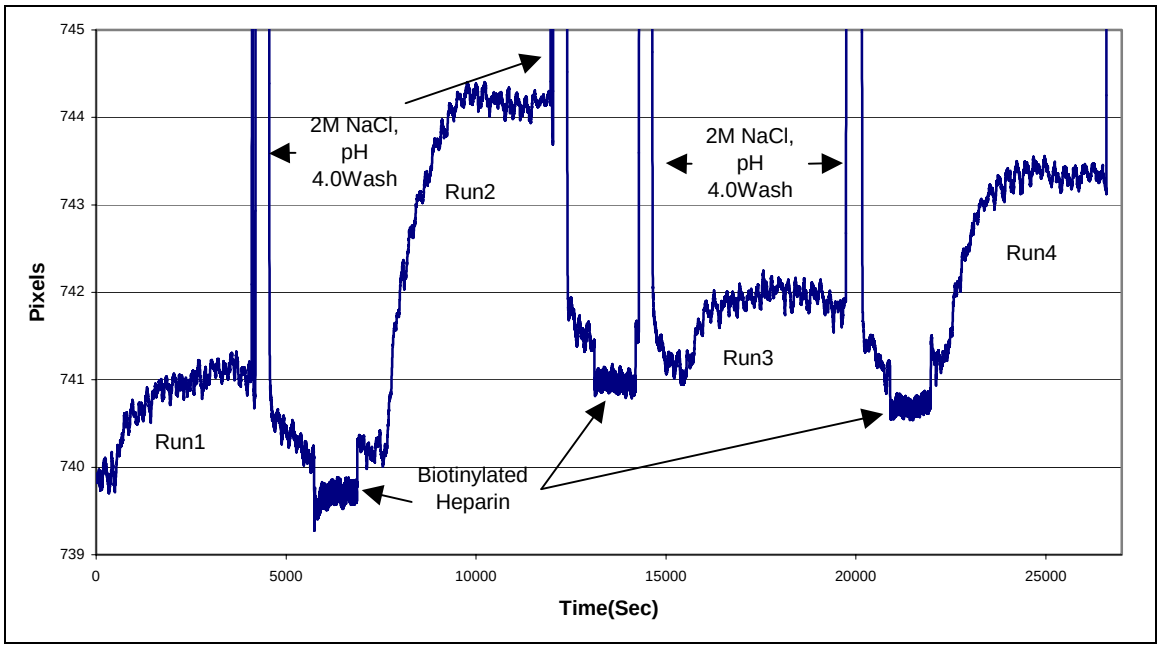

Figure 4.8, Benefits of unwashed biotinylated heparin refreshing. Despite using 37.5 nM FGF-2 for each association there are varying amounts of binding depending on the chip surface condition. A wash cycle after the heparin refreshing severely retards the amount of FGF-2 that can bind to the surface. Run1 exhibits 1.256 pixels of association, run 2 has 4.056 pixels, run 3 has 0.809 pixels, and run 4 has 2.191 pixels. This scenario that highlights the importance of heparin refreshing was completed 2 times on 2 different chips.

Washing the mSAM chip with 2.0 M NaCl, 20 mM sodium acetate at pH 4.0 has been reported to remove all of the heparin binding protein from the surface (Ibrahimi et al., 2004). Unfortunately, this does not occur in our system and as more associations are performed more and more protein builds up on the chip. This is seen as an increase in the pixel that the system baselines at. This buildup can even be seen in Figure 4.8 after only 4 runs. The initial baseline for this particular chip was at 739.9 pixels and the subsequent runs were at 740.2, 741.2, and 741.2 pixels. Initially the rate of buildup is small and does not affect the binding kinetics or amount of surface binding. As more and more

associations are performed though the amount of surface build up increases as well as the rate of accumulation. Eventually the surface kinetics and amount of binding during association are compromised and the chip is no longer suitable for further data collection.

Despite this buildup, good data can be collected and analyzed. Normalization of the data shows that while the amount bound by the surface varies, the kinetics do not. Figure 4.9a and 4.9b show how normalizing can correct for the variations in amounts of surface binding. The 3 associations (50 nM, 37.5 nM, 37.5 nM) show different amounts of binding, 13.1, 8.41, and 7.4 pixels respectively, but the normalized data looks amazingly similar.

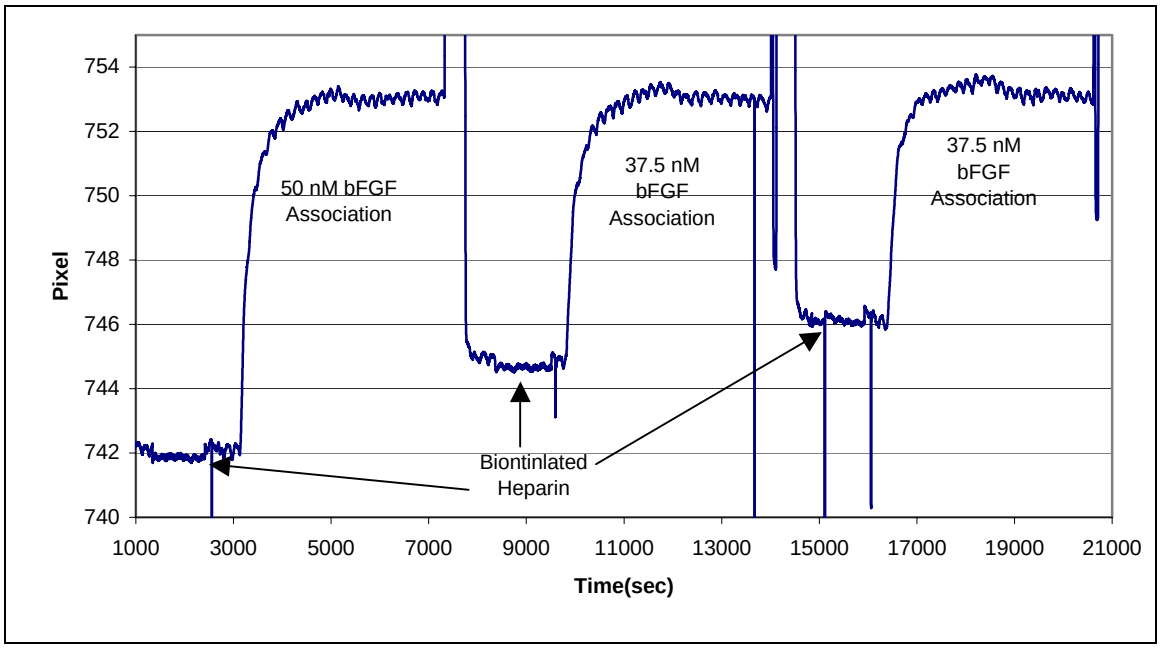

Figure 4.9a

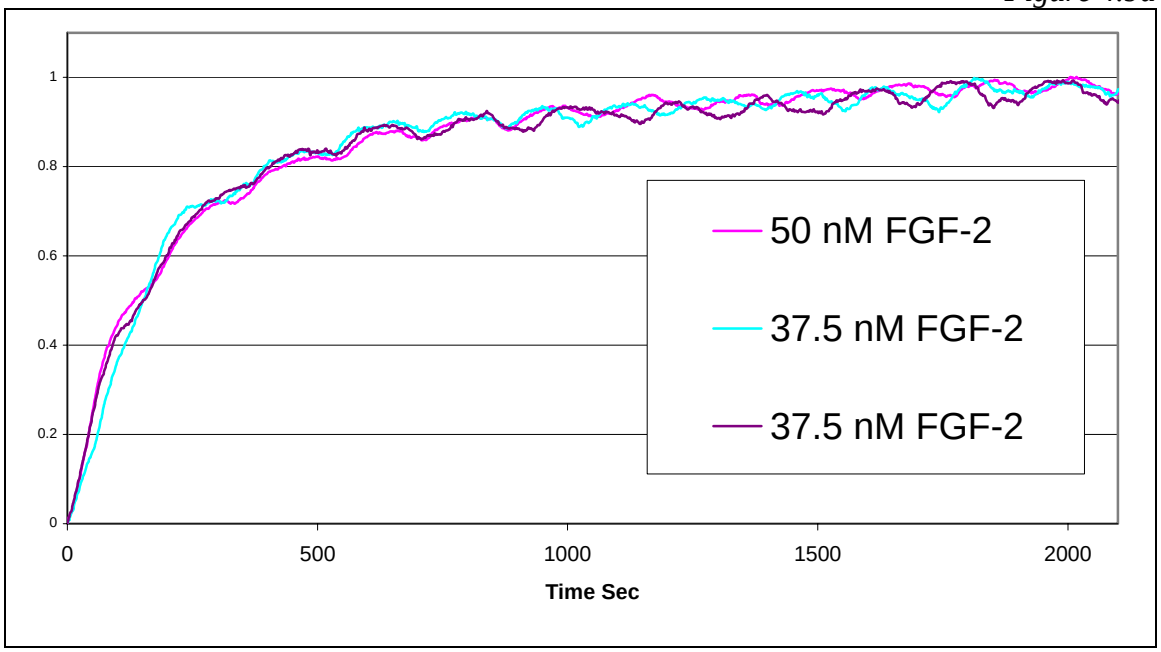

Figure 4.9b, Figure 4.9a shows three associations of FGF-2 in 50 nM, 37.5 nM, and 37.5 nM concentrations that exhibit binding of 13.1, 8.41, and 7.4 pixels. They all have different amounts of surface binding, but when normalized, as shown in Figure 4.9b, they are nearly alike despite different concentrations and amount bound. This figure is representative of over 20 associations (Specifically 10 at 37.5 nM and 4 at 50 nM) on 4 chips.

Data Fitting

To determine the association and disassociation rate constants a combination of curve fitting and linearization is needed. The collected data is normalized by dividing R by R_{max}, determined for each individual run, to scale the curve from zero to 1. Next Y_{max} and k_{obst} are determined by utilized a least squares analysis for Equation 11 of the association data. Next k_{obst} is plotted vs. the protein concentration to produce a linear relation ship with a slope of k_a and a y-intercept of k_d (Morton & Myszka, 1996). A noticeable oscillation is present in the collected data from the interactions of variations in flow rate and the temperature control function of the Reichert SPR system. This oscillation was found to not have an effect on the calculation of k_{obst} when there were more than 1.5 pixels of FGF-2 association. No further function fitting was necessary.

$$R = Y_{\max 1}\left(1 - e^{-k_{obst}\, t}\right)$$

Equation 10

$$k_{obst} = Ck_a - k_d$$

Equation 11

Quantifying FGF-2 heparin interactions

Four chips were using to perform 25 associations under optimum conditions. Seven associations were measured on the Jan 27, 2005 chip, nine on the February 9, 2005 chip, five on the Feb 22, 2005 chip, and 4 on the March 16, 2005 chip. Of these, 21 exhibited an association in excess of 1.5 pixels and were used to determine the kinetic rate constants for FGF-2 with heparin.

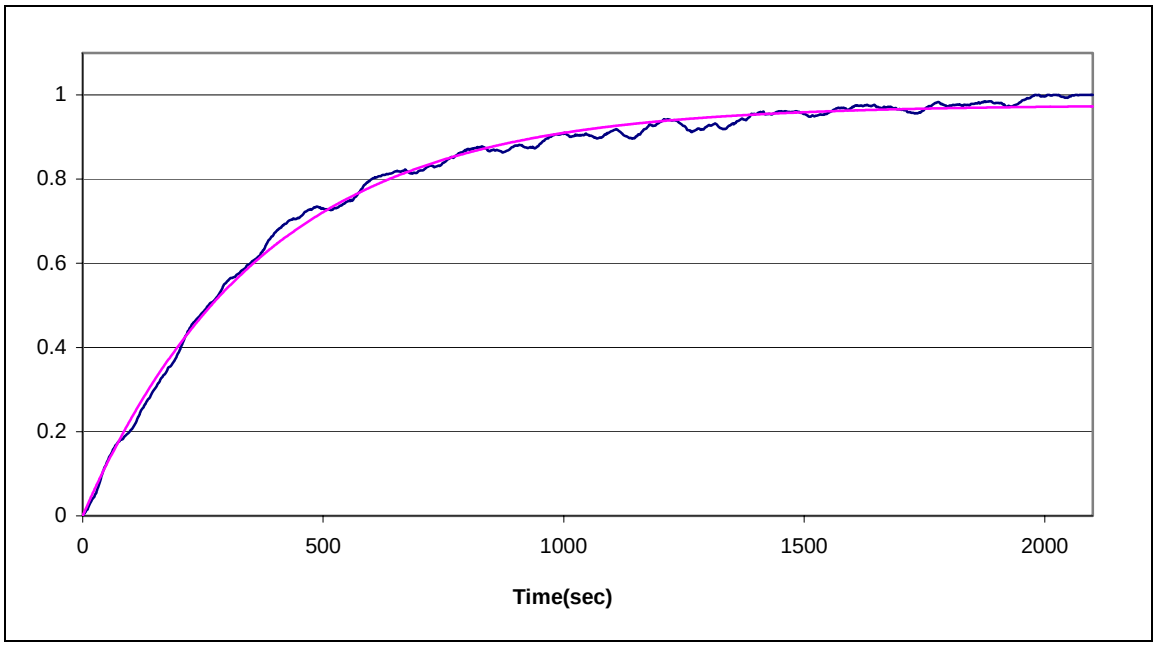

Figure 4.10, A plot of the calculated value versus the actual data from a 37.5 nM FGF-2 association. The calculated values were determined by applying least squares analysis to Equation 10. This figure is representative of 25 (Specifically 10 at 37.5 nM) associations on 4 chips.

To determine the rate constants the individual runs were normalized and fit to Equation 10 using a least square analysis. The calculated k_{obst} was then plotted versus the concentration of FGF-2 (M). For example, in Figure 4.10 the k_{obst} was found to be 0.002685 s^{-1}. The calculated k_{obst} data (Figure 4.11) was then linearized to determine the rates of association and dissociation during the kinetics.

When examining all of the associations, the rate of association, k_a, was found to be 7.157 x 10^4 $M^{-1}s^{-1}$, the rate of dissociation constant, k_d, was found to be 6.045 x 10^{-4} s^{-1}, and K_D was found to be 8.3 nM. The R^2 value of 0.44 is not ideal and is an indication of variation between the measured data. The sources of these variations are not known, but the data does show a strong trend.

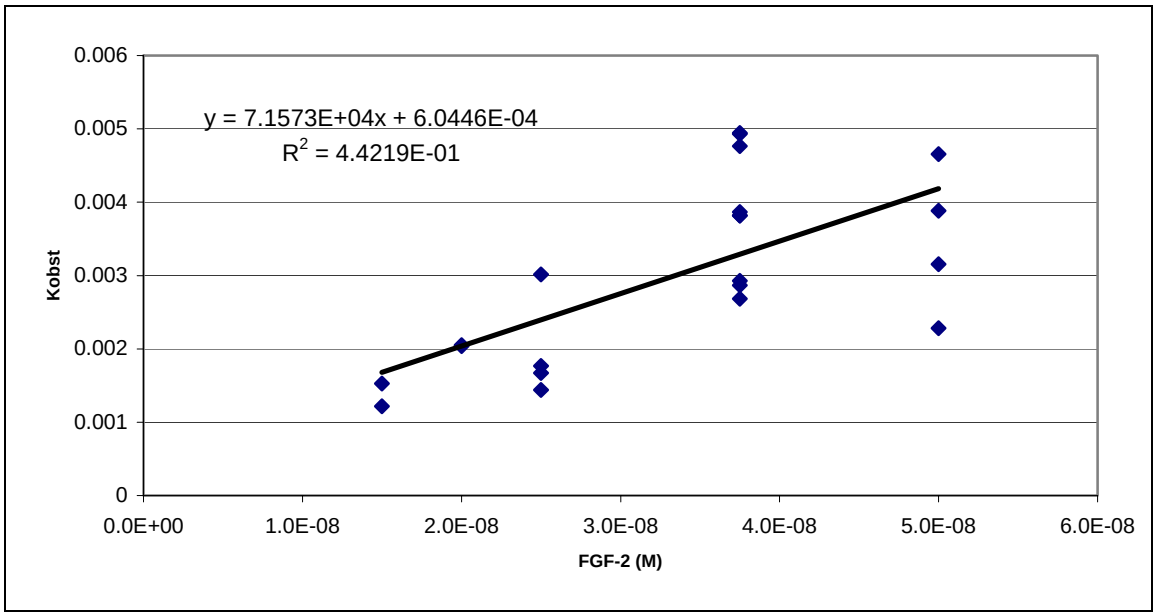

Figure 4.11, K_{obst} versus FGF-2 concentration to solve for the kinetic rate constants for 15nM to 50 nM FGF-2 solution. Note the similarity between the calculated Kobst between 37.5 and 50 nM FGF-2 solution. This figure is composed of 21 associations from 4 different chips.

However an analysis of the individual chips showed a stronger correlation. The first two associations on a chip typically showed different rate constants then the later associations. This difference between the initial association and later ones has been noted before and it is common to automatically excluded the first two associations on a chip (Dr. T.E. Ryan, Reichert Inc., personal communication). Figure 4.12 shows the results when one examines chips 2 and 3 individually and Figure 4.13 shows the results when the associations from chips 2 and 3 are considered together. The exclusion of the first two runs produces an excellent relationship for chip 3 ($k_a = 1.597 \times 10^5$ $M^{-1}s^{-1}$, $k_d = 1.08 \times 10^{-3}$ s^{-1}, $R^2 = 0.993$) and good correlation for chip 2 ($k_a = 1.280 \times 10^5$ $M^{-1}s^{-1}$, $k_d = 8.6 \times 10^{-4}$ s^{-1}, $R^2 = 0.678$). When the results of chips 2 and 3 are examined together reasonable relation was noted 3 ($k_a = 1.238 \times 10^5$ $M^{-1}s^{-1}$, $k_d = 5.4 \times 10^{-4}$ s^{-1}, $R^2 = 0.797$).

Chips 1 and 4 were not examined further as they produced poor results. Chip 1 produced a poor relationship when examined individually (R^2 =0.47) and contained only 3 points after excluding the first two associations and any associations with less than 1.5 pixels of binding. Chip 1 was the first time surface refreshing was employed. Most of the early runs had no surface refreshing and produced low amounts of total binding. Only a limited number of the later runs were performed with the surface refreshing as employed for all of the associations in chips 2 and 3 and as a results the chip produced only 3 quantifiable associations. Chip 4 only had associations performed at one concentration and as a result was not suitable for this type of analysis.

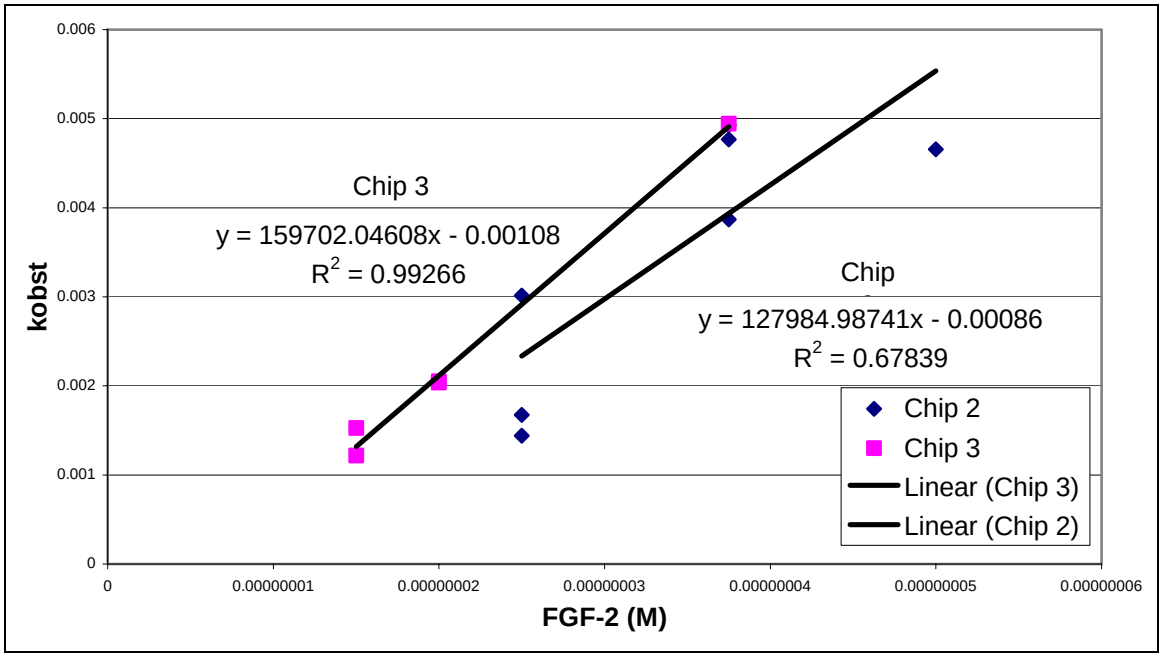

Figure 4.12 K_{obst} versus FGF-2 concentration for chips 2 & 3 to solve for the kinetic rate constants for the individual chips. The shown data excludes the first two associations for a given chip. This figure is composed of 11 associations from 2 different chips.

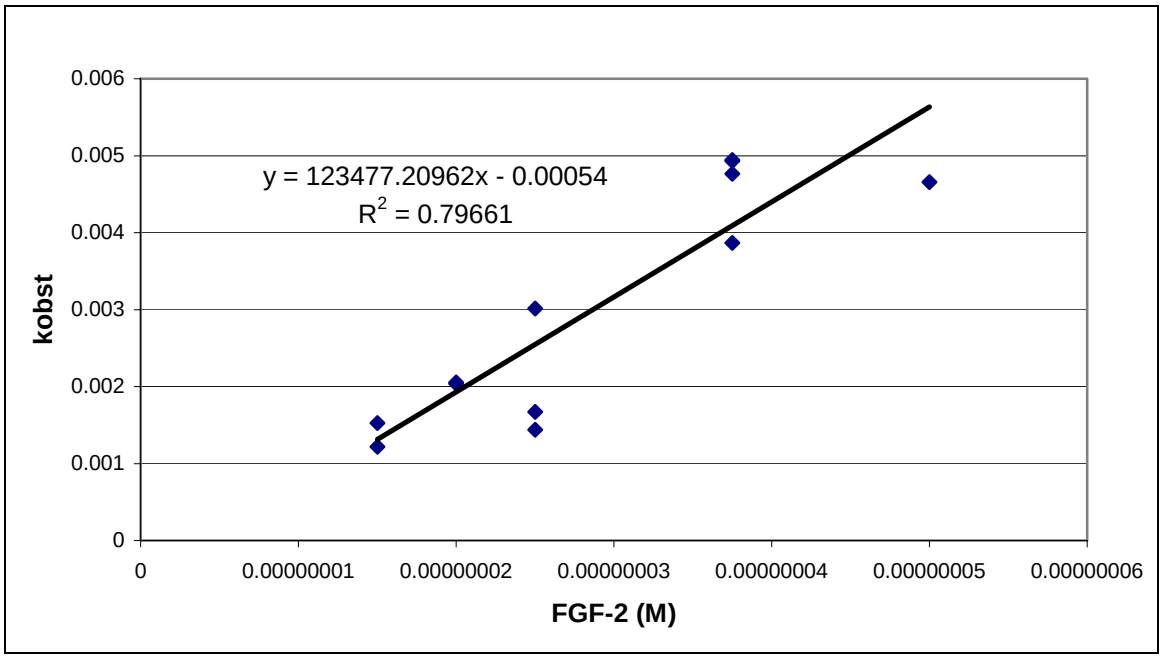

Figure 4.13 K_{obst} versus FGF-2 concentration for chips 2 & 3 to solve for the kinetic rate constants for the combined data. The shown data excludes the first two associations for a given chip. This figure is composed of 11 associations from 2 different chips.

Chips 2 and 3 both produced excellent data that likely differed because of their different surface conditions and the effects of rebinding. The surface slowly changes and the baseline increases as runs are performed on the chip, but this change is not consistent or well understood. Chip 3 had approximately 2 pixels of buildup on its surface, while chip 2 had approximately 6 pixels of build up. Chip 3 showed less variation in the calculated relationship (R^2 =0.993) then chip 2 (R^2 =0.678). Neither chip results are inherently better given the variations are likely an effect of surface conditions. In such a case it is better to utilize the combined results from chips 2 and 3 for analysis that considers a range of surface conditions ($k_a = 1.238 \times 10^5$ $M^{-1}s^{-1}$, $k_d = 5.4 \times 10^{-4}$ s^{-1}, R^2 =0.797).

Mass Transfer Limitations

With any rapid reaction or binding there is the possibility of mass transfer becoming the rate-limiting step for the event. That is the result of an inability of the binding protein to diffuse to the binding surface faster then the binding occurs. To avoid this problem it is recommended to utilize a high solution flow rate that keeps the flow cell well mixed and a chip surface with a low binding capacity that lowers the rate of removal of the binding protein from the solution near the binding surface (Myszka, 1997; Schuck 1997).

Sometimes mass transfer limitations cannot be avoided by optimizing flow rates or surface densities. In these cases one must utilize analytic methods to examine the data. One such approach is to use a two-compartment model where one compartment represents the solution flowing over the chip and another represents the solution adjacent to the binding surface, Equation 1 (Myszka, 1997). Another option is to put less weight on the rapid binding that initially occurs and weight the data as the association approaches equilibrium. Near equilibrium, the filled binding and limited number of un bound sites reduce the effective surface density and results in non-mass transfer limited kinetics (Schuck & Minton, 1996).

$$A \underset{k_m}{\overset{k_m}{\leftrightarrow}} A^* + B \underset{k_d}{\overset{k_a}{\leftrightarrow}} AB \quad .$$

Equation 12

Two-Compartment Model

There are many ways to deal with mass transfer limitations. Ideally they can be avoided by optimizing flow rate and surface density. When planning and setup alone are

not enough analytical methods exist to solve the problem. Fortunately the setup used did not operate in a mass transfer limited regime. This is a result of the high flow rate and surface chemistry that were employed. Clamp, a kinetic rate solving software program, was used to analyze several of the associations with a two-compartment model (Figure 4.14). It showed that the concentration of FGF-2 in both compartments was the same; as a result we implemented a well-mixed single compartment model, as presented in Chapter 1, for the data analysis.

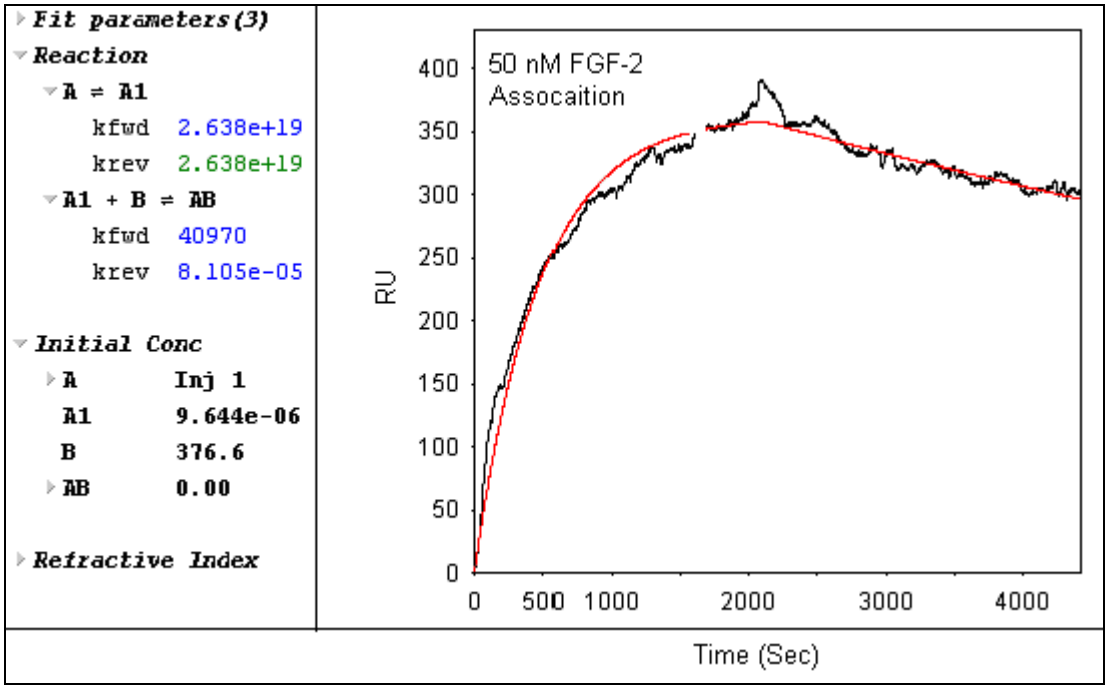

4.14, The results of a two-compartment model simulation in Clamp of 50 nM association. For the graph the x-axis is time in seconds and the y-axis is RU of bound FGF-2. A represents the FGF-2 in the bulk solution, A1 is the FGF-2 near the surface, B is the binding site on the bound heparin, and AB is the FGF-2-heparin complex. Note the significant high kinetic rate of transport between the compartments of nearly 2.6 x 10^{19}. This is much greater the calculated rate of association and indicates that two compartments have the same concentration. This figure is representative of 25 (Specifically 4 at 50 nM) associations on 4 chips.

Another means to analyze the data for mass transport limitations is to vary the flow rate of the system. This varies Reynolds number of the flow cell and how well mixed the solution in the flow cell is. When one can vary the flow rate of the system without affecting the effective kinetic rate, one can assume the system is limited only by the rate of association and not by the rate of mass transport. Figure 5.15 shows no change in the kinetic rate when the flow rate is lowered 17% from the normal flow rate of 0.64 ml/min to 0.53 ml/min. A flow rate of 0.21 ml/min is shown to illustrate the effects of mass transport limitations on an association. All of the associations that were used for analysis were performed under non-mass transport limited conditions.

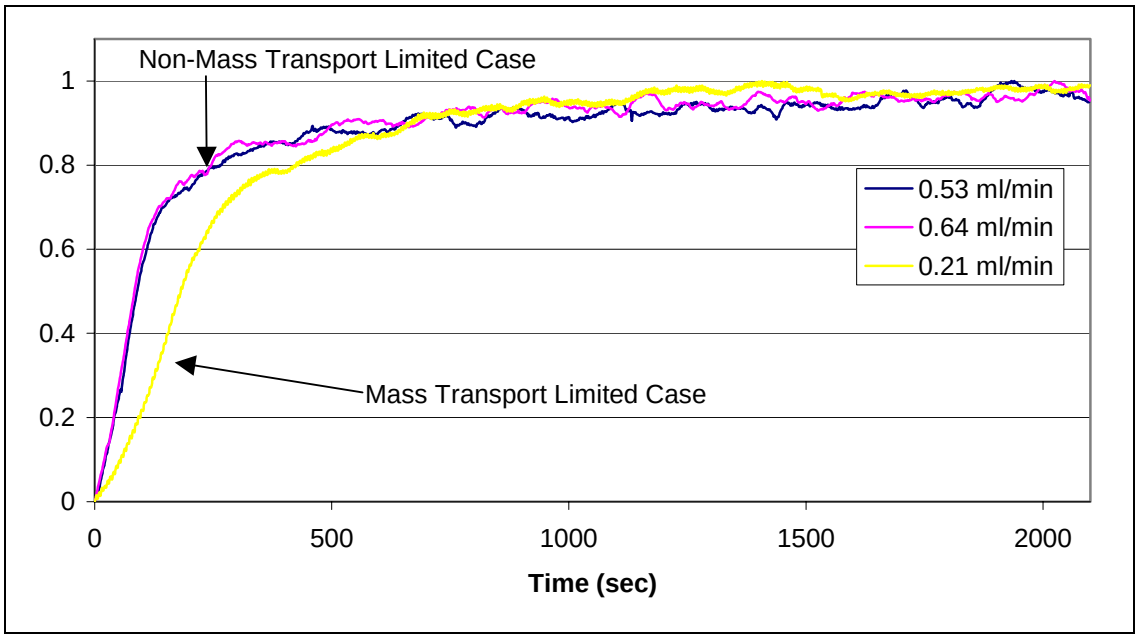

Figure 5.15. The normalized results of 3 consecutive associations of 50 nM FGF-2 to a heparin covered mSAM surface at different flow rates. Note the extreme similarity between the 0.64 ml/min (normal flow rate) and the 0.53 ml/min association. This indicates that association is not mass transport limited at the flow rate employed in this study. The 0.21 ml/min association illustrates the effects of mass transport limits on the rate of association. This figure is representative of 3 associations on a single chip.

A third means to analyze an association for a mass transport limitation is to plot dR/dt versus R, where R is the amount of binding from the association at a given time (Schunk & Minton, 1996). Figure 5.16 illustrates idealized graphs. An ideal non-mass transport limited case will show a straight line, while a mass transport limited case would posses a maximal effective association rate (dR/dt) that it could not surpass.

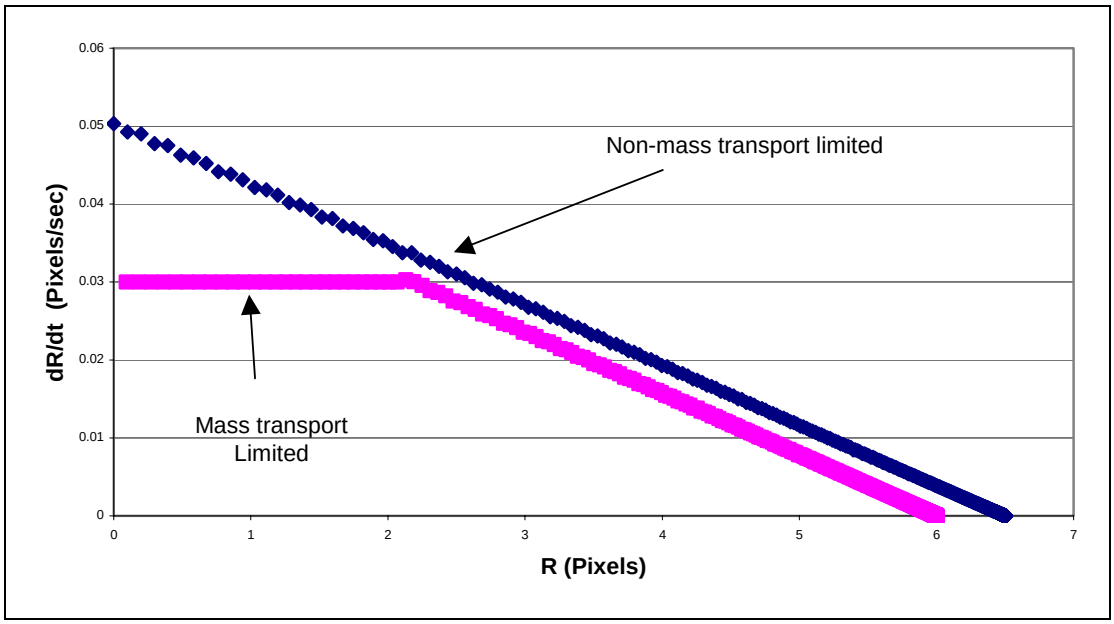

Figure 5.16, An example of what a non-mass transport limited and mass transport limited dR/dt versus R graph would look like. This data was created to illustrates this scenario and the absolute values are of no significance. Note the leveling off of the transfer limited case and the complete linear relationship of the non-mass transfer limited situation.

The associations presented in Figure 5.15 are reformatted in Figure 5.17 a, b, and c to check for the presence of mass transfer limitations by examining dR/dt versus R. All of the cases exhibit possible mass transfer limitations as shown in Figure 5.15. That is the association's dR/dt versus R is not completely linear and it has a maximal effective association rate. The 0.21 ml/min association exhibits the greatest influence of mass

transfer limitations and the .0.64 ml/min and 0.52 ml/min associations exhibited nearly equal amounts of mass transfer limitations. This is consistent with Figure 5.15.

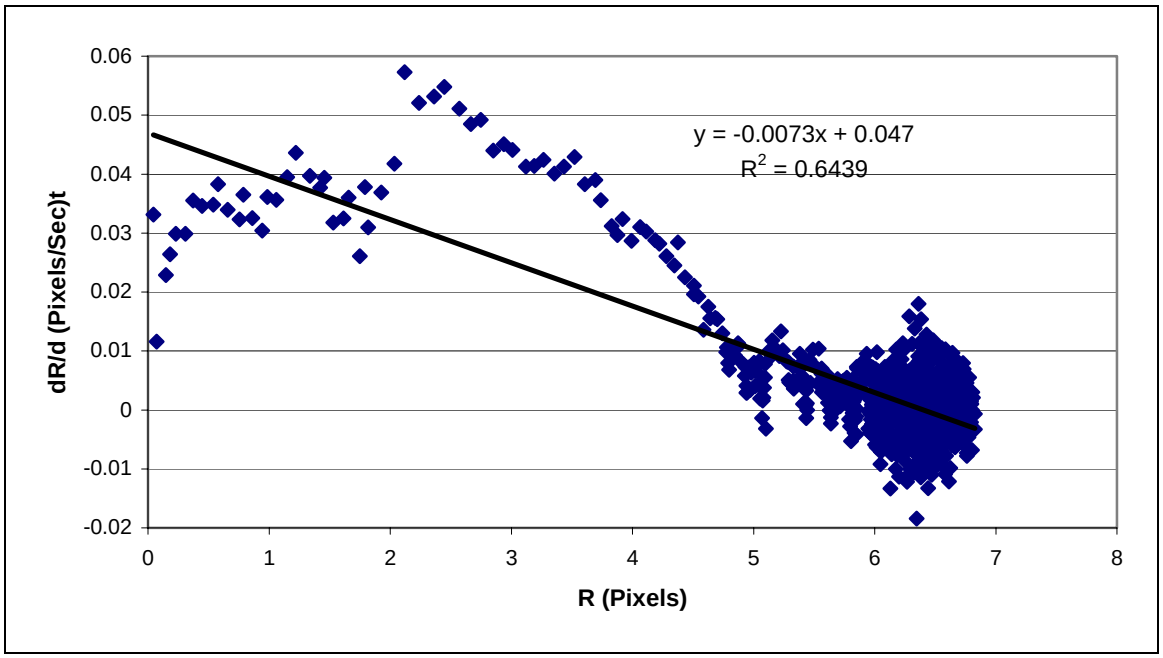

Figure 5.17a, dR/dt versus R for 0.64 ml/min 50 nM FGF-2 association

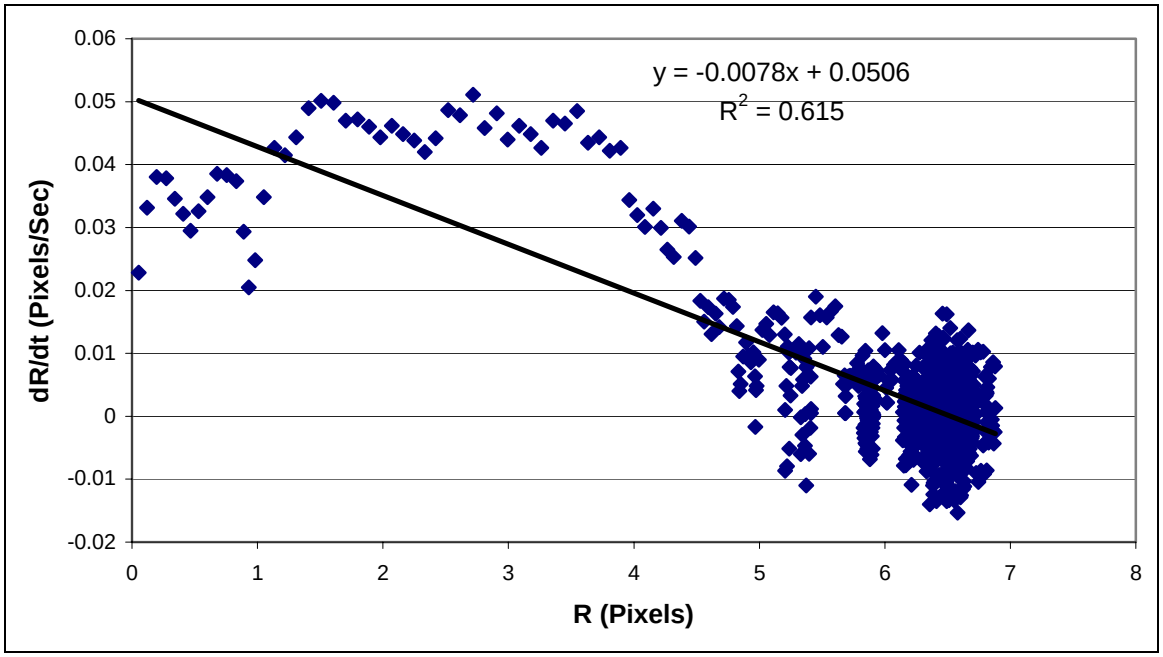

Figure 5.17b, dR/dt versus R for 0.53 ml/min 50 nM FGF-2 association

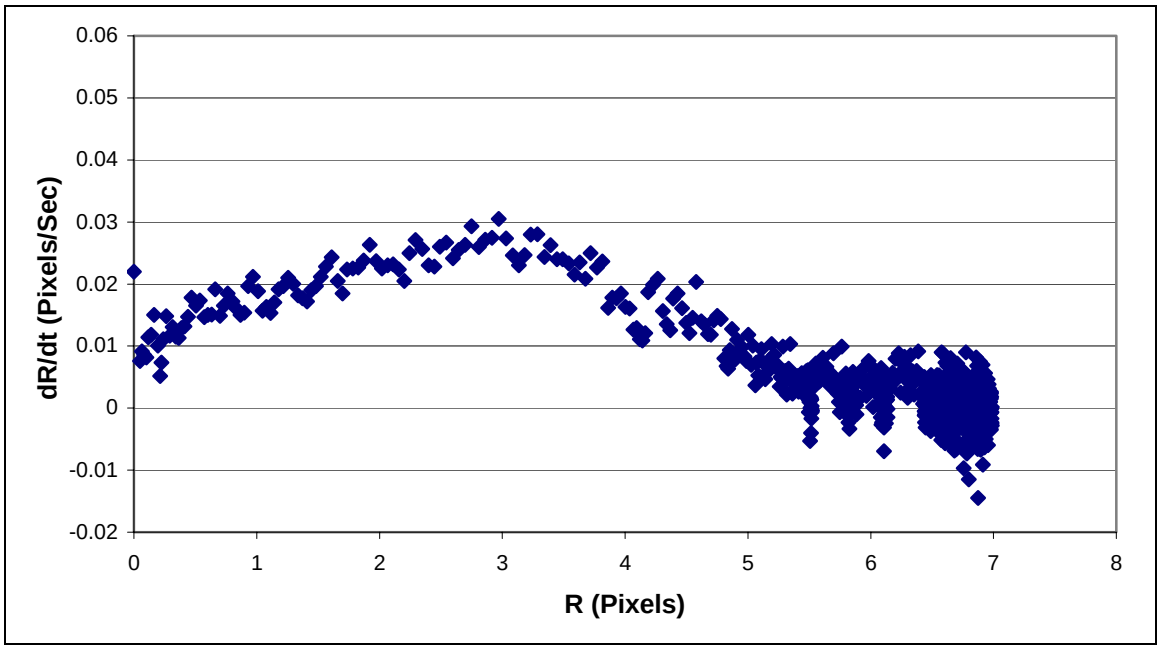

Figure 5.17c, dR/dt versus R for 0.21 ml/min 50 nM FGF-2 association.
These Figures are calculated from the 5 point average R from the associations shown in Figure 5.13. Note the possibility of mass transport limitations in all cases.

The association of 50 nM FGF-2 with a heparin bound surface was checked in several ways for mass transfer limitations. The two-compartment model analysis and the variation of the Reynolds's number by varying the flow rate showed no mass transfer limitations at the flow rate of 0.64 ml/min. However the analysis of association rate versus extent of binding suggested a mass transfer flow rate limitation was present at a flow rate of 0.64 ml/min. What has been shown is that accounting for mass transfer limitations with a two-compartment model does not improve the quality of quantification and that varying the flow rate in the system does not change the rate of association when operating near .64 ml/min. This suggests that there are no mass transport limitations or if they are present they do not affect the quantification and can be disregarded.

Other SPR Issues

Often it is assumed that the binding follows a first order reaction as shown in Equation 1. However, this is usually not the case. It is common for the data to deviate from the expected first order equation to a multi term equation. This can be cause by heterogeneity of the binding sites, mass transport limitations, or steric interferences. Proteins coupled directly to the chips surface by amine coupling attach to the surface in random orientations, which results in groups with different binding affinities. Some configurations will only bind the protein in solution at high concentrations, further complicating the calculations of rate constants (Schuck, 1997). Steric interferences can be avoided by utilizing a low surface density and using compounds as spacers between the binding protein and the chip surface (Schuck & Minton, 1996).

Rebinding

When molecules bind to another, their dissociation caused by the removal of the ligand in solution. disassociation does not automatically return them to the surrounding solution. Rather they can rebind to the same site or a nearby site (Gopalakrishnan et al., 2005). This rebinding makes determining the true kinetic rate constants difficult if not impossible. What is seen is a limited amount of slow rate disassociation that usually occurs in a non-exponential fashion. Typically this situation arises in systems with a high affinity for the protein of study (Gopalakrishnan et al., 2005). Physiologically this has an advantage as it may cause prolonged activation or stimulation when it occurs with signal molecules.

Several papers suggest the use of a low surface density and high flow rate being sufficient to avoid rebinding (Schuck, 1997). Unfortunately these measures may not be

enough. One possible solution is the use of a compound in the solution used for disassociation that will bind the free protein but will not bind to the surface or bind to proteins when bound to the surface. This will reduce the amount of free binding and allow a better calculation of the disassociation constant.

Heparin was used for some of the disassociations to allow the analysis of the effects of rebinding of FGF-2 to the surface bound heparin. The heparin in solution competed with the bound heparin for FGF-2 after it disassociated from surface bound heparin. A concentration of heparin that did not interact with the surface or induce an index shift was desired. Figure 4.18 shows that while 30 μM heparin solution induces an index shift or interacts with the surface 15 μM does not. All FGF-2 disassociation used concentrations of 15 μM or less.

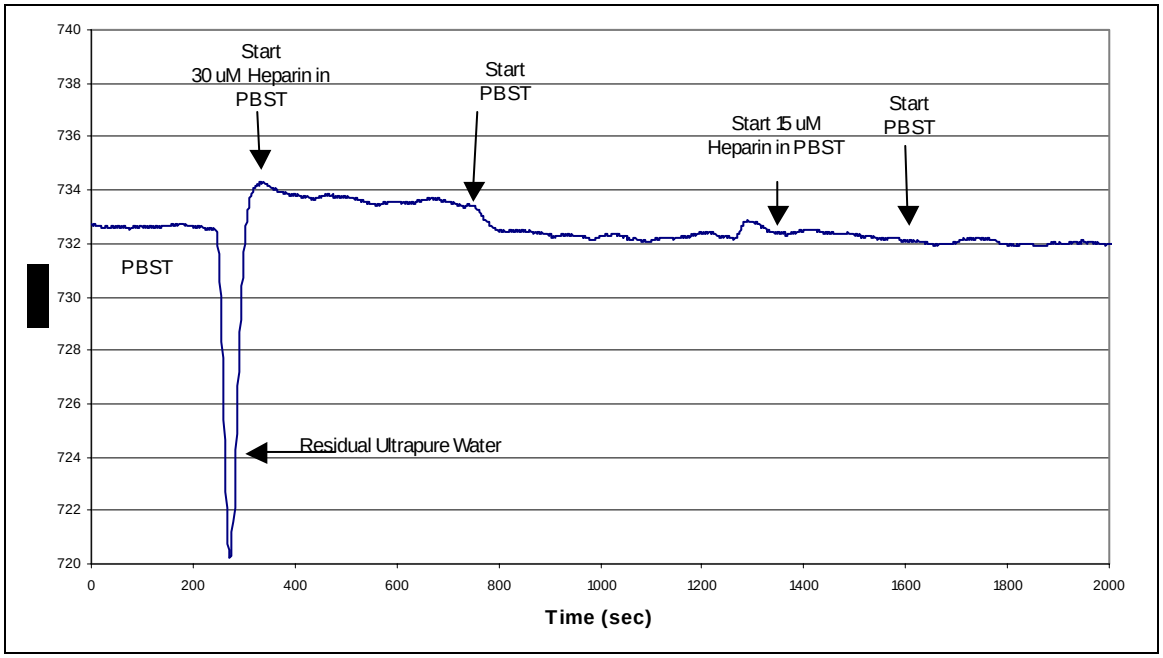

Figure 4.18, Analysis of Heparin solutions for use in disassociation after association of FGF-2 with a heparin bound surface. Note 30 μM heparin causes a significant index shift while 15 μM heparin does not. While this type of comparison was only performed once on one chip, No index shift was associated with heparin solutions on 12 runs on 4 chips.

Figure 4.19 shows the extent of the rebinding problem in the disassociation of FGF-2 from surface bond heparin. In the case of using just PBST for the disassociation, nearly no disassociation from the surface was observed. However, when heparin was introduced into the disassociation solution to compete with surface bound heparin for released FGF-2, a dose dependent disassociation was noted.

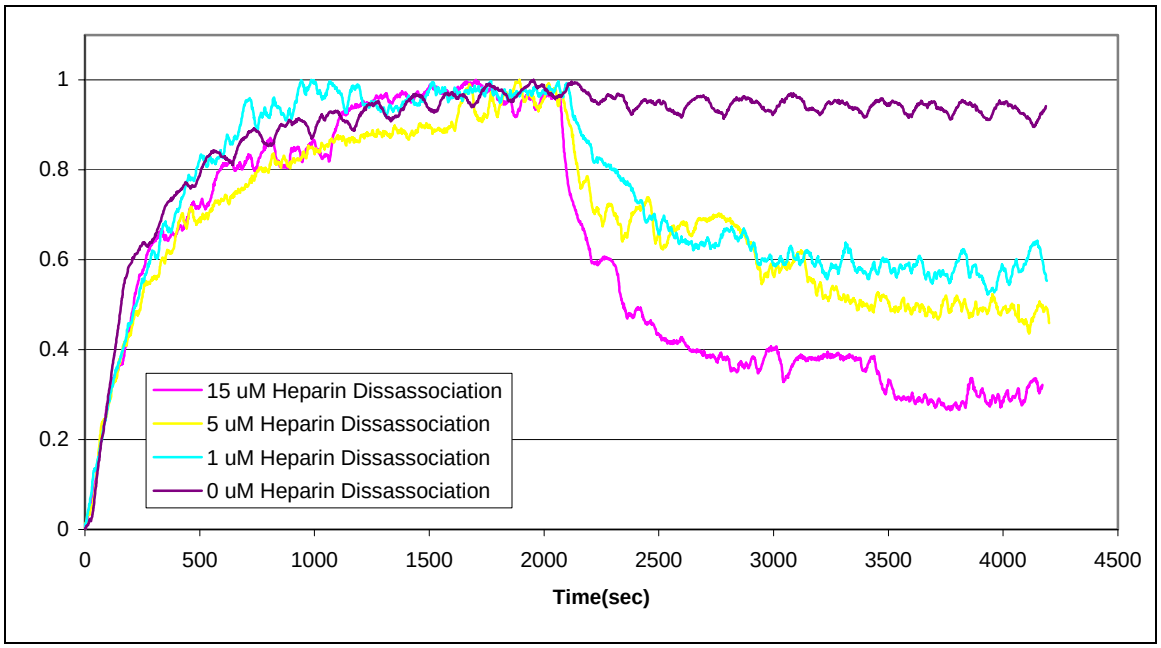

Figure 4.19, A normalized 37.5 nM FGF-2 in PBST pH 7.4 association to a heparin covered mSAM for 2100 seconds, followed by a 2100 second period of disassociation with different heparin concentrations. Note the effect the dose dependent effect heparin concentration has on disassociation. This figure is representative of 12 associations (2 sets of +/- heparin in the dissociation fluid) on 3 chips.

The effects of heparin concentration on disassociation were quantified by fitting to a simple first order disassociation model (Equation 12). The first 240 seconds were analyzed to determine the effective disassociation rate and displayed in Table 4.1 & Figure 4.20. The heparin concentration has a dose dependent effect on the effective disassociation rate constant The R^2 values for the calculate rate constant vary from a quite good 0.97 to a rather poor 0.62. This is in small part caused by noise and the reality that the presence of rebinding makes this system a non-first order disassociation.

$$R = R_0 e^{e^{-k_d t}}$$

Equation 13

Heparin Concentration in Disassociation Solution (μM)	Effective rate of Disassociation, k_d, (s^{-1})	R^2
0	1.098×10^{-4}	.62
1	5.041×10^{-4}	.97
5	7.734×10^{-4}	.61
15	1.291×10^{-3}	.96

Table 4.1, Effective rates of disassociation fit to Equation 12. This figure is representative of 12 associations on 3 chips.

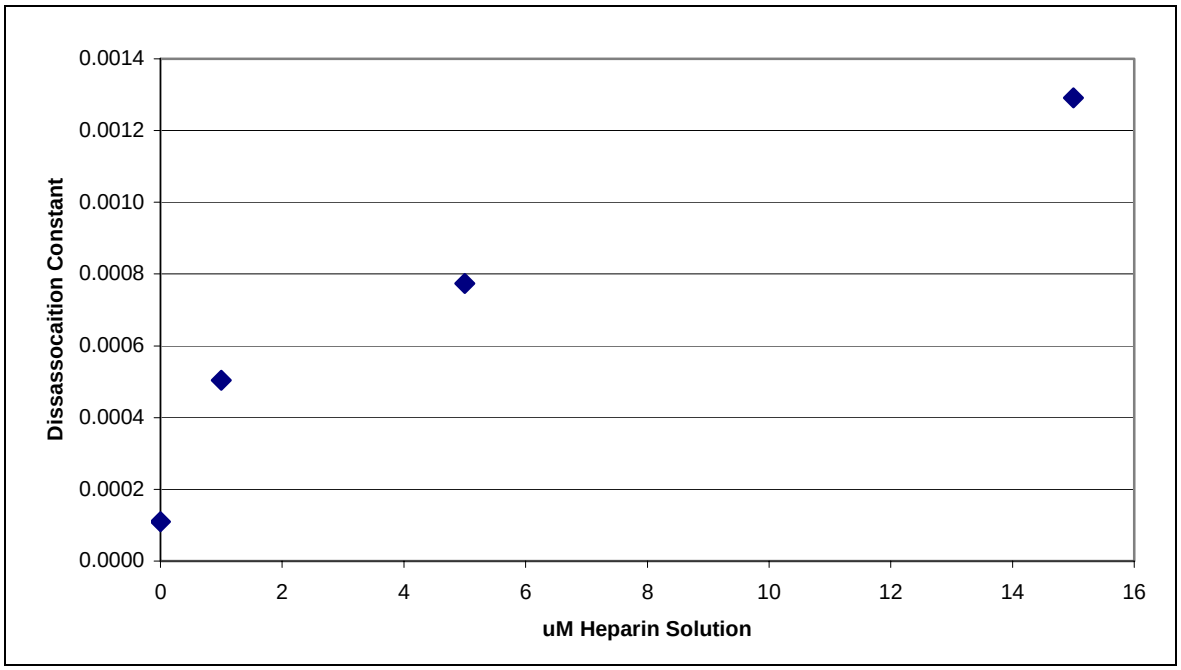

Figure 4.20, Rate of disassociation constant versus heparin concentration in disassociation solution. Note the linearity of the association.

Other FGF-2 Heparin studies

As presented in Chapter 1, several studies have examined the interactions of FGF-2 and heparin using SPR analysis (Table 4.1). There results differ from our results (k_a of 7.157×10^4 $M^{-1}s^{-1}$; k_d o 6.045×10^{-4} s^{-1}), for many reasons. The other studies all utilize a CMD chip that is known for non-specific binding.

Wu et al. (2003) use a non-circulated cuvettes based system. They do not discuss if the system is mass transfer limited or discuss the suitability of their binding chemistry for interaction analysis. With the missing information it is hard to properly assess their study. Alexakis et al. (2004) do not present rate constants; rather they found, k_D, the ratio of k_a to k_d. They also make no mention of weather their system is mass transfer limited.

Ibrahimi et al. (2004) is an excellent study. Their system is not mass transfer limited and they utilize a well characterized SPR system and binding chemistry. However, their study is not perfect. In their study they utilized FGF-2 amine coupled to a CMD chip that they passed 50-800 nM heparin solutions to measure binding. This is a very concentrated solution of heparin that could exhibit different binding kinetics. Furthermore, it is better to design you system to reflect the realities of the extra cellular environment. Typically heparin and heparan sulfate are bound to the cell and FGF-2 is found a very low concentrations in the intercellular solution, not like in this study where FGF-2 is bound to the surface with high concentrations of heparin in solution. They also mention non-specific binding accounting for up to 20% of the observed, uncorrected FGF-2-heparin association.

Table 4.2 lists a summary of all studies, including this study, which examined FGF-2 interactions with heparin. Our rate of association (7.157×10^4 $M^{-1}s^{-1}$) is similar to Wu et al. ($5.4 \pm 0.7 \times 10^4$ $M^{-1}s^{-1}$), slightly faster the Presta et al., but significant slowly then the value calculated by Ibrahimi et al. ($k_a = 1.1 \times 10^7 \pm 4.71 \times 10^5$ $M^{-1}s^{-1}$). Kd of our system (K_d=8.446 nM) was quite similar to Alexakis et al. (K_d =10.6+/1.4.4 nM). Much like the association constants, our rate of disassociation ($k_d = 6.045 \times 10^{-4}$ s^{-1}) is similar to Presta et al. ($k_d = 3.8 \times 10^{-4} \pm 1.92 \times 10^{-2}$ s^{-1}), slightly slower the Wu et

al.(k_d=3.85+/-10^{-3} s^{-1}) , and slightly faster than Ibrahimi et al. (k_d =.43+/-1.92x10^{-2} s^{-1}). While our values differ from the other studies, they are similar enough to be caused by different procedures, equipment, or supplies.

Authors	SPR System	Method To bind Heparin to System	Rate Constants
Alexakis et al. 2004	Biacore,	Amine Couple Streptavidin To Surface; Bind Biotinylated Heparin To Streptavidin	K_d =10.6+/1.4.4 nM where $K_d = k_d/k_a$
Ibrahimi et al. 2004	Biacore 3000	Amine Couple Albumen Heparin To Surface; Amine Couple FGF-2 To Surface	k_a =1.1 x 10^7 +/- 4.71 x 10^5 ($M^{-1}s^{-1}$) k_d =.43+/-1.92x10^{-2} (s^{-1})
Kirtland (this paper)	Reichert	Amine Couple Streptavidin To Surface; Bind Biotinylated Heparin To Streptavidin	k_a = 1.238 x 10^5 $M^{-1}s^{-1}$ k_d =5.4x10^{-4} s^{-1} K_d=4.88 nM
Presta et al. 2005	Not listed	Couple Biotinylated Heparin To Streptavidin Coated Surface	k_a=9 x 10^3 +/- 4.71 x 10^5 ($M^{-1}s^{-1}$) k_d=3.8x10^{-4}+/-1.92x10^{-2} (s^{-1})
Wu et al. 2003	IAsys,	Amine Couple Glycol Chitosan To Surface; Glycaminated Heparin To Glycol Chitosan	k_a=5.4 +/- 0.7 x 10^4 ($M^{-1}s^{-1}$) k_d=3.85+/-10^{-3} (s^{-1})

Table 4.2 (copy of Table 1.2), A compilation of results from studies that quantified the binding of FGF-2 and heparin using SPR, including this study (Kirtland).

IGFBP-3 Heparin Interactions

IGF-BP3, a heparin binding protein, was passed over the heparin surface mSAM chip developed in Chapter 3. Although the study of this binding interaction was limited (see Appendix), it did further confirm the utility of our SPR system for studying heparin-binding interactions.

Chapter 4 Conclusions

The Reichert system was successfully employed to quantify the interactions of FGF-2 and surface bound heparin. The collected data was not mass transfer limited and was fir to a well mixed, single compartment model. Rebinding was a significant issue

that was particularly evident in the disassociation phase. Heparin was added to the disassociation solution to enable the disassociation of FGF-2 and determination of the dissociation rate directly. The rebinding was reduced in a dose dependent manor with heparin concentration.

Chapter 5: Summary and Future Work

Summary:

The primary goals of this thesis were to (1) couple heparin to mSAM chips, using these heparin coupled chips, (2) quantify the interactions of FGF-2 with heparin using a Reichert SPR instrument. These goals were achieved. A heparin coated chip surface was created by coupling streptavidin by amine chemistry to a mSAM chip and biotinylated heparin was attached through the interaction of biotin and streptavidin (Chapter 3). This surface exhibited little if any non-specific binding and no mass transfer limitations. It successfully bound heparin binding proteins (FGF-2, IGF-BP3), but not non-heparin binding proteins (IGF-I). Analysis of FGF-2 was successfully completed and a rate of association of $7.2 \times 10^{4}\ M^{-1}s^{-1}$ and a rate of disassociation of $6.0 \times 10^{-4}\ s^{-1}$ were calculated from the association data. A dissociation rate of $1.1 \times 10^{-4}\ s^{-1}$ was calculated from the dissociation data in the presence of soluble heparin to prevent rebinding. The rates for dissociation are quite comparable. The literature from other studies using other SPR systems indicated a wide range of individual rate measurements but our overall affinity was not dissimilar and we are confident that our procedure does lead to reproducible and reliable rate measurements.

Recommendations for Future Work

While this study completed all of its goals, it also raised some new questions and areas for improvement. The most obvious source of noise in the system came from the variations in flow from the peristaltic pump. The recurrent oscillation in the collected data was ever present. Future work to explore different pump types or configurations to

minimize the effects of pump noise would be beneficial. A reduction in noise would allow the quantification of lower concentrations of growth factors.

The procedure to bind heparin to the mSAM chip successfully produced a surface that would bind heparin binding proteins with low non-specific binding. Future studies could examine the interactions of other heparin binding proteins such as VEGF or PDGF. For example, we did do a limited number of studies looking at IGFBP-3 binding to heparin (Appendix). More accurate association and disassociation rate constants are always useful and determining the quantitative values on the same heparin surface would allow better comparison of how these heparin-binding growth factors might compete for heparin and heparan sulfate proteoglycans in vivo

While the interactions of only FGF-2 and heparin are important, the reality is that the intercellular space is a complex mixture of compounds. We showed that heparin affects the disassociation rate of FGF-2 from surface bound heparin. Another area of possible study would be to examine the effects of heparin in the association solution. This would likely affect the overall rate and extant of surface binding and could tell us more about the activation of cellular pathways. Wu et al. (2003) examined the effects of different heparin fragments in the association solution on the rate constants. They showed that different heparin fragment types had an effect on the association and disassociation constant rates. Future work to explore the effects of varied heparin or heparin sulfate concentrations on the extent or rate of binding. This would also allow better comparisons of how growth factors and heparin and heparan sulfate proteoglycans interact in vivo.

Ideal interactions between molecules are not effected by the binding of one or the other to a surface. In theory the same constants should be determined whether FGF-2 or heparin is bound to the surface In this study we bound heparin to the surface. Possible future studies could use amine chemistry to bind FGF-2 to an mSAM surface to see if similar rate constants can be calculated.

Heparin and heparan sulfate can be modified by the cell in a multitude of possibilities. These modifications may affect there binding properties. Future works may bind different types of heparin / heparan sulfate to mSAM chip to examine the effects different heparin/ heparan sulfate modifications. Cells have a variety of heparin types out side their cell membranes. More information would all a better understanding of the in vivo behavior of growth factors.

Our system typically had a constantly changing surface density of heparin. For a given association concentration the extent of binding was always changing. Another possible area of future work would be to develop a method to quantify the amount of heparin bound to the chip surface. Osmond et al (2002) used thrombin as a means to measure the amount of heparin on a chip surface, but their correlations applied to specific heparin types bound with particular methods. Future work could develop a correlation between thrombin binding and the amount of our heparin on a chips surface. Knowing the amount of heparin on the surface could improve the calculations used to determine rate constants or allow one to maintain a constant heparin density.

References

Akhouri, R., A. Bhattacharyya, et al. (2004). "Structural and functional dissection of the adhesive domains of Plasmodium falciparum thrombospondin-related anonymous protein (TRAP)." Biochem J 379(Pt 3): 815-822.

Alexakis, C., P. Mestries, et al. (2004). "Structurally different RGTAs modulate collagen-type expression by cultured aortic smooth muscle cells via different pathways involving fibroblast growth factor-2 or transforming growth factor-beta1." FASEB10: 1147-1149.

Amara, A., O. Lorthioir O, et al. (1999). "Stromal cell-derived factor-1alpha associates with heparan sulfates through the first beta-strand of the chemokine." J Biol Chem 274(34): 23916-23925.

Arteel, GE., S. Franken S, et al. (2000). "Binding of selenoprotein P to heparin: characterization with surface plasmon resonance." Biol Chem 381(3):265-268.

Badellino, K., P. Walsh (2001). "Localization of a heparin binding site in the catalytic domain of factor XIa." Biochemistry 40(25): 7569-7580.

Barth, H., C. Schafer, et al. (2003). "Cellular binding of hepatitis C virus envelope glycoprotein E2 requires cell surface heparan sulfate." J Biol Chem 278(42): 41003-41012.

Biacore, AB (2005). Biacore Webpage http://www.biacore.com Accessed: April 14, 2005.

Bengtsson, E., A. Aspberg, et al. (2000). "The amino-terminal part of PRELP binds to heparin and heparan sulfate." J Biol Chem 275(52): 40695-40702.

Berry, D., Z. Shriver, et al. (2004). "Quantitative assessment of FGF regulation by cell surface heparan sulfates." Biochem Biophys Res Comm 314(4): 994-1000.

Birkmann, A., M. Ensser, et al. (2001). "Cell surface heparan sulfate is a receptor for human herpesvirus 8 and interacts with envelope glycoprotein K8." J Virol 75(23): 11583-11593.

Caldwell, E., A. Andreasen, et al. (1999)."Heparin binding and augmentation of C1 inhibitor activity." Arch Biochem Biophys 361(2): 215-222.

Capila, I., M. Hernaiz, et al. (2001). "Annexin V--heparin oligosaccharide complex suggests heparan sulfate--mediated assembly on cell surfaces." Structure 9(1): 57-64.

Capila, I., V. VanderNoot, et al. (1999). "Interaction of heparin with annexin V." FEBS Lett 446(2-3): 327-330.

Chua, C., N. Rahimi, et al. (2004). “Heparan Sulfate Proteoglycans Function as Receptors for Fibroblast Growth Factor-2 Activation of Extracellular Signal-Regulated Kinase 1 and 2.” Circ Res 94: 316-323.

Cochran, S., C. Li, et al. (2003). “Probing the interactions of phosphosulfomannans with angiogenic growth factors by surface plasmon resonance.” J Med Chem 46(21): 4601-4608.

Cooper, M. (2003). “Label-free screening of bio-molecular interactions.” Anal Bioanal Chem 377(5): 834-842. Review.

Dessy, R. (2005). Professor Emeritus, Virginia Polytechnic Institute and State University. Personal Communication.

Diamandis, E., T. Christopoulos. (1991). “The biotin-(strept)avidin system: principles and applications in biotechnology.” Clin Chem 37(5): 625-636. Review.

Dong, J., C. Peters-Libeu, et al. (2001). “Interaction of the N-terminal domain of apolipoprotein E4 with heparin.” Biochemistry 40(9): 2826-2834.

Earp, R., and R. Dessy (1998). Surface Plasmon Resonance. Commercial Biosensors: Applications to Clinical Bioprocess, and Environmental Samples. G. Ramsay, John Wiley & Sons, Inc.: 99-164.

Eckert, R., H. Ragg (2003). ”Zinc ions promote the interaction between heparin and heparin cofactor II.” FEBS Lett 541(1-3): 121-125.

Faham, S., R. Hileman, et al. (1996). “Heparin structure and interactions with basic fibroblast growth factor.” Science 271(5252): 1116-1120.

Faham, S., R. Linhardt, et al. (1998). “Diversity does make a difference: fibroblast growth factor-heparin interactions.” Curr Opin Struct Biol 8(5): 578-586. Review.

Fannon, M., K. Forsten, et al. (2000). “Potentiation and inhibition of bFGF binding by heparin: a model for regulation of cellular response.” Biochemistry 39(6): 1434-1445.

Fannon, M., M. Nugent. (1996). “Basic fibroblast growth factor binds its receptors, is internalized, and stimulates DNA synthesis in Balb/c3T3 cells in the absence of heparan sulfate.” J Biol Chem 271(30): 17949-17956.

Forsten, K., R Akers, et al. (2001). “Insulin-like growth factor (IGF) binding protein-3 regulation of IGF-I is altered in an acidic extracellular environment.” J Cell Physiol 189(3): 356-365.

Forsten, K., N. Courant, et al. (1997). “Endothelial proteoglycans inhibit bFGF binding and mitogenesis.” J Cell Physiol 172(2): 209-220.

Forsten, K., M. Fannon, et al. (2000). “Potential mechanisms for the regulation of growth factor binding by heparin.” J Theor Biol 205(2): 215-230.

Francis, G., M. Ross, et al., (1992). “Novel recombinant fusion protein analogues of insulin-like growth factor (IGF)-I indicate the relative importance of IGF-binding protein and receptor binding for enhanced biological potency.” J Mol Endocrinol 8: 213-223

Friedrich, U., A. Blom, et al. (2001). “Structural and energetic characteristics of the heparin-binding site in antithrombotic protein C.” J Biol Chem 276(26): 24122-24128.

Futamura, M., P. Dhanasekaran, et al. (2005). “Saito H. Two-step mechanism of binding of apolipoprotein E to heparin: implications for the kinetics of apolipoprotein E-heparan sulfate proteoglycan complex formation on cell surfaces.” J Biol Chem 280(7): 5414-5422.

Gapalakrishnan, M., K. Forsten-Williams, et al. (2005). Ligand Rebinding: Self-consistent Mean-field Theory and Numerical Simulation Applied to SPR Studies.” Chemistry and Biology of Heparin and Heparan Sulfate. H.G. Garg, Elsevier Ltd.

Garcia-Olivas, R., J. Hoebeke, et al. (2003). “Differential binding of platelet-derived growth factor isoforms to glycosaminoglycans.” Histochem Cell Biol 120(5): 371-382.

Gaus, K., E. Hall. (1999). “Surface Plasmon Resonance Measurement of the Binding of Low-Density Lipoprotein at a Heparin Surface.” J Colloid Interface Sci 217(1): 111-118.

Guerrini, M., T. Agulles, et al. (2002). “Minimal heparin/heparan sulfate sequences for binding to fibroblast growth factor-1.” Biochem Biophys Res Commun 292(1): 222-230.

Guerrini, M., A. Naggi, et al. (2005). “Complex glycosaminoglycans: profiling substitution patterns by two-dimensional nuclear magnetic resonance spectroscopy,” Analytical Biochemistry 337(1): 35-47.

Hoffman, M., J. Engbring, et al. (2001). “Cell type-specific differences in glycosaminoglycans modulate the biological activity of a heparin-binding peptide (RKRLQVQLSIRT) from the G domain of the laminin alpha1 chain.” J Biol Chem 276(25): 22077-22085.

Ibrahimi, O., F. Zhang, et al. (2004). “Kinetic model for FGF, FGFR, and proteoglycan signal transduction complex assembly.” Biochemistry 43(16): 4724-4730.

Jang, J., J. Hwang, et al. (2004). “Identification and kinetics analysis of a novel heparin-binding site (KEDK) in human tenascin-C.” J Biol Chem 279(24): 25562-25566.

Joyce, J., T. Tung, et al. (1999). “The L1 major capsid protein of human papillomavirus type 11 recombinant virus-like particles interacts with heparin and cell-surface glycosaminoglycans on human keratinocytes.” J Biol Chem 274(9): 5810-5822.

Kappler, J., S. Franken, et al. (2000). “Glycosaminoglycan-binding properties and secondary structure of the C-terminus of netrin-1.” Biochem Biophys Res Commun 271(2): 287-291.

Kett, W., R. Osmond, et al. (2003). “Avidin is a heparin-binding protein. Affinity, specificity and structural analysis.” Biochim Biophys Acta 1620(1-3): 225-234.

Laffont, I., V. Shuvaev, et al. (2002). “Early-glycation of apolipoprotein E: effect on its binding to LDL receptor, scavenger receptor A and heparan sulfates.” Biochim Biophys Acta 1583(1):99-107.

Lahiri, J., L. Isaacs, et al. (1999). “A strategy for the generation of surfaces presenting ligands for studies of binding based on an active ester as a common reactive intermediate: a surface plasmon resonance study.” Anal Chem 71(4):777-790.

Liekens, S., E. De Clercq, et al. (2001). “Angiogenesis: regulators and clinical applications.” Biochem Pharm 61(3): 253-270.

Lin, Y., R. Pixley, et al. (2000). “Kinetic analysis of the role of zinc in the interaction of domain 5 of high-molecular weight kininogen (HK) with heparin.” Biochem 39(17): 5104-5110.

Lookene, A., M. Nielsen, et al. (2000). “Contribution of the carboxy-terminal domain of lipoprotein lipase to interaction with heparin and lipoproteins.” Biochem Biophys Res Commun 271(1): 5-21.

Lookene, A., R. Savonen, et al. (1997). “Interaction of lipoproteins with heparan sulfate proteoglycans and with lipoprotein lipase. Studies by surface plasmon resonance technique.” Biochem 36(17): 5267-5275.

Lookene, A., P. Stenlund, et al. (2000). “Characterization of heparin binding of human extracellular superoxide dismutase.” Biochem 39(1): 230-236.

Lustig, F., J. Hoebeke, et al. (1996). “Alternative splicing determines the binding of platelet-derived growth factor (PDGF-AA) to glycosaminoglycans.” Biochem 35(37): 2077-12085.

Lustig, F., J. Hoebeke, et al. (1999). “Processing of PDGF gene products determines interactions with glycosaminoglycans.” J Mol Recognit 12(2): 112-120.

Mach, H., D. Volkin, et al. (1993). “Nature of the interaction of heparin with acidic fibroblast growth factor.“ Biochem 32(20): 5480-5489.

Martin, L., C. Blanpain, et al. (2001). “Structural and functional analysis of the RANTES-glycosaminoglycans interactions.” Biochem 40(21): 6303-6318.

Miyamoto, K., N. Kodera, et al. (2002). “Specific interactions between cryogel components: role of extra domain A containing fibronectin in cryogelation.” Int J Biol Macromol 30(3-4): 205-212.

Morton T., D. Myszka, et al. (1995). “Interpreting complex binding kinetics from optical biosensors: a comparison of analysis by linearization, the integrated rate equation, and numerical integration.” Anal Biochem 227(1): 176-185.

Moscatelli, D. (1992). “Basic fibroblast growth factor (bFGF) dissociates rapidly from heparan sulfates but slowly from receptors. Implications for mechanisms of bFGF release from pericellular matrix.” J Biol Chem 267(36): 25803-25809.

Moulard, M., H. Lortat-Jacob, et al. (2000). “Selective interactions of polyanions with basic surfaces on human immunodeficiency virus type 1 gp120.” J Virol 74(4): 1948-1960.

Mulloy, B., M. Forster, et al. (1993). “N.M.R. and molecular-modeling studies of the solution conformation of heparin.” Biochem J 293: 849.

Myszka, D. (1997). “Kinetic analysis of macromolecular interactions using surface plasmon resonance biosensors.” Curr Opin Biotechnol 8(1): 50-57.

Myszka, D., T. Morton, et al. (1997). “Kinetic analysis of a protein antigen-antibody interaction limited by mass transport on an optical biosensor.” Biophys Chem 64(1-3): 127-137.

Nielsen, P., Y.Gho, et al. (2000). “Identification of a major heparin and cell binding site in the LG4 module of the laminin alpha 5 chain.” J Biol Chem 275(19): 14517-14523.

Nielsen, P., Y. Yamada (2001). “Identification of cell-binding sites on the Laminin alpha 5 N-terminal domain by site-directed mutagenesis.” J Biol Chem 276(14): 10906-10912.

Nugent, M., R. Iozzo (2000). “Fibroblast growth factor-2.” Int J Biochem Cell Biol 32(2): 115-120. Review.

Neuenschwander, P. (2004). “Exosite occupation by heparin enhances the reactivity of blood coagulation factor Ixa.” Biochem 43(10): 2978-2986.

Ornitz, D., N. Itoh, (2001). “Fibroblast growth factors.” Genome Biol 2(3): reviews 3005.1–3005.12.

Osmond, R., W. Kett, et al. (2002). “Protein-heparin interactions measured by BIAcore 2000 are affected by the method of heparin immobilization.” Anal Biochem 310(2): 199-207.

Padera, R., G. Venkataraman, et al. (1999). “FGF-2/fibroblast growth factor receptor/heparin-like glycosaminoglycan interactions: a compensation model for FGF-2 signaling.” FASEB J 13(13): 1677-1687.

Pei, R., X. Cui, et al. (2000). “Real-time immunoassay of antibody activity in serum by surface plasmon resonance biosensor.” Talanta 53(3): 481-488.

Pellegrini, L. (2001). “Role of heparan sulfate in fibroblast growth factor signalling: a structural view.” Curr Opin Struct Biol 11(5): 629-634. Review.

Pethe, K., M. Aumercier, et al. (2000). “Characterization of the heparin-binding site of the mycobacterial heparin-binding hemagglutinin adhesin.” J Biol Chem 275(19): 14273-14280.

Pharmacia Biosensor AB (1991). BIAcore Methods. Uppsala, Sweden, Pharmacia Biosensor AB.

Pharmacia Biosensor AB (1994). BIAtechnology Handbook. Uppsala, Sweden, Pharmacia Biosensor AB.

Presta, M., P. Oreste, et al. (2005). “Antiangiogenic activity of semisynthetic biotechnological heparins: low-molecular-weight-sulfated Escherichia coli K5 polysaccharide derivatives as fibroblast growth factor antagonists.” Arterioscler Thromb Vasc Biol 25(1): 71-76.

Qureshi, M., S. Wong, (2002). “Design, production, and characterization of a monomeric streptavidin and its application for affinity purification of biotinylated proteins.” Protein Expression and Purification 25(3): 409-415.

Raman, R., V. Sasisekharan, et al. (2005). “Structural Insights into Biological Roles of Protein-Glycosaminoglycan Interactions.” Chem & Biol 12(3): 267-277.

Raman, R., G. Venkataraman G, et al. (2003).“Structural specificity of heparin binding in the fibroblast growth factor family of proteins.” Proc Natl Acad Sci USA 100(5): 2357-2362.

Ricard-Blum, S., O. Feraud, et al. (2004). “Characterization of endostatin binding to heparin and heparan sulfate by surface plasmon resonance and molecular modeling: role of divalent cations.” J Biol Chem 279(4): 2927-2936.

Rifkin, D., D. Moscatelli, (1989). “Recent developments in the cell biology of basic fibroblast growth factor.” J. Cell Biol 109: 1-6.

Reichert Inc. (2005). Reichert Inc. Webpage http://www.reichert.com Accessed: April 14, 2005.

Sadir, R., F. Baleux, et al. (2001). “Characterization of the stromal cell-derived factor-1alpha-heparin complex.” J Biol Chem 276(11): 8288-8296.

Safran, M., M. Eisenstein, et al. (2000). “Oligomerization reduces heparin affinity but enhances receptor binding of fibroblast growth factor 2.” Biochem. J 345: 107–113.

Schlessinger, J., A. Plotnikov, et al. (2000). “Crystal structure of a ternary FGF-FGFR-heparin complex reveals a dual role for heparin in FGFR binding and dimerization.” Mol Cell 6(3): 743-750.

Schuck, P. (1997). “Use of surface plasmon resonance to probe the equilibrium and dynamic aspects of interactions between biological macromolecules.” Annu Rev Biophys Biomol Struct 26: 541-566. Review.

Shuvaev, V., I. Laffont, et al. (1999). “Kinetics of apolipoprotein E isoforms-binding to the major glycosaminoglycans of the extracellular matrix.” FEBS Lett 459(3): 353-357.

Silin, V., and A.Plant. (1997) “Biotechnological applications of surface plasmon resonance.” Trends in Biotechnology 15(9): 353-359.

Silin, V., H. Weetall, et al. (1997). “SPR Studies of the Nonspecific Adsorption Kinetics of Human IgG and BSA on Gold Surfaces Modified by Self-Assembled Monolayers (SAMs).” J Colloid Interface Sci 185(1): 94-103.

Smith, S., R. Sreenivasan, et al. (2003). “Mapping of regions within the vaccinia virus complement control protein involved in dose-dependent binding to key complement components and heparin using surface plasmon resonance.” Biochim Biophys Acta 1650(1-2): 30-39.

Sommer, A., D. Rifkin (1989). “Interaction of heparin with human basic fibroblast growth factor: protection of the angiogenic protein from proteolytic degradation.” J Cell Phys 138(1): 215-220.

Stearns, N., D. Prigent-Richard, et al. (1997). “Synthesis and characterization of highly sensitive heparin probes for detection of heparin-binding proteins.” Anal Biochem 247(2): 348-356.

Stenberg, E., B. Persson, et al. (1991). “Quantitative determination of surface concentration of protein with surface plasmon resonance using radiolabeled proteins.” J Colloid Interface Sci 143(2): 513-526.

Stenlund, P., M. Lindberg, et al. (2002). “Structural requirements for high-affinity heparin binding: alanine scanning analysis of charged residues in the C-terminal domain of human extracellular superoxide dismutase.” Biochem 41(9): 3168-3175.

Tkachenko, E., E. Lutgens, et al. (2004). “Fibroblast growth factor 2 endocytosis in endothelial cells proceed via syndecan-4-dependent activation of Rac1 and a Cdc42-dependent macropinocytic pathway.” J Cell Sci 117(Pt 15): 3189-3199.

Utt, M., B. Danielsson, et al. (2001). "Helicobacter pylori vacuolating cytotoxin binding to a putative cell surface receptor, heparan sulfate, studied by surface plasmon resonance.” FEMS Imm Medl Microbiol 30(2): 109-113.

Vives, R., R. Sadir, et al. (2002). “A kinetics and modeling study of RANTES(9-68) binding to heparin reveals a mechanism of cooperative oligomerization.” Biochem 41(50):14779-14789.

Walker, A., J. Turnbull, et al. (1994). “Specific heparan sulfate saccharides mediate the activity of basic fibroblast growth factor.” J. Biol. Chem 269: 931-935.

Williams K., C. Chua, et al. (2005). “The kinetics of FGF-2 binding to heparan sulfate proteoglycans and MAP kinase signaling.” J Theor Biol 233(4): 483-499.

Wu, X., Y. Xu, et al. (2003). “Surface plasmon resonance analysis to evaluate the importance of heparin sulfate groups' binding with human aFGF and bFGF.” J Zhejiang Univ Sci 4(1): 86-94.

Yakovlev, S., S. Gorlatov, et al. (2003).”Interaction of fibrin(ogen) with heparin: further characterization and localization of the heparin-binding site.” Biochem 42(25): 7709-7716.

Zhang, F., M. Fath, et al. (2003). “A highly stable covalent conjugated heparin biochip for heparin-protein interaction studies.” Anal Biochem 304(2): 271-273.

Zhang, F., F. Ronca, et al. (2004). “Structural determinants of heparan sulfate interactions with Slit proteins.” Biochem Biophys Res Commun 317(2): 352-357.

Appendix: IGFBP-3-Long-R3-IGF-I Interactions

Acknowledgement

The majority of the work presented in this section was performed by Abbie Bellis with the assistance and oversight of David Rand Kirtland.

Introduction

The Reichert SR 7000 was used to analyze the effects of pH on the interactions of insulin-like growth factor binding protein-3 (IGFBP-3) with surface bound recombinant insulin like growth factor-I (Long R3-IGF-I). Long R3-IGF-I is a mutant form of IGF-I that is reported to not bind insulin like growth factor binding proteins (IGFBP) at the normal physiological pH (7.4) (Francis et al., 1992). This small study was focused on quantifying the effect of pH on the interaction of IGFBP-3 with surface coupled Long R3-IGF-I.

Method

The procedures, hardware, and materials used for this study were the same as presented in Chapter 2, except for a few small differences. The Long R3-IGF-I was attached to an mSAM surface by offline amine coupling. Instead of being performed on the SPR until while collecting data the association was performed on the lab bench and with overnight incubation to maximize attachment. This technique consumes fewer materials, but the exact quantity of protein bound is unknown.

The mSAM surface was activated with 250 μl of 0.2 M EDC (Pierce, Rockford, IL) and 0.05M NHS (Aldrich Chemical, St. Louis, MO) solution for 12 minutes at room temperature. The chip was then rinsed with 20mM sodium acetate(Fischer Scientific, Pittsburgh, PA), pH 5.4, to remove any remaining compounds. Next, 200 μl of

0.0125μg/μl LongR3 IGF-I(Cell Sciences Inc., Canton, MA) in 20 mM, pH 5.4, sodium acetate, pH 5.4, solution was placed on the chip and incubated over night at 4° C. The next day the chip was rinsed twice with 200μl and then covered with 200μl for 10 minutes with 1.0 M ethanolamine (Sigma, St. Louis, MO), pH 8.5, to remove any remaining reactive NHS esters. The surface was then washed using ultrapure water to remove any unbound compounds before mounting the chip.

The prepared chip then mounted as explained in Chapter 2 and the SPR unit was used to examine the interactions of IGFBP-3 (Upstate Biotechnology, Lake Placid, NY) with the bound Long R3-IGF-I. Concentrations of 5, 10, 15, and 25 nM IGFBP-3 in PBST were examined primarily at pH 5.8, 6.2, 6.8, and 7.4. The associations were performed for 300 seconds at 0.8 ml/min using a recycle loop.

Results

The results were examined using the same, first order single site model presented in Chapter 1 and fit using a least squares analysis to calculated k_{obst} as shown in Figures 1a & 1b. Figure 2 illustrates the similarity between the k_{obst} at 5.8 and 7.4 pH. There is little if any difference between the rate constants at the different pH.

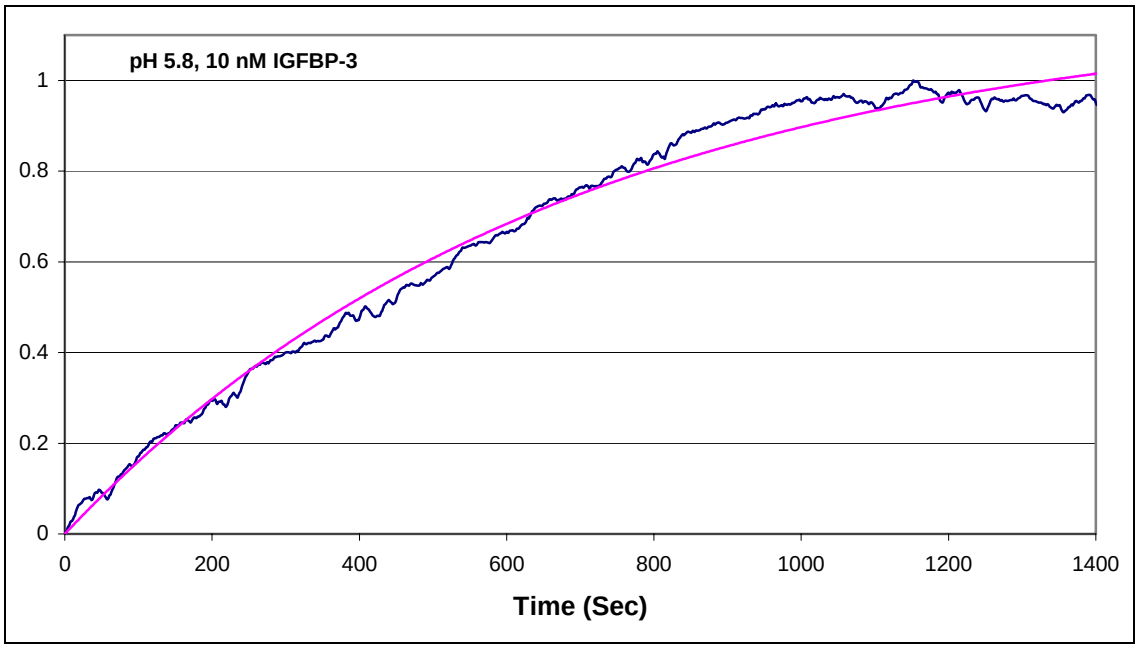

Figure 1a

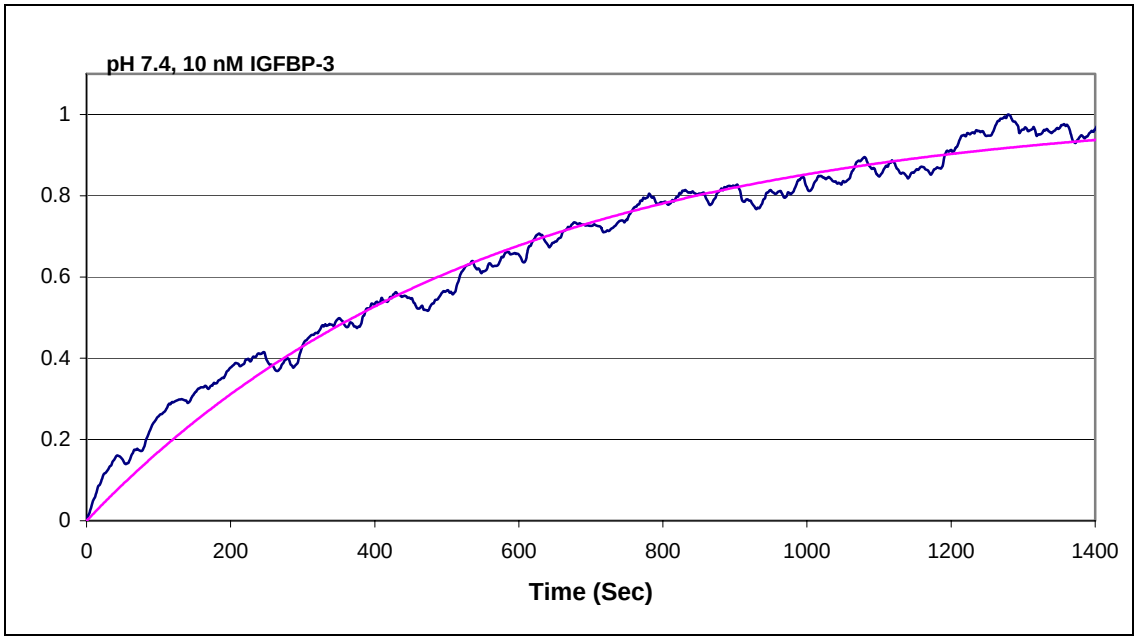

Figure 1b

A plot of the calculated value versus the actual data from a 10 nM IGFBP-3 association for pH 5.8 (a) and pH 7.4 (b). The calculated values were determined by Appling least squares analysis to Equation 9. Each figure is representative of 12 runs on 2 chips at 10 nM IGFBP-3.

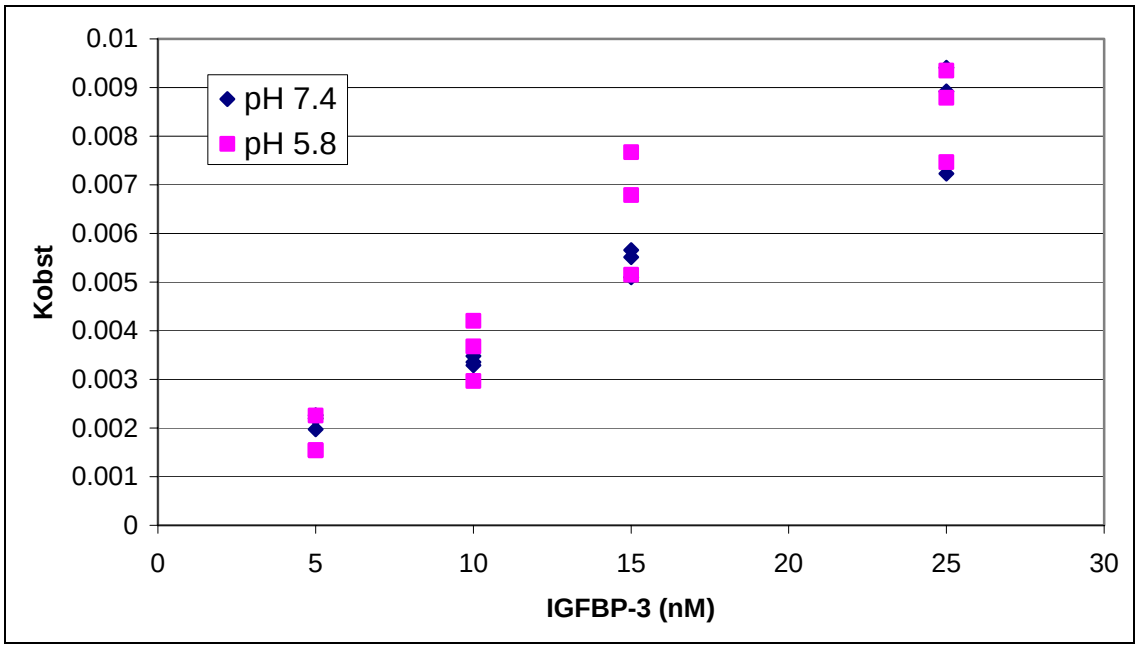

Figure 2. K_{obst} versus concentration of IGFBP-3 at 5.8 & 7.4 pH. Note the amount of overlap between the two pH's.

Conclusion

The data collected in this study showed no significant difference in the binding of IGFBP-3 with surface coupled Long R3-IGF-I between pH 5.8 and 7.4. This does not mean that pH is unimportant in the biological behavior of their interaction. The pH may affect some other aspect of the IGFBP-3 : Long R3-IGF-I complex, for example surface coupling of IGFBP-3 (Forsten et al., 2001), but it was not found to impact the specific binding. Confirmation of this via surface coupling of IGFBP-3 and solution binding of LongR3-IGF-I was not performed but would be a valuable additional study.

Appendix: IGFBP-3-Heparin Interactions

Introduction

The Reichert SR 7000 was used to analyze the effects of pH on the interactions of insulin-like growth factor binding protein-3 (IGFBP-3) with surface bound recombinant heparin. Heparin is known to interact with IGFBP-3. The interactions of IGFBP-3 with other molecules have been shown to be pH dependent (Forsten et al., 2001) and it is not known if there is a pH dependence for the interaction with heparin. This small study was focused on quantifying the effect of pH on the interaction of IGFBP-3 with surface coupled heparin.

Method

The procedures, hardware, and materials used for this study were the same as presented in Chapter 2. The same procedure to prepare and setup a heparin coupled mSAM was utilized as well. 37.5 nM IGFBP-3 (Upstate Biotechnology, Lake Placid, NY) in PBST at pH 5.8,and 7.4 were associated with the surface bound heparin. For the disassociation 15 μM heparin (Cat # 03003, Celsus Labs, Cincinnati OH) was used to minimize the effects of rebinding. The associations and disassociations were performed for 2100 seconds at 0.64 ml/min using a recycle loop.

Results

Figure 1 shows the results of associating IGFBP-3 with the heparin bound surface at pH 5.8 and pH 7.4 pH. No differences in the rates of association or disassociation between the two pHs were noted. The association and disassociation constants were calculated using clamp and found to be $k_a = 9.74 \times 10^4 \pm 1.68 \times 10^3$ $M^{-1}s^{-1}$ and $k_d = 4.68 \times 10\text{-}^4 \pm 4.27 \times 10\text{-}6$ s^{-1}.

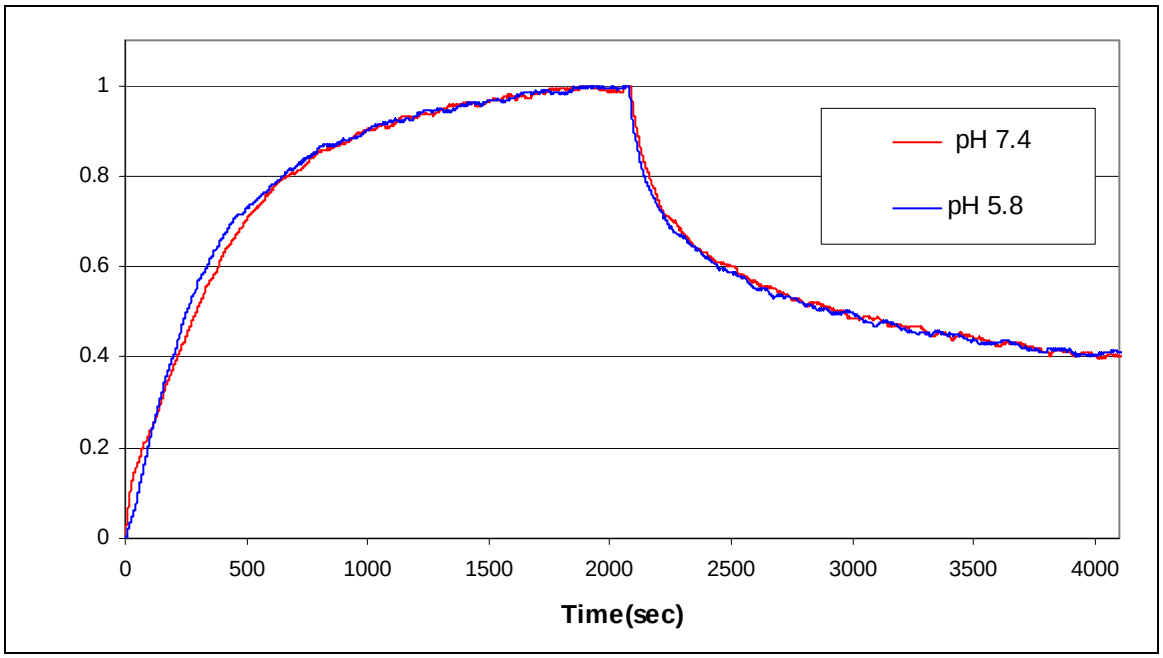

Figure 1, Association and disassociation of 37.5 nM IGFBP-3 with surface bound heparin at 5.8 pH and 7.4 pH. The disassociation was performed with 15 μM heparin in PBST solution. Note the lack of difference between the runs. The figure is representative of 5 runs on 2 chips.

Conclusion

The data collected in this study showed no significant difference in the binding of IGFBP-3 with surface coupled heparin between pH 5.8 and 7.4. This does not mean that pH is unimportant in the biological behavior of their interaction; just that pH does not affect the rate of their association or disassociation.

Vita

David Rand Kirtland

David Rand Kirtland was born in Charlottesville Virginia in 1978 to Dr. Howard and Barbara Kirtland. He grew up in Franklin, PA, and graduated from Franklin Area High School in the spring of 1997. In May 2002, he graduated from Cornell University, Ithaca, NY, with a Bachelor of Science in Chemical Engineering with a concentration in bioengineering. He enrolled at Virginia Polytechnic Institute and State University, Blacksburg, VA, in Jan of 2004 and is expected to complete his Masters of Science in Biomedical Engineering in May 2005.